Alkaline Iodine as an Oxidant for Uranium. IV.

By G. S. DESHMUKH and M. K. JOSHI

(Received January 10, 1955)

New volumetric methods of estimating uranium based on the reduction of U(VI) to U(IV) and re-oxidation of the latter by selenious acid or alkaline ferricyanide have been recently reported from our Laboratories[1,2]. In these procedures uranium was actually determined by performing iodometric titrations of the excess oxidising agents and also by estimating the products. Thus in the selenious acid method the metallic selenium was weighed and in the ferricyanide procedure the $K_4Fe(CN)_6$ formed was titrated directly with standard solution of $Ce(SO_4)_2$.

The oxidising action of iodine in alkaline medium is well known[3,4]. Its use as an oxidant for tetravalent uranium, however, finds little mention in the existing literature. Preliminary experiments showed that when an aqueous solution of iodine in KI was added to uranous sulphate solution followed by NaOH, rapid oxidation of U(IV) to U(VI) occurred. It was interesting therefore to study this redox process in some detail and utilize it for the quantitative determination of uranium.

Experimental

Uranyl sulphate solution was prepared by dissolving E. Merck's extra pure sodium uranate in sulphuric acid. Its uranium content was determined by the classical oxinate method. An aliquot volume of the uranyl sulphate solution was taken in a stoppered flask and reduced by means of pure zinc and H_2SO_4 in the cold. It was allowed to stand for about 15 minutes until the yellow colour of the uranyl sulphate changed to apple green characteristic one of the uranous sulphate. The contents of the flask were filtered through a Gooch crucible and the unreacted zinc was washed several times with dilute H_2SO_4 and then with distilled water. A stream of air was now bubbled through the cold uranous solution for five minutes to oxidise any U(III) formed to U(IV)[5].

An inert atmosphere was maintained by passing a slow stream of nitrogen gas, and a measured excess of standard iodine solution was added and then followed by 3N NaOH solution until a yellow precipitate was obtained. The contents of the flask were left over for 15~20 minutes, acidified and the unreacted iodine was determined in the usual way by titration with standard thiosulphate to the starch end point. In another set, the alkali was just neutralised with dilute H_2SO_4, followed by an excess of borax-boric acid buffer to maintain a pH 8~10 appropriate for iodine-arsenite reaction. The buffer solution was prepared by dissolving 8% and 4% by weight of crystallised borax and pure boric acid respectively in water as recommended by Chapin[6]. The unused iodine was then titrated with standard As_2O_3 solution to the starch end point.

The difference in the volume of thiosulphate and arsenious oxide before and after the reaction thus corresponds to the iodine consumed for the

TABLE I

Expt. No.	Normality of $Na_2S_2O_3$(N)	Vol. of Thio $=I_2$ reacted (ml.)	Normality of As_2O_3(N)	Vol. of $As_2O_3=I_2$ reacted (ml.)	Weight of uranium (g.) Oxinate method (x)	$Na_2S_2O_3$ Method (a)	As_2O_3 Method (b)	Difference x—a	x—b
1.	0.09781	25.80	0.1000	25.25	0.3008	0.3006	0.3007	0.0002	0.0001
2.	0.1000	20.20	"	20.20	0.2406	0.2406	0.2406	nil	nil
3.	0.08322	21.30	"	17.75	0.2118	0.2113	0.2113	0.0005	0.0005
4.	0.1030	15.20	"	15.65	0.1866	0.1866	0.1864	nil	0.0001
5.	0.1000	10.10	"	10.10	0.1203	0.1203	0.1203	nil	nil
6.	0.08320	10.65	"	8.85	0.1059	0.1056	0.1054	0.0003	0.0005
7.	0.1030	7.60	"	7.825	0.09330	0.09330	0.09320	nil	0.0002
8.	0.1000	5.05	"	5.05	0.06015	0.06015	0.06015	nil	nil
9.	0.1030	4.15	"	4.55	0.05401	0.05403	0.05419	0.0002	0.00018
10.	0.05000	5.05	0.05000	5.05	0.03006	0.03007	0.03007	0.00001	0.00001
11.	0.06035	3.65	"	4.40	0.02635	0.02624	0.02620	0.00011	0.00011

1) G. S. Deshmukh and M. K. Joshi, *Z. anal. Chem.*, 143, 334—339 (1954).
2) G. S. Deshmukh and M. K. Joshi, *Ber.* 88, 186—187 (1955).
3) E. Rupp, *Arch. Pharmaz*, 245, 6 (1907).
4) Abel, *Z. anorg. allgem. Chem.*, 76, 396 (1912).
5) A. I. Vogel, "A Text-Book of Quantitative Inorganic Analysis", Longmans, Green and Co., London, p. 318 (1951).
6) R. M. Chapin, *J. Am. Chem. Soc.*, 41, 351 (1919).

CHEMISTRY HALL LIBRARY

oxidation of U(IV) to U(VI). The amount of uranium was calculated as follows,

$$I_2+2NaOH \longrightarrow 2NaI+H_2O+O \quad \text{.....(i)}$$

$$UOSO_4+O \longrightarrow UO_2SO_4. \quad \text{.....(ii)}$$

Thus, $1U \equiv I_2 \equiv 2Na_2S_2O_3 \equiv 2/1As_2O_3$.

It follows that 1 ml. of 0.1 N $Na_2S_2O_3$ or As_2O_3 is equal to 0.01191 g. of uranium. Results of a series of experiments are returned in Table I. It will be seen that they are in fair agreement with those obtained by the classical oxinate procedure.

Iodine reacts with hydroxyl ions to form iodide and the extremely unstable hypoiodite; the latter is rapidly converted into iodate and iodide by self-oxidation-reduction[7].

$$I_2+2OH^- \rightleftarrows I^-+IO^-+H_2O \quad \text{.....(iii)}$$

$$3IO^- \rightleftarrows 2I^-+IO_3^- \quad \text{.....(iv)}$$

Since reaction (ii) is very fast and iodate rarely acts as an oxidising agent in alkaline medium. it is evident that tetravalent uranium is oxidised to the hexavalent state by hypoiodite, which in turn is reduced to iodide. After the oxidation process is completed and the system is acidified, an amount of iodine equivalent to the iodate formed is libereted according to the following equation,

$$5NaI+NaIO_3+3H_2SO_4 \longrightarrow 3I_2+3Na_2SO_4+3H_2O \quad \text{(v)}$$

This is titrated with standard $Na_2S_2O_3$ or As_2O_3 which corresponds to the unreacted iodine.

Titrations of U(IV) to U(VI) are generally carried out at elevated temperatures and involve the risk of aerial oxidation[8,9]. Since in the present method an excess of the oxidant is used in an inert atmosphere this possibility is eliminated. An additional advantage of this method, besides its simplicity and accuracy, is the use of As_2O_3, as a primary standard.

7) A. I. Vogel, "A Text-Book of Quantitative Inorganic Analysis", Longmans, Green and Co., London, p. 329 (1951).

8) N. Birnbaum and S. M. Edmonds, *Ind. Eng. Chem., Anal. Ed.*, 12, 155 (1940).

9) E. Miller and A. Flath, *Z. Elektrochem.*, 29, 500 (1923).

Summary

A new method for the determination of uranium based on the reduction of U(VI) to U(IV) and re-oxidation of the latter by alkaline iodine is described. The excess iodine is titrated with standard $Na_2S_2O_3$ or As_2O_3 and the results are found to be accurate and reproducible.

The authors are indebted to Prof. S. S. Joshi for facilities given to them and kind interest in the work. The award a U. P. Scientific Research Committee Scholarship (to M. K. J.) is also gratefully acknowledged.

Department of Chemistry, Banaras Hindu University, Banaras, India

---

A New Method of Drawing the Potential Energy Surface

By Shin SATO

(Received March 8, 1955)

Introduction

The calculation of the potential energy of a polyatomic system, which is necessary for the discussion of molecular structure or chemical reaction, is mathematically so difficult that the so-called "semi-empirical method" devised by Eyring and his collaborators has been widely used to interpret many chemical reactions[1]. The results obtained by this method, however, are found to have several weak points when being compared with the experimental data. In the present paper a new method of drawing the potential energy surface for the system of three atoms is proposed and compared with Eyring's method.

1) S. Glasstone, K. J. Laidler and H. Eyring, "The Theory of Rate Processes" McGraw-Hill Book Company, Inc., New York and London (1941).

Approximate Function for the Anti-bonding State of Two Atoms

When two atoms approach each other, there appear two energy states generally; the one is bonding and the other anti-bonding. The potential energy of the bonding state can be obtained experimentally as a function of the distance between two atoms. As is well known, the curves for many diatomic molecules are conveniently approximated by the Morse function[2],

$$E_{\text{bond}}=D_e\left[e^{-2\beta(r-r_e)}-2e^{-\beta(r-r_e)}\right]. \quad (1)$$

For the anti-bonding state, however, the curves cannot be obtained experimentally and the function is not yet proposed. The present author researched the function and found that the equation

2) P. M. Morse, *Phys. Rev.* **34**, 57 (1929).

$$E_{ant}=\frac{D_e}{2}[e^{-2\beta(r-r_e)}+2e^{-\beta(r-r_e)}], \qquad (2)$$

where D_e, β and r_e are constants which appear in the equation (1), is in good agreement with results calculated by James-Coolidge-Present[3] and Hirschfelder-Linnett[4] for the $^3\Sigma_u$ state of hydrogen molecule, which is shown in Fig. 1. Their results seem to be

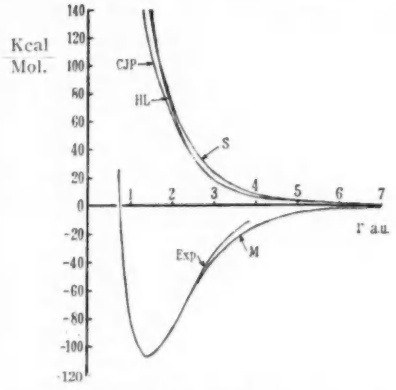

Fig. 1. Potential energy curve of hydrogen molecule.
Exp=Experimental; M=Morse curve; CJP=Coolidge, James and Present calculations; HL=Hirschfelder and Linnett calculations; S=Curve used by the present author.

the best ones at present. The applicability of this function for the anti-bonding states of other diatomic molecules cannot be ascertained because of no existing data. In the present method, one needs the energy curve for the anti-bonding state and the relation of (2) is assumed until the more suitable function is found.

Potential Energy for the System of Three Atoms

On the other hand, the potential energy curve of the system of two atoms A and B is approximated from the analogy of the well-known Heitler-London method for hydrogen molecule, as follows.

$$E_{bond}=(Q_{AB}+\alpha_{AB})/(1+S^2_{AB})$$
$$=(Q_{AB}+\alpha_{AB})/(1+k) \qquad (3)$$

and

$$E_{ant}=(Q_{AB}-\alpha_{AB})/(1-S^2_{AB})$$
$$=(Q_{AB}-\alpha_{AB})/(1-k) \qquad (4)$$

where $k=S^2_{AB}$ and Q_{AB}, α_{AB} and S_{AB} are Coulomb, exchange and overlap integrals respectively, all of which are functions of the distance between two atoms A and B.

For the potential energy of the system of three atoms A, B and C, London derived an equation by making some approximations and his equation has been used by Eyring et al. to interpret many simple chemical reactions[1]. The present author, by making a slightly different assumption $S^2_{AB}=S^2_{BC}=S^2_{CA}=k$, has derived the equation

$$E=\frac{1}{1+k}\left\{Q_{AB}+Q_{BC}+Q_{CA}\right.$$
$$\left.-\sqrt{\frac{2}{1}[(\alpha_{AB}-\alpha_{BC})^2+(\alpha_{BC}-\alpha_{CA})^2+(\alpha_{CA}-\alpha_{AB})^2]}\right\}, \qquad (5)$$

where Q_{ij}, α_{ij} and k have the same meanings as in equations (3) and (4). The London equation does not contain the term k, which corresponds to the square of overlap integral and may be so small compared with unity in the range of the internuclear separation under consideration that the equation (5) does not differ very much from London's equation.

Thus one can calculate the potential energy of the system of three atoms A, B and C as functions of r_{AB}, r_{BC} and r_{CA} from the above equations; assuming k as a constant for the system considered, one can obtain Q_{ij} and α_{ij} as functions of r_{ij} by substituting eqs. (1) and (2) in eqs. (3) and (4) respectively and these functions are substituted in the equation (5).

In Eyring's method Q_{ij} and α_{ij} are calculated by putting $k=0$ and by assuming that the Coulomb fraction ρ is a constant for the system of two atoms, while the present method is based on the relation of (2) and the assumption of k.

Potential Energy Surface for Hydrogen Atom-molecule Reaction

As a first attempt to make use of the method just described, the author has drawn the potential energy surface for hydrogen atom-molecule reaction, which has been already treated by Eyring's method[1].

The calculation for two configurations of an equilateral triangle (a) and a straight-line (b) indicates that the latter configuration is more stable than the former one as is seen from Fig. 2. Since only the lowest state is necessary for the present discussion, the surface has been drawn in the linear configuration. The result of calculation on the assumption of $k=0.18$ is given in Fig. 3,

3) H. M. James, A. S. Coolidge and R. D. Present, *J. Chem. Phys.*, **4**, 187 (1936).
4) J. O. Hirschfelder and J. W. Linnett, *J. Chem. Phys.*, **18**, 130 (1950).

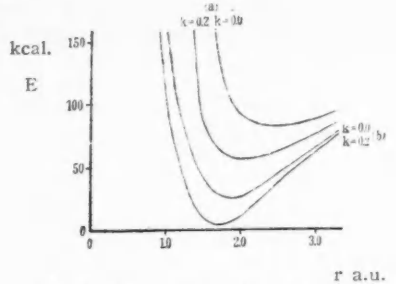

Fig. 2. Comparison of two configurations.
(a) equilateral triangle; (b) straight-line

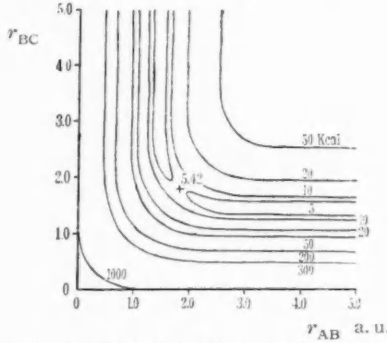

Fig. 3. Potential energy surface for the system of three hydrogen atoms in the linear configuration.

where r_{AB} is the distance between hydrogen atoms A and B and r_{BC} is the distance between B and C in the linear configuration of A-B-C. The vicinity of the saddle point in Fig. 3 is enlarged in Fig. 4. The diagram

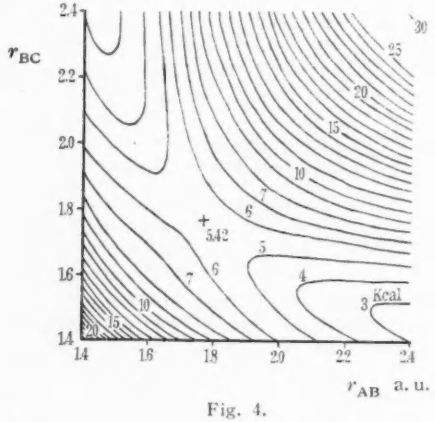

Fig. 4.

obtained differs essentially from Eyring's one which has two saddle points and a basin[4]; the present result has only one saddle point and no basin, coinciding with that of the non-empirical calculation[5]. The calculations with various values of k show the same situation, which seems, then, to be accompanied by the present method.

Comparison of the Two Methods

According to the theory of absolute reaction rates, the energy value at the saddle point, after allowing for zero-point energies, corresponds to the activation energy of hydrogen atom-molecule reaction. The results calculated by the two methods are given in Table I together with the experimental data.

TABLE I
ACTIVATION ENERGY OF HYDROGEN ATOM-MOLECULE REACTION

(kcal./mol.)

Observed	Calculated					
	Eyring			Present		
	ρ	E_c [a]	E_a [b]	k	E_c	E_a
5.0 ± 0.5 [3]	0.14	14	...	0.0	23.8	...
				0.1	13.4	...
7.0 ± 0.5 [7]	0.20	7.63	8.50	0.18	5.42	4.99
				0.2	3.59	...

a) without allowing for zero-point energies.
b) after allowing for zero-point energies.

Inspecting the table one can easily find that if $\rho>0.20$ is used in Eyring's method the better value may be obtained. If this is done, however, the minimum of the basin which appears in Eyring's diagram becomes lower than the minimum of the hydrogen molecule. This result might suggest the possibility of a stable linear complex H-H-H which has not been observed. Moreover Eyring's method cannot be applied in the range of $r<1.0$ a.u., as is seen from Fig. 5.

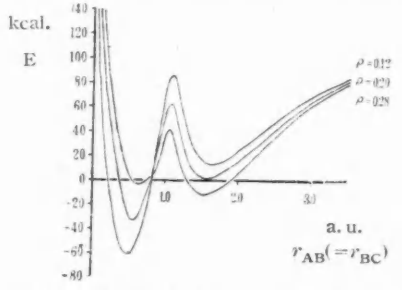

Fig. 5. Potential energy curves along the diagonal section of the surface for various values of ρ by Eyring's method.

5) J. O. Hirschfelder, H. Diamond and H. Eyring, *J. Chem. Phys.* 5, 697 (1937).
6) A. Farkas and L. Farkas, *Proc. Roy. Soc.* (London) *A152*, 124 (1935).
7) K.H. Geib and P. Harteck, *Z. physik. Chem.* (Bodenstein Festband) 849 (1931).

which shows the potential energy curves along the diagonal section of the surface for the various values of ρ. The minimum of the curves at 1.5 a.u. in Fig. 5 corresponds to the basin described above.

On the other hand, the present method gives a more reasonable value for the activation energy of hydrogen atom-molecule reaction and is bearable even in the range of $r<1.0$ a.u., as in seen from Fig. 6.

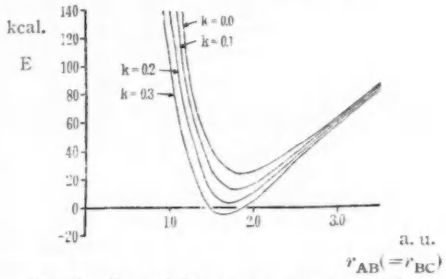

Fig. 6. Potential energy curves along the diagonal section of the surface for various values of k by the present method.

Summary

A new method of drawing the potential energy surface has been devised and compared with Eyring's semi-empirical method. The points different from the latter method are that an appropriate function for the anti-bonding state of a diatomic molecule is assumed and the overlap integral is not ignored. The so-called Coulomb fraction in Eyring's method is not used and the London equation has been slightly modified.

As an example the activation energy of hydrogen atom-molecule reaction has been calculated. So far as this reaction is concerned, the present method gives more reasonable value than Eyring's method.

The present author wishes to express his hearty gratitude to Prof. S. Shida for his interest and advice and to Mr. I. Yasumori, Mr. J. Higuchi and Mr. K. Fueki for their helpful discussions and suggestions.

Laboratory of Physical Chemistry,
Tokyo Institute of Technology,
Tokyo

Rheology of Surface Films. IV. Viscoelastic Properties of 6-Nylon Films at Air/Water Interface[1]

By Kiyoshi INOKUCHI

(Received March, 22, 1955)

Introduction

For the study of the fundamental rheological properties of surface films, it is desirable to investigate first a simple elastic film, being formed by a substance of known structure, which facilitates the interpretation of the experimental data in terms of molecular structure. Second, it is also necessary to extend the research to the viscoelastic films, in order to complete the investigation of surface rheology. In the course of this study, the author found[2] that the spread film of 6-nylon is a favorable material for our present purpose mentioned above, since it behaves as a purely elastic body at large areas, whereas it became viscoelastic when the compression advanced beyond a certain area. The aim of this report is to describe the rheological characteristics of 6-nylon film in detail in relation to their dependence to the degree of compression, magnitude of stress, temperature, and molecular weight of the sample, and to attempt some discussions thereupon.

Experimental

Materials.—Samples of poly-ε-capramide (6-nylon), whose molecular weights were controlled with benzoic acid, were kindly furnished from the Research Laboratory of Toyo Rayon Co. The average molecular weights were viscometrically determined[3], and the following results were obtained: 17300, 9100, 4600, 2800, and 1000. Unless otherwise stated, the sample of molecular weight 17300 was mainly used. Prior to the measurement, all the samples were washed with water, alcohol, and benzene, and dried in vacuum.

1) Presented at the Annual Meeting of the Chemical Society of Japan, April, 1954, Tokyo.
2) T. Tachibana and K. Inokuchi, *J. Colloid Sci.*, 8, 341 (1953).
3) M. Watanabe, *J. High Polymer* (Japan), 6, 216 (1949).

Spreading Condition.—The sample was spread from a mixed solution of benzene and phenol (3 : 1 in volume) on distilled water. The film was initially spread to 90 Å²/residue from 0.05% solution. Before compression, about twenty minutes were allowed for the equilibrium to be attained. Unless otherwise stated, the film was compressed down to a desired area at a rate of 60 cm²/min. and held at least for two hours before measurement. Film compression mainly studied was attained down to about a few Å²/residue.

Apparatus.—Surface rheometer used was the electromagnetic driving type reported in the foregoing paper[4]. The size of the trough and the detailed measures of the apparatus were the same as shown there. The apparatus was set in an air-thermostatted cabinet and the humidity in it was maintained at an almost saturated state by hanging up some water-immersed cloths in the cabinet. The temperature control of water in the trough was carried out by passing the thermostatted water into the jacket at the bottom of the trough. The temperature near the surface of the water was measured by means of a thermistor. Accuracy of temperature control was about ±0.5°C. The stress being applied to the film at all compressions was always controlled so that a suitable amount of strain (within 2 degrees of angle) occurred under shearing stress. The duration of the measurement was limited within about thirty minutes.

For the numerical evaluation of the viscoelastic quantities, equations (4) and (5) in the previous paper[4] were used with the implicit assumption that the film under test is isotropic and homogenous. With less compressed films, this assumption may be approximately valid. With highly compressed films, however, in which the films are no longer isotropic, and this assumption will not necessarily be valid, no accurate evaluation but more approximation of the viscoelasticity was attained.

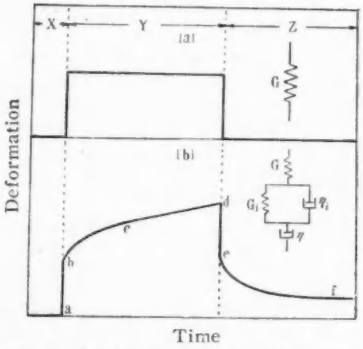

Fig. 1. Strain-time curves of 6-nylon. (a), at less compressed film, (b), at compressed film beyond about 40 Å²/residue. X represents the dead time, Y, the time, the stress being applied, and Z, the time after the stress is removed.

4) K. Inokuchi, This Bulletin, 27, 432 (1954).

Results and Discussion

General Remarks on the Rheological Properties.—As shown in Fig. 1, the strain-time curve of 6-nylon film was divided into two types according to the degree of compression of the film, i.e., a simple elastic type of less compressed film (about 75–40 Å²/residue) and a viscoelastic type of considerably compressed film (less than about 40 Å²/residue). For convenience' sake, the descriptions will be divided into two parts: time-independent mechanical property and a time-dependent one.

Part I. Time-independent Mechanical Property (Instantaneous Elasticity)

(1) Effect of Stress

It was found that the stress-strain relation generally depends upon the past history of shearing when the stress was first applied to the film. So, experiments, involving repeated process of application and removal of stress, were performed. Successive strains were thus obtained, stresses being gradually increased. Typical examples of these patterns, determined with the film at 42 Å²/residue were shown in Fig. 2. It is seen that,

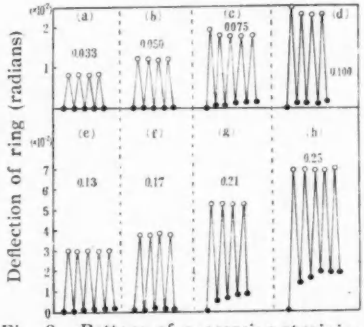

Fig. 2. Pattern of successive straining of the film at 42 Å²/residue at 28°C, stress being varied in each run, the values of which are indicated above each figure in dyne per cm. Open circles represent the instantaneous strain under stress, and full circles, the strain under removal of the stress.

at moderately small stress, each strain was perfectly identical, no hysteresis being observed as in Fig. 2 a-b. Under large stresses, however, considerable shortening of each strain was evident at the first one or two cycles, though it became less marked upon further repetition of straining tending to a limiting value as in Fig. 2 c-h, especially in h.

It is worthy of noticing that the film become more rigid as the rhythmic strain was

applied to the film. Such a phenomenon may well be compared to "rheopexy" or "work hardening" at bulk. It is plausible to consider that the elasticity of film, simply set up by compression, involves certain unstability in bond formation. Thus, it is presumable that the rhythmic motion, applied to the film, orients and aligns the film molecules, thereby accelerating the attainment of more stable bond formation. Such a mechanism may also be inferred from the property of the ordinary fibre, in which the increase of the tensile strength develops under extension.

When the plots were made using the first value of each strain series, a linear stress-strain relationship was obtained which bent down at larger stress as in Fig. 3. On the

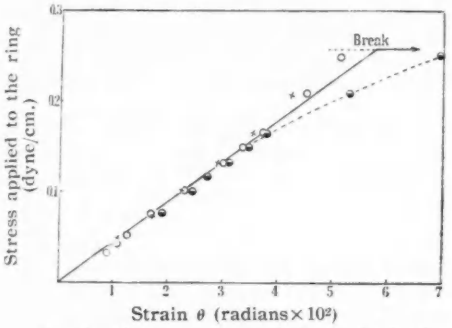

Fig. 3. Stress-strain relation obtained from Fig. 2. Half circle plots were obtained from the first strain of each group of the strain cycles, open circles, from the fourth strain. Crosses represent the plots obtained five minutes after rupture of the film.

other hand, if the curve were plotted using the fourth value of strain series, the nearly straight line was obtained almost up to the point of rupture. Even once the rupture took place under too large stress, only several minutes were sufficient for recovering the film structure. In Fig. 3, crosses indicate that the strain, determined five minutes after rupture, is in good coincidence with those before rupture.

Nearly linear relation between stress and strain was generally observed with films at large areas, where only an instantaneous elastic response appeared under stress. On the other hand, with films at small areas, where creep appeared under stress, the plots tended to bend towards the strain-axis above a certain value of stress, though they produced a good straight line at moderately small stresses. Hysteresis was negligible as far as the linear portion was concerned. It was thus presumed that the film at all compressions would be Hookean for at least moderately small stress.

The stress-strain curves at constant rate of strain were also determined, since they are significant for studying the film properties, especially the properties of weakening or fatigue preceding the rupture, which cannot adequately be analysed in terms of viscoelastic deformation alone. The form of the curves are of course dependent on the rate of strain, and the family of the curves depicted in Fig. 4, were obtained under a

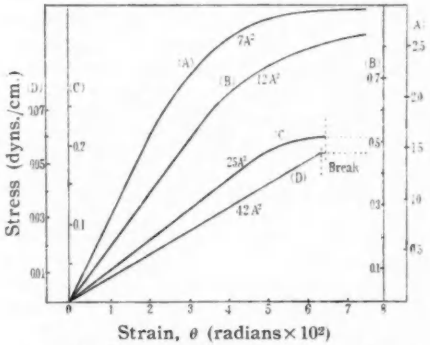

Fig. 4. Stress-strain curves of 6-nylon at constant rate of strain (1.05×10⁻² radian per minute). Curve (A), 7 Å²/residue; (B), 12 Å²/residue; (C), 25 Å²/residue; and (D), 42 Å²/residue. Temperature 20°C.

fixed rate of strain. In this figure, it is seen that at large areas, e.g., at 42 Å²/residue, a good straight line up to the film rupture was obtained, whereas as the area decreased, the plastic portion became evident before rupture set in. In addition, we see that with reducing area, elastic modulus (the slope of the linear portion) remarkably increased, but the strain at yield (length of the elastic portion) became shorter and shorter. Moreover, it is noticed that with highly compressed films (12 and 7 Å²/residue), the creep after yield was well-definable, without causing any gross rupture. Such behavior clearly represents that the film which was simply "brittle" at less compressed state, transformed to "tough" as the compression proceeded, the mechanical properties becoming closer to that of bulk.

It is really surprising that the film at less compressed state, not at highly compressed one, actually exhibits an ideal elastic behavior, which can hardly be seen at the ordinary bulk materials, upon which some discussions will be made in the next paper.

(2) Effect of Aging Time at Constant Temperature

Time effect of elasticity was examined. In Fig. 5, instead of the actual value of the

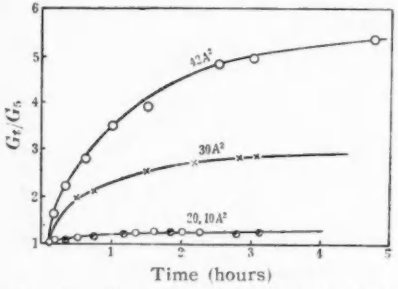

Fig. 5. Effect of aging time on the instantaneous modulus of rigidity at temperature 20°C. Abscissa indicates the aging time, t, defined as the time measured from the end of compression, ordinate, the ratio of rigidity at time $t(G_t)$ for that at 5 minutes of $t(G_5)$.

elastic modulus, ratio of instantaneous elastic modulus at time t for that of five minutes after the end of the compression, was plotted against the gelation time. It is seen that within the first ten minutes, there occurred a rapid increase in the modulus of elasticity, but this was followed by a very gradual approach to a steady state. Moreover, it was found that such an aging effect was remarkable with films at large areas, whereas it became less serious with highly compressed films. The large effect of aging at less compressed films may well be accounted for by the greater ease of orientation and alignment of the film molecules, which tends to form the stable bond than in the case of high compression. It is also noticed from these curves that the time of about two hours, which was allowed to elapse before all the measurements other than this were started, is practically sufficient to attain the steady state of elasticity.

(3) Effect of Temperature

When the temperature was raised to 38°C and chilled at the initial temperature, considerable increase in rigidity was noted, indicating that the temperature hysteresis does exsist. But when the sample was spread at moderately high temperature (38°C), and cooled and held at about 7°C for about ten hours, hysteresis was practically eliminated between the curves for increasing and decreasing temperature as seen in Fig. 6.

Temperature dependence of the instantaneous elastic modulus G, defined as S/θ, was depicted in Fig. 6. It was seen that the plots may yield a straight line, with negative inclination which was similar for films at all compressions. Thus, the following equation may hold between G and temperature, T.

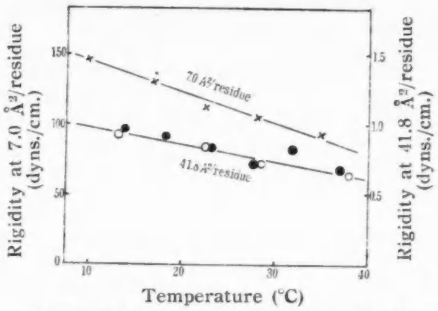

Fig. 6. Effect of temperature on the instantaneous modulus of rigidity. Rate of temperature change, 0.1°C per minute. Crosses show the plots at 7.0 Å²/residue, circles, those at 41.8 Å²/residue. The degree of temperature hysteresis was seen by the open and full circles, the former being those obtained with increasing temperature, the latter with decreasing temperature.

$$G=a+bT \tag{1}$$

where a, and b, are constants, b being negative. Such a temperature dependence is the same as the bulk material of nylon whose tensile strength decreased with increase in temperature[5].

According to Wieland and Snyder[6], the stress, F, can be resolved as follows

$$F=F_u+F_s, \tag{2}$$

where F_u represents energy term, and F_s, entropy term. The entropy term, F_s, is given by the relation

$$F_s=T(\partial F/\partial T)_\theta. \tag{3}$$

Since our present discussion is confined to the Hookean elastic part,

$$F=G\cdot\theta$$

Thus,

$$F_s=T\cdot\theta\cdot(dG/dT). \tag{4}$$

Assuming that F_u is independent of temperature, it follows from the equation (1), (2), and (4) that F_t is negative because of the negative sign of dG/dT (or b), and this term decreased, as the strain increased, whereas the stress due to energy, F_u possesses increasing positive value with increasing strain.

5) T. Alfrey, "Mechanical Behaviors of High Polymers", p. 518 (1948).

6) W. B. Wiegand and I. W. Snyder, *Trans. Inst. Rubber Ind.*, 10, 234 (1934).

If we compare this thermal data with that of rubber[7], this film corresponds to that of highly stretched rubber in which advanced degree of crystallization occurs. When this film is compared to that of resting muscle[8], in which F_u is increased, and F_s decreased with advancing strain, the property is analogous to the highly organized structure of resting muscle. From those observations, it is suggested that 6-nylon film is not rubber-like, but of rather orderly arranged crystalline structure. Such a view may also be inferred from the property of crystallite formation in bulk.

(4) Relation between Elastic Modulus and Film Concentration

Change in modulus of rigidity with reducing area was quantitatively examined. By performing the compression at constant rate, it was possible to overcome the hysteresis of elasticity and to characterize the transformation of the film phase. Fig. 7

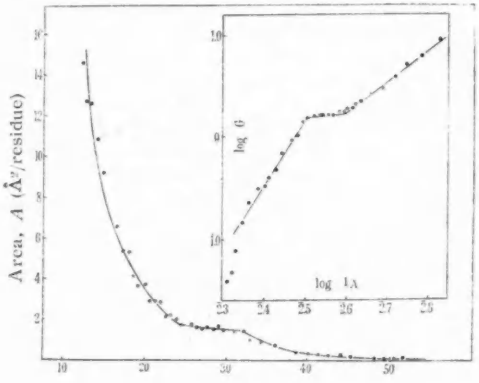

Fig. 7. Rigidity-area (G-A) curve obtained under a constant rate of compression (9.6 cm²/minute). Inset indicates the log G—log $1/A$ relation.

shows the rigidity-area curve, which was determined at a compression rate of 9.6 cm²/min. It is seen in this figure that the modulus increased continuously as the compression proceeded down to about 33 Å²/residue, where a plateau started. Further compression did not appreciably increase the rigidity until the areas of 24 Å²/residue was reached after which the rigidity was found to increase again with reducing area, this time more steeply. To make clear this relation, the logarithm of both modulus of rigidity G, and the reciprocal of area, $1/A$—a surface concentration—was plotted as seen in the inset of the figure. It is seen that these plots at larger areas than the plateau fall on a straight line with slight deviation, while those at smaller areas than the plateau produced a fairly good straight line. Thus, it was found that the experimental results were charcterized by the slopes of the lines, namely by the value p of the following equation

$$G=c(1/A)^p \qquad (5)$$

where c and p are constants. At larger and smaller areas than the plateau, p's were approximately calculated as 6 and 3, respectively. It may be that a film structure, once established at large areas, transformed to another type according to the degree of compression. The plateau region is thought to be a transition state of film structure under compression. As will be mentioned in the next paper, the plateau in the rigidity-area curve was consistent with the plateau which appeared in the pressure-area curve.

If we assume an approximate value as the thickness of the film under test, the modulus of rigidity in bulk would be calculated from the value of surface modulus of rigidity, G. The film thickness was presumed from the spreading amount and the density of the solid. The modulus of rigidity in bulk, corresponding to the area of 40 Å²/residue was calculated as 1.2×10^7 dyns./cm², whereas those corresponding to the area of 20 Å²/residue and 7.0 Å²/residue, were 4.6×10^7, and 5×10^8 dyns./cm², respectively. Uéno and Fuchino[9] obtained 55 kg./cm² as Young's modulus of elasticity of unstretched fibre of 6-nylon, from which the modulus of rigidity in bulk was calculated as 1.9×10^9 dyns./cm², assuming the poisson ratio 0.4. Although, with the film of high compression, precise evaluation of the film rigidity is impossible because of the failure of the isotropy of the film, the general trend is that the value calculated from the surface modulus at large areas was considerably smaller than that in bulk, whereas the values became closer to each other with reducing area. Such a disagree- ment of rigidity modulus between the bulk and the surface film would not be surprising, because the structure of spreading film is generally not the same as that in bulk. Such a difference in structure, however, is thought to be less pronounced as the compression advanced to form multimolecular layers, since the values at high compression became close to that of bulk.

7) E. Guth, *Ann. N.Y. Acad. Sci.*, 47, 723 (1947).
8) E. Guth, *Ann. N.Y. Acad. Sci.*, 47, 743 (1947).
9) S. Ueno and K. Fuchino, *J. Textile Research (Sen'i-gakukai-shi)*, 45, 324 (1951).

(5) Molecular Weight Dependence of Gelation Area

The area, at which the film first manifests elasticity under compression is significant for the study of the film structure, and is called here "gelation area" (A_g), the unit being Å²/residue. Fig. 8 shows how the gelation

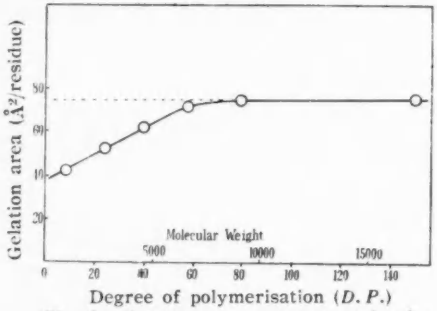

Fig. 8. Gelation-area versus molecular weight relation.

area is affected by the molecular weight of the spead material. It was found that the gelation area versus degree of polymerisation *D. P.* plots yielded a straight line showing an increase in A_g with increase in *D. P.*, so long as *D. P.* is not very high. However, with *D. P.* above a certain value, it tended to a maximum value of about 75 Å²/residue.

It is apparent that the gelation area inevitably necessitates the mutual contact of the neighboring molecules. So, the gelation area must closely be related to the degree of molecular extension. Since at the gelation point, the molecules are linked together, the degree of molecular extension would chiefly be determined by the flexibility of molecular chain.

With molecules, whose chain length is relatively short, the smaller value of A_g would be expected, the lower *D. P.* is, because the moleculer extension due to the flexibility of the molecular chain might be come less pronounced with decreasing chain length. In an extreme case of monomer films, A_g would be very close to the co-area of the residue itself. As seen in Fig. 8, extrapolation of the A_g-*D. P.* curve to zero *D. P.* yielded about 37 Å²/residue, which is fairly consistent with the co-area of residue, lying flat on water surface (molecular model gives 40.2 Å²/residue).

On the other hand, with the molecule, whose chain length is sufficiently long, it will be expected that the area per residue is independent of *D. P.*, since further increase in *D. P.* beyond a certain limit, would merely cause repetition of the flexible unit of chain. This was experimentally verified as shown in Fig. 8, in which A_g became independent of *D. P.*, when *D. P.* was over about 80.

It is generally accepted that chain polymers in solution take a spatial configuration of nearly random coiling, if there is no special interaction between chains. Applying this analogy to the surface, and assuming a two-dimensional random-coil model for the chain configuration of the film molecules, it can be deduced from simple statistical calculations that the mean area occupied by one molecule is proportional to *D. P.*, that is, the mean area per residue is independent of *D. P.* except for the chains of extremely short length. This seems to explain the above experimental result.

It must be noticed, however, that the maximum value of A_g is only twice as the co-area of residue, which is too small if we assume the two-dimensional random coil of a molecular chain. Moreover, it is surmised that, if the random coil of the molecular chain might be assumed, the value of *D. P.* at point of levelling off of the curve should be far small, being less than one-tenth of that in Fig. 8, at most. These results lead us to the postulation that the configuration of molecular chains at water surface is not likely in the case of random-coil, but may presumably be an extremely stretched one, possessing less flexibility. Such a molecular configuration may rather be favorable for the alignment and association between adjacent molecular chains which lead to the formation of rigid gel-structure.

(6) Molecular Weight Dependence of the Film Elasticity

Instantaneous modulus of rigidity was plotted against the molecular weight of the

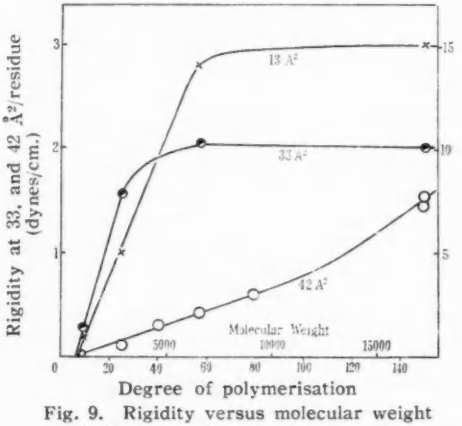

Fig. 9. Rigidity versus molecular weight relations at various areas.

sample at various areas. As depicted in Fig. 9, two types of the curve were obtained. At a highly compressed state (13 and 33 Å²/residue), rigidity increased proportionally with *D. P.* as far as *D. P.* is relatively low, but they approached asymptotically to a maximum value when *D. P.* was over about 80. Moreover, it was found that extrapolation to zero rigidity failed to pass through the origin, cutting the *D. P.* axis by about 5. Such a form of the curve is entirely similar to that obtained with material in three-dimensional state[10]. Kanamaru and Koyama[11] also obtained the similar curve with nylon fibre.

On the other hand, the spreading at a less compressed state, 42 Å²/residue, failed to exhibit the saturation curve as shown above. That is, the rigidity increased linearly with *D. P.* up to *D. P.* value of about 150. Extrapolation of the curve to zero rigidity coincided with the same point for the more compressed film.

Although the current view[12,13] of the strength-*D. P.* relation of the fibre or yarn is that the mechanical strength of material is affected by the two factors, the one is a frictional force between the chains (*D. P.*-dependent), and the other a primary valence force of the main chain (*D. P.*-independent)., it is not suggested that the strength of the spread film can readily be explained from this view point. The author should like to consider that the degree of cristallite formation is intimately related to this phenomenon. As is generally accepted, fine structure of the crystalline polymers are considered to consist of the dense, tightly packed crystalline regions interspersed with less-dense amorphous regions, and the latter, being weaker than the former in mechanical strength, may be determinant for the establishment of the overall mechanical property. It is further believed that one and the same molecule may pass through two or more amorphous regions. Thus, it will be expected that the mechanical strength becomes independent of *D. P.*, when *D. P.* is sufficiently high. A similar consideration may also be applied for the case of the compressed film of 6-nylon, for instance at 13 and 33 Å²/residue, since, as will be described in the next paper, the structure of the compressed film is thought to bear considerable resemblance to that in bulk.

10) A. M. Sookne and M. Harris, *Ind. End. Chem.*, 37, 478 (1945).
11) K. Kanamaru and F. Koyama, *J. Chem. Soc. Japan (Ind. Chem. Sec.)*, 1273, 46, (1943).
12) K. H. Meyer, and H. Mark, Der Aufbau der Hochpolym. org Naturstoffe (Leipzig, 1930), p. 153.
13) R. R. Sulivan, *J. Appl. phys*, 13, 157 (1947).

With the films at large areas, however, the condition may be somewhat unfavorable for the crystallite formation, because the molecular configuration is confined within the two-dimensional plane, and the molecules are more loosely packed than in the above case. It follows that, due to the imperfect crystallite formation, amorphous region extends to a longer part of the molecule, and the mechanical strength may become dependent of *D. P.* up to a higher value of *D. P.* Thus, the simple increase in rigidity with *D. P.* at 42 Å²/residue may result. Such a view must be verified further with various kinds of material, and experiments with spreading films, which facilitate the control of the concentration of molecules with the same material, may be very useful for the investigation of this problem.

(7) Effect of pH of the Substrate Water

Gelation areas were measured under various pH of the substrate water (Fig. 10). Control

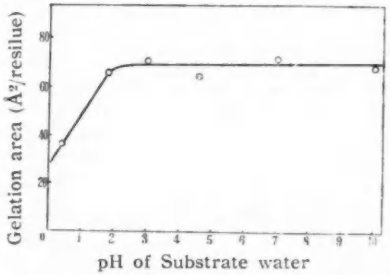

Fig. 10. Effect of pH of the substrate water upon the gelation-area, temperature 13–16°C.

of pH was carried out with hydrochloric acid and sodium hydroxide, and a glass electrode system was used to measure pH values. It was found that gelation area markedly decreased on the acidic substratum, though no remarkable influence was observed in the pH range between 2 and 10. On the 2 N sulfuric acid aqueous solution, the film failed to exhibit the elasticity above the areas of about 40 Å²/residue. Below this area, the film elasticity was found to decrease on the strong acidic solution. Such a result may well be consistent with the plausible view that the hydrogen bridge between the iminogroup of one residue and the carbonyl of another is respon sible for the film elasticity, since such a bond would be very weak on high acidic substratum.

Part II. Time-dependent Mechanical Properties

(1) Formal Analysis of the Strain-time Curve under Constant Shear Stress

Since, as mentioned above, the mechanical properties of the film at compressed state was complicated, it seemed convenient to represent the behavior with a series of the mechanical models: an instantaneously recoverable spring having an elastic modulus G, atime-dependent slowly recoverable spring of elastic modulus G_i set in parallel with a dashpot of viscosity, η_i, and a non-recoverable viscosity, η (see the inset of Fig. 1). The delayed elastic response is generally represented by a series of definite numbers of retardation times. So we now examine how many retardation mechanisms are necessary to represent practically the form of the experimental curve for delayed elasticity. As a typical example of the analysis, the strain-time curve at the area of 7.0 Å^2/residue was used.

According to the usual analysis of rheology[14], the form of the curve for the delayed elastic response is expressed by the following equation

$$\gamma=\sum_{i=1}^{i} A_i(1-e^{-t/\tau_i}), \qquad (6)$$

where γ represents the delayed elastic strain at time t, A_i, a constant, and τ_i a retardation time. Letting Q be equal to $(\Sigma A_i-\gamma)$, which corresponds to the distance between "b-c" curved line and "p-c" straight line measured along the strain axis of Fig. 11 (shadow region), the equation (6) follows,

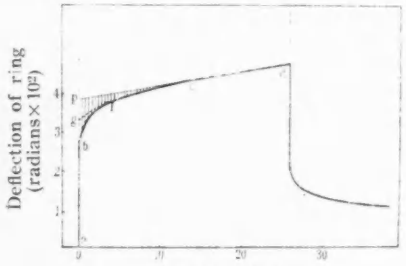

Fig. 11. Strain-time curve at 7.0 Å^2/residue, temperature 35°C. Stress applied to the ring, 5.0 dynes per cm.

$$Q=\sum_{i=1}^{i} A_i e^{-t/\tau_i} \qquad (7)$$

Letting τ_1, τ_2,..., a series of the retardation times involved in the film, be arranged in the decreasing order of magnitude and assuming that τ_1 is preferentially large compared with the other retardation times, τ_2, etc., log Q, when plotted against time, should give a straight line for large value of t. Except for the region of the initial several minutes, the above relation was valid in Fig. 12 (circle plots), which shows a straight

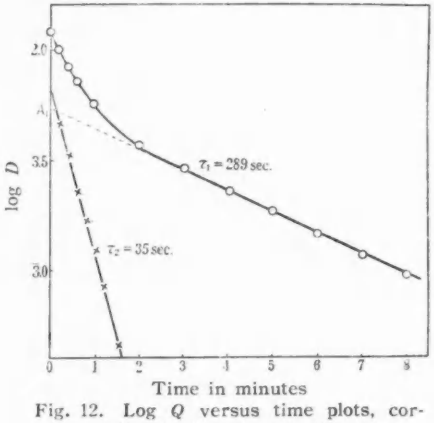

Fig. 12. Log Q versus time plots, corresponding to the curve in Fig. 11.

line intersecting log Q axis at A_1. Putting this straight line back into Fig. 11, the dotted line "f-g" was obtained, which represents the equation (7) involving single retardation time. From this figure, it can readily be seen that single retardation mechanism does not serve to represent the experimental data with sufficient accuracy.

If the relation mentioned above proved to hold, equation (7) further predicts that log $(Q-A_1e^{-t/\tau_1})$ should also become linear with large value of t, provided $\tau_1>\tau_2$. This was also valid as shown in the lower part of Fig. 12 (cross plots), from which τ_2, and A_2 were obtained from the inclination of the linear part of the line and the intercept on the ordinate axis, respectively. Since, in the present experimental conditions, it was difficult to determine the accurate form of the curve of the initial period of several seconds, a further series of retardation times following τ_2, was not taken into our consideration.

In brief, it was found that duplicate retardation mechanisms, in which longer and shorter retardation times are involved, seem adequate to describe the delayed elastic response of this film. If the initial displacement of the ring due to an instantaneous elasticity and the creep of constant rate of motion are represented by θ_0, and λt, respectively, where λ stands for the rate constant of motion, the overall strain of the ring, θ, would be expressed by the following equation of the six parameter model,

$$\theta=\theta_0+A_1(1-e^{-t/\tau_1})+A_2(1-e^{-t/\tau_2})+\lambda t. \qquad (8)$$

A similar degree of agreement between equa-

14) T. Alfrey, "Mechanical Behaviour of High Polymers," Intersci. Publ. New York, (1948), p. 58.

tion (8) and the observed curve was found to hold for all the data obtained with films at high compression, though films at less compression, e.g., 20 to 30 Å²/residue, where the contribution of the time-dependent strain was comparatively small, single retardation time was found to be practically adequate to express the delayed elastic strain. Such a form of the creep curve was just similar to that of the three-dimensional hydrogels of agar-agar, reported by Fujita and others[15].

Assuming that $G=KS/\theta_0$, $G_1=KS/A_1$, $G_2=KS/A_2$, $\eta_1=G_1\tau_1$, $\eta_2=G_2\tau_2$, and $\eta=KS/\lambda$, S represents the stress applied, and K, a constant involving shape factor, numerical values of the various areas, were obtained as shown in Table I.

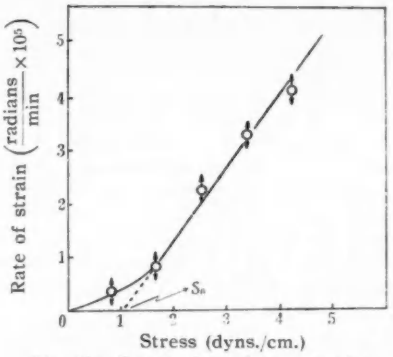

Fig. 13. Stress dependence of the rate of stationary flow at the film of 7.0 Å²/residue.

TABLE I

VARIOUS PARAMETES IN THE MECHANICAL MODEL IN C.G.S. UNIT TEMPERATURE 20°C

C.G.S. unit / Area Å²/residue	Instantaneous Elasticity	Delayed Elastic Parameters						Stationary Flow Viscosity
	G	G_2	τ_2	η_2	G_1	τ_1	η_1	η_f
42	0.38	—	—	—	—	—	—	—
25	1.6	—	—	—	19.5	113	2.2×10^3	7.8×10^3
12	11.2	109	17	1.9×10^3	107	72	7.7×10^3	1.3×10^4
7	112.3	1590	27	4.3×10^4	675	126	8.5×10^4	7.0×10^5

Although the observed values obtained with the same film were considerably reproducible, those obtained with a different run of experiments were found to scatter to a considerable extent. This seemed to be more pronounced at highly compressed film, while it was less serious at large areas. This may be due to the difficulties of obtaining conditions of forming exactly the same gel-structure.

(2) Stationary Flow Properties

(a) **Effect of Stress.**—Stress effect on λ of equation (8) was examined. As shown in Fig. 13, λ-S plots curved at small stress, with convex curvature against the strain axis, while, at higher stress, λ increased linearly with increasing stress, although the experimental plots scattered to some extent. If the intercept of the straight line on the stress axis was represented by S_0, such plots would be approximated by the equation,

$$\theta_f=K(S-S_0)t/\eta \qquad (9)$$

where θ_f is the displacement due to the flow, η, a parameter having the dimension of surface viscosity. Such a flow behavior, which is well-known as Bingham's plastic flow, was always observed in all the flow region of the films.

(b) **Effect of Temperature.**—The effect of temperature on η was also studied. It was found that the viscosity decreased with increasing temperature as should be expected. To make this clear, the logarithm of η was plotted against the reciprocal of the absolute temperature ($1/T$) as depicted in Fig. 14.

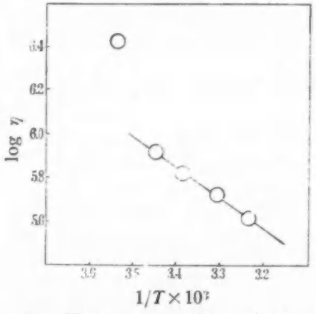

Fig. 14. Temperature dependence of the viscosity coefficient (η_f) at the film at 7.0 Å²/residue.

We see that the temperature dependence of the viscosity follows the well-known Andrade

15) H. Fujita, K. Ninomiya and T. Homma, This Bulletin, **26**, 20 (1953).

equation and the corresponding apparent activation energy E was approximately estimated as 6.4 kcal./mole. This value is in good agreement with that obtained in bulk[16], and, from this, it is assumed that the flow mechanism of such films is similar to that in bulk. Although it is difficult to know what this means, such a magnitude of energy may suggest that the strength of flow unit involved in it is the interaction of a secondary nature as would be expected from the molecular structure of 6-nylon, which permits the hydrogen bondings between NH and CO of adjacent chains of molecules.

Such a temperature dependence was almost the same for all compressions of the film. It was found, however, that the films, which were compressed to the areas of 12—15 Å²/residue, were the exception. Although the films of such a degree of compression took no special attitude as far as the stress effect was concerned, the viscosity of this film decreased far more markedly with rise of temperature than that of the other compressions. The author[17] reported a surface film of ovalbumin which suffered melting at room temperature under a certain condition. The fact observed here with 6-nylon may have some similarity with this phenomenon. Detailed mechanism requires further studies.

(3) Transcient Creep Properties

As is understood from the equation (8), these properties can be characterized by the parameters A_i, and τ_i. It was found that the values of both parameters was considerably less reproducible compared with the instantaneous elasticity and stationary flow, the experimental errors amountung to about 30% or more. In Fig. 15, instead of A_1, the modulus of retarded elasticity G_1, defined by KS/A_1, was plotted, together with τ_1, against stress. Fig. 16 gives the temperature dependence of G_1 and τ_1. We can see in these figures that the values of G_1 decreased with increasing stress. It is to be noted that the delayed elasticity is non-Hookean unlike the instantaneous elasticity. The value of G_1 decreased with increasing temperature, in a manner just similar to G. Because of the negative sign of the temperature dependence of G_1, the nature of the delayed elasticity was considered to be energy effect rather than entropy effect, as was the case with instantaneous elasticity.

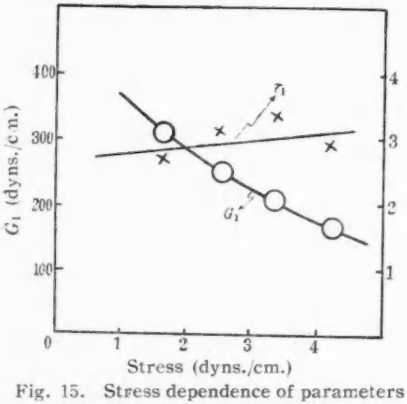

Fig. 15. Stress dependence of parameters in the delayed elastic mechanism. The area, 7.0 Å²/residue. Circles represent the delayed elasticity (G_1), crosses, the retardation time (τ_1).

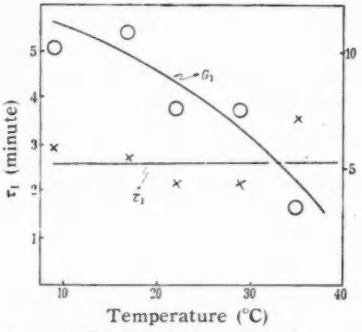

Fig. 16. Temperature dependence of each parameters in the delayed elastic mechanism. The area, 7.0 Å²/residue. Circles represent the delayed elasticity G_1, crosses, retardation time, τ_1.

The dependence of τ_1 upon the stress as well as temperature was considerably scattered, being similar to the Fujita's[15] data obtained with agar-agar hydrogel. Although definite conclusion could not be drawn on either stress or temperature effect on the retardation times, it would be likely that the retardation time is little influenced by temperature or stress. Such charactersitics of A_1 and τ_1 were similar also in the case of A_2 and τ_2.

(4) Stress-relaxation Test at Constant Shear Strain

(a) **Formal Analysis of the Curves.**—This test was carried out by reading the microammeter of the circuit of the rheometer at suitable intervals of time, when the current passed through the coil was controlled by adjusting the potentiometer so that the deflection of the ring, which occurred instantaneously after applying the stress, was held

16) K. Fuchiro, H. Okada, and N. Sagane, *J. High Polymer Chem.* (Japan), **7**, 19 (1950).

17) K. Inokuchi, This Bulletin, **26**, 500 (1953).

constant throughout the experiment. A family of the curves in Fig. 17, obtained at different

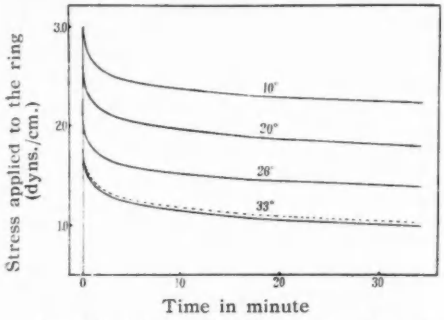

Fig. 17. Stress-relaxation curves at constant shear strain of the film at 7.0 Å$_2$/residue at varying temperatures. Deflection of the ring, 2.5×10^{-2} radians.

temperatures showed that considerably fast decay of the stress appeared at the early stage of time, followed by a slow decay at longer periods of time. Results of duplicate experiments are also indicated with a dotted line for the curve of 33°C. In general, relaxation of slow decay is relatively reproducible, whereas that of fast decay showed less reproducibility.

It was considered here that the experimental curves obtained could be expressed by a series of several Maxwellian relaxations as being written by the following equation

$$S=A\Sigma_i' e^{-t/\tau_i'}$$

where S represents the stress applied, τ_i' a constant termed as a relaxation time, and A_i', a constant. Check of the equation was made just in the same manner as was the case of the creep test in the foregoing section. As a result, it was found that three elements of Maxwellian relaxation were at least necessary to fit the whole data of the experimental plots except for the initial stage several seconds. In the present film, τ_1', τ_2' and τ_3', have the order of magnitude of 10^4, 10^2 and 10^1 second, respectively. Such a trend was always found with each curve obtained. Assuming that $G_i'=S_i/A_i'$, where $S=\sum S_i$, each value of the parameters, G and τ, were calculated as seen in Table II. Accurate determination of the numerical values of the third relaxation mechanism was, however, rather difficult, so we had to be contented with approximations.

(b) **Temperature Dependence of the Relaxation Times.**—Assuming Arrhenius equation, apparent activation energies, E'_1 and E'_2, corresponding to τ_1' and τ_2', respectively were obtained by plotting logarithms of τ_1' and τ_2' against $1/T$. It is to be noticed that temperature dependence of both relaxation times markedly differed, that is, longer relaxation time, τ_1', is considerably temperature-dependent, giving $E'_1\fallingdotseq5$ kcal./mole, whereas shorter relaxation time, τ_2', exhibited almost no temperature dependence, namely $E'_2\fallingdotseq0$.

TABLE II

VARIOUS PARAMETERS OF THE MECHANICAL MODEL OBTAINED FROM THE STRESS-RELAXATION CURVES IN Fig. 17

Parameters in C. G. S. unit / Temperature (°C)	G_1'	G_2'	G_3'	τ_1'	τ_2'
10	44.9	5.6	3.9	2.1×10^4	1.4×10^2
20	37.6	5.2	5·2	1.5×10^4	1.6×10^2
26	29.4	4.6	7.8	1.4×10^4	1.3×10^2
33	22.2	4.8	4.8	0.9×10^4	1.4×10^2

Activation energy of longer relaxation time, 5 kcal./mole, is fairly consistent with that of flow obtained with the creep curve in the preceding section. This value of activation energy for relaxation is in good harmony with the view that the gel-structure of this film consists of cross-linking at points of contact of a secondary strength. The fact that the shorter relaxation time was independent of temperature, is inferred from the result of the creep test that the retardation time, τ_1, failed to exhibit any definite temperature dependence.

Although, at the present stage, molecular interpretation of the temperature-independent relaxation mechanism is not clear, it would be reasonable to suppose that this relaxation is chiefly associated with the frequency factor in Arrhenius equation, presumably with the activation entropy for relaxation. In any case, it was pointed out here that the compressed film under test involves at least two kinds of relaxation mechanism of different modes.

(5) Correspondence between the Two Mechanical Models

In the above description, two types of mechanical model were presented: the one (model A), obtained from the creep test, the other (model B), from the stress relaxation test. If each parameter operating in the models is linear in nature, both models should be equivalent to each other, and values of parameters of one model are obtainable, when those of the other are known. In order to study the extent of correspondence of the mechanical models, duplicate measurements of creep and stress-relaxation were carried out with one and the same film, since the data

obtained from the experiments on different films scattered considerably even when the same experimental conditions were considered to be secured. The results obtained were arrayed by means of the mechanical models in Fig. 18, in which respective numerical values of each parameter were given in c.g.s. unit. It was stated above that six parameters were adequate to express the overall form of the curves up to the initial several seconds. For the sake of simplicity, however, the mechanical models of four parameters were used in this connexion, parameters belonging to the shortest retardation times (within one minute) being neglected. In this figure, blackets in model (A) give the values calculated from model (B).

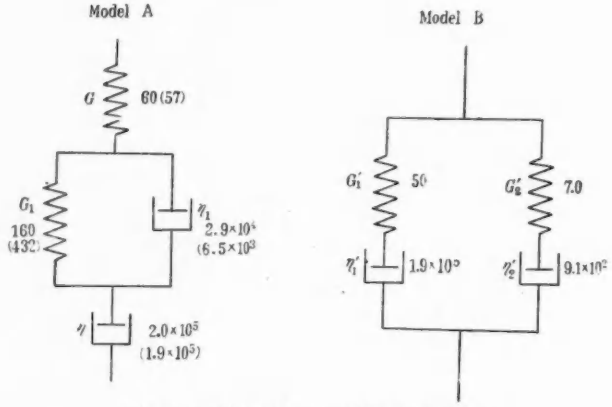

Fig. 18. Mechanical models of 6-nylon.

It is indicated that satisfactory agreement was obtained between the observed and calculated values, so far as instantaneous elasticity and stationary flow viscosity are concerned. As to the delayed elastic part, however, considerable disagreement of the values was seen. Such a degree of departure may well be expected, since it was shown above that parameters operating in the delayed elastic mechanisms as well as those in the shorter relaxation ones were considerably irreproducible, and that the delayed elasticity is non-Hookean (non-linear).

Such a state of affairs makes it difficult to draw a definite conclusion as to the consistency of the model of delayed elastic mechanism. It may, however, be said that our mechanical models presented above are sound for describing the static viscoelastic behaviors of the film, so far as the simple elastic part and stationary flow part are concerned.

Summary

(1) Using a surface-rheometer, the strain-time curves at constant shear stress, the stress-relaxation curves at constant strain, and the stress-strain curves at constant rate of strain were determined with the spread films of 6-nylon at air/water interface, and the rheological data were measured in relation to their dependence upon stress, temperature, and molecular weight of the sample under varying compressions, and were arrayed in the light of the mechanical models.

(2) It was found that the rheological characteristics of the film were classified into two types according to the degree of compression, i.e., a simple elastic type at large areas which involves a Hookean elasticity alone, and a viscoelastic type at considerably small areas, which is characterized by an instantaneous elasticity, the delayed elasticity, and stationary flow under constant stress.

(3) The stress-strain curves at constant rate of strain revealed that the film, which was simply brittle at large areas transformed to tough as the compression proceeded, the mechanical properties resembling to that in bulk.

(4) It was also observed that the film strength, which was readily set up after compression, was considerably improved by the rhythmic strains applied to it, indicating the two-dimensional rheopexy.

(5) Instantaneous elastic modulus versus area curve showed a conspicuous plateau at the areas from about 33 to 24 Å^2/residue, which suggests that at least two different phases are experienced during the process of compression.

(6) Temperature dependence of the instantaneous elasticity suggests that the elasticity is mainly due to the energy effect rather than entropy effect.

(7) Molecular weight variations of the film elasticity and of the gelation area were examined together with their pH dependence of the substratum, and discussions were made in molecular terms.

(8) The stationary flow under constant stress behaved as a plastic flow, which is characterized by a yield stress above which flow practically begins to occur. Apparent activation energy of flow was estimated as about 6 kcal./mol.

(9) Overall forms of the strain-time curves and of the stress-relaxation ones were found to be well fitted by the mechanical models of six parameters.

(10) From the temperature dependence of the relaxation times, it was suggested that at least two different modes of relaxation mechanism do exist within the films of high compression.

The author wishes to express his hearty thanks to Prof. T. Tachibana for his helpful advice and encouragement throughtout thiswork. The author is also indebted to Prof. S. Oka (Gakushuin University), Dr. K. Suzuki (Tokyo University of Education), and Dr. T. Nakagawa (University of Tokyo) for valuable criticism of this work.

Department of Chemistry, Faculty of Science, Ochanomizu University, Tokyo

---

Spectrochemical Study of Microscopic Crystals. VIII.[1] *Absorption Spectra of Dicyclopentadienyl-compounds of Iron and Cobalt*

By Shoichiro YAMADA, Akitsugu NAKAHARA and Ryutaro TSUCHIDA

(Received April 7, 1955)

Since the first preparation of dicyclopentadienyl-iron[2], a number of reports have appeared on the dicyclopentadienyl-compounds of various metals. Although the measurement of pleochroism is expected to afford valuable information about the linkages within the complexes, none of the former investigators have dealt with this property. In this paper we will report on the quantitative dichroism measurement with crystals of dicyclopentadienyl-iron (II) and dicyclopentadienyl-cobalt (III) perchlorate, and discuss the results of the measurements.

Experimental

Materials.—Dicyclopentadienyl-iron was prepared from cyclopentadienyl-magnesium bromide and tris-(2,4-pentanediono)-iron (III) in orange, monoclinic needles elongated along the [100] m.p. 173°C. The optical measurements were made on the prism face with polarized light having its electric vector along and perpendicular to the (100)-plane.

Dicyclopentadienyl-cobalt (III) perchlorate was prepared according to the method of Wilkinson et al.[3] from tris-(2,4-pentanediono)-cobalt (III) and cyclopentadienyl-magnesium bromide. The yellow, prismatic crystals thus obtained exhibit a straight extinction on the prism face. The optical measurements were made on this face with the electric vector along the directions of extinction.

Measurements.—Quantitative dichroism measurements were performed at room temperature in the region covering from 2400 to 7000 Å by Tsuchida-Kobayashi's microscopic method[4]. The symbol, α, represents absorption coefficient per mm. of a crystal. Molecular absorption coefficients, K, were estimated from the relation, $K = 10\,\alpha M/\rho$, where M and ρ denote formula weight of a compound and density of a crystal, respectively.

Results and Discussion

Dicyclopentadienyl-iron (II).—The results of the measurements are shown in Fig. 1 and Table I. The A- and B-absorption represent the absorption with the electric vector along and perpendicular to the *a*-plane of the crystal, respectively. Based on the

1) Paper VII of this series, S. Yamada, A. Nakahara, Y. Shimura and R. Tsuchida, This Bulletin, 28, 222 (1955).

2) T. J. Kealy and P. L. Pauson, *Nature*, 168, 1039 (1951); S. A. Miller, J. A. Tebboth and J. F. Tremayne, *J. Chem. Soc.*, 1952, 632.

3) G. Wilkinson, *J. Am. Chem. Soc.*, 74, 6148 (1952).

4) R. Tsuchida and M. Kobayashi, "The Colours and the Structures of Metallic Compounds." Zoshindo, Osaka, 1944, p. 180. See also the previous papers of this series.

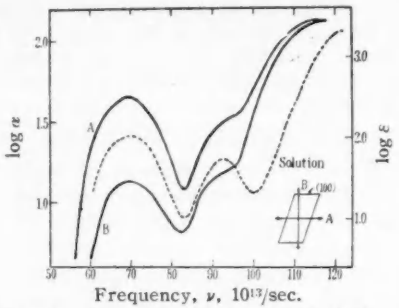

Fig. 1. Absorption spectra of $Fe(C_5H_5)_2$. The spectra of the aqueous solution (dotted curve) is taken from Ref. (7).

rings. Taking into consideration the orientation of the molecules in the crystal[5,6], the components of the molecular absorption coefficients (Fig. 2) were estimated, and shown in Table II. Dicyclopentadienyl-iron in the crystalline state is seen to exhibit in the region of the present measurement three band maxima at about 70, 94 and 120×10^{13}/sec., which almost correspond with the maxima observed for the solution of the compound[7]. Comparing the absorption curves of dicyclopentadienyl-iron with those of other compounds of iron[8], it is supposed that the absorption bands at 70 and 94×10^{13}/sec. should correspond to such absorption bands as would appear when the iron atom comes into co-ordinate linkage with ligands. Those bands, therefore, may be considered as due mainly to the co-ordinate linkages around the central metal atom of the complexes. Based on the former investigations on the absorption spectra of metallic complexes[9], it is also supposed that the band at about 120×10^{13}/sec. should be due to the electronic transitions in the cyclopentadienyl rings in coordination with the metal atom, being designated as a specific band.

TABLE I

ABSORPTION MAXIMA OF DICYCLOPENTADIENYL-IRON IN THE CRYSTALLINE STATE

	Band I			Band II			Specific Badd		
	ν, 10^{13}/sec.	$\log\alpha$	K	ν, 10^{13}/sec.	$\log\alpha$	K	ν, 10^{13}/sec.	$\log\alpha$	K
A-abs.	69.1	1.65	558×10^2	93.4	1.47	368×10^2	117	2.15	176×10^2
B-abs.	69.6	1.14	172×10^2	93.0	1.14	172×10^2	120	2.15	176×10^2
	$\alpha_A/\alpha_B=3.24$			$\alpha_A/\alpha_B=2.14$					

crystal analysis[5,6], it is seen that the A-absorption represents the main characteristic of the component absorption of the molecule with the electric vector perpendicular to the cyclopentadienyl-rings, and the B-absorption represents the one along the pentagonal

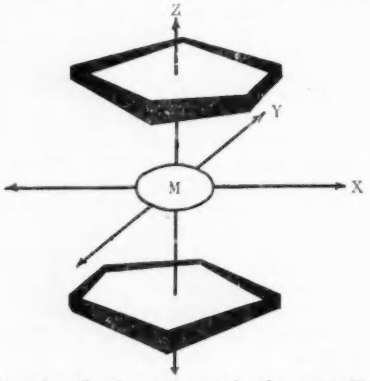

Fig. 2. Configuration of the metallic dicyclopentadienyl-compounds.

TABLE II

	Band I	Band II
K_z	94400	56400
K_x	17200	17200
K_z/K_x	5.48	3.28

For the bands at 70 and 94×14^{13}/sec., *Z-absorption, the absorption with the electric vector perpendicular to the pentagonal rings, has much larger intensity than X-absorption, absorption with the electric vector parallel to the pentagonal rings;* $K_z/K_x=5.48$ for the band at 70×10^{13}/sec., and $K_z/K_x=3.28$ for the band at 94×10^{13}/sec.

As to the specific band at about 120×10^{13}/sec., which may be ascribed to transitions in the cyclopentadienyl-radicals in coordination with the metal atom, *the absorption with electric vector along the rings is slightly hypsochromic to that perpendicular to the above.*

Dicyclopentadienyl-cobalt (III) Perchlorate.—Results of the measurements are shown in Fig. 3 and Table III. A-absorption

5) E. O. Fischer and W. Pfab, *Z. Naturforsch.*, **7b**, 377 (1952).

6) P. F. Eiland and R. Pepinsky, *J. Am. Chem. Soc.*, **74**, 4971 (1952); J. D. Dunitz and L. E. Orgel, *Nature*, **171**, 121 (1953).

7) L. Kaplan, W. L. Kester and J. J. Katz, *J. Am. Chem. Soc.*, **74**, 5531 (1952).

8) K. Sone, This Bulletin, **25**, 1 (1952), etc.

9) Absorption bands of such a kind were previously named "specific bands." See R. Tsuchida and M. Kobayashi, This Bulletin, **13**, 476 (1938).

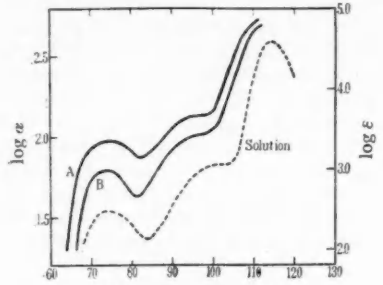

Fig. 3. Absorption spectra of $Co(C_5H_5)_2ClO_4$. The spectra of the aqueous solution (dotted curve) is taken from Ref. (3).

TABLE III

ABSORPTION MAXIMA OF DICYCLOPENTADIENYL-COBALT (III) PERCHLORATE IN THE CRYSTALLINE STATE

	Band I		Band II	
	ν, 10^{13}/sec.	$\log \alpha$	ν, 10^{13}/sec.	$\log \alpha$
A-abs.	74.4	2.0	97.0	2.2
B-abs.	74	1.79	97	2.06
	$\alpha_A/\alpha_B=1.62$.		$\alpha_A/\alpha_B=1.38$	

and B-absorption denote absorption with electric vector along and perpendicular to the direction of elongation. The compound exhibits three absorption bands at 74, 96 and about 115×10^{13}/sec., which almost coincide with the band maxima reported for the solution[10]. By analogy with dicyclopentadienyl-iron (II), the band at 115×10^{13}/sec. may be readily assigned to the specific band, which is due to the electronic transitions in the cyclopentadienyl-rings of the cobaltic compound. The two bands at the longer wave-length of dicyclopentadienyl-cobalt are supposed to be due to the electronic transitions of co-ordination electrons or electrons closely related to the co-ordinate linkages. The crystal structure of the present compound has not yet been determined. But it is reasonable that we should expect for this compound a similar rule on dichroism to that for the corresponding iron-compound. Thus, for the bands directly connected with the co-ordinate linkages in the dicyclopentadienyl-cobalt (III)-complex, the *Z*-absorption should be stronger than the *X*-absorption. The results of the present measurements, therefore, indicate that the *B*-absorption represents the main characteristic of the component absorption with the electric vector along the pentagonal rings. On the basis of the above assumption, the dichroism of this compound is seen to be quite similar to that of the corresponding iron-compound. Thus for both the bands, *absorption is stronger with electric vector perpendicular to eth pentagonal rings than with the vector along the cyclopentadienyl-rings.*

For the specific band at 115×10^{13}/sec., *absorption with electric vector along the rings is slightly hypsochromic to that perpendicular to the above.*

General Rules on the Dichroism.—From what is described in the foregoing part of this paper may be derived the following rules on the dichroism which are common for dicyclopentadienyl-iron (II) and -cobalt (III) complexes: (1) *For the two bands at the longer wave-length, due mainly to the co-ordination electrons around the metal atom, Z-absorption is highly hyperchromic to X-absorption, and* (2) *for the specific band, Z-absorption is slightly bathochromic to X-absorption.*

Rule (1) means that, for the bands which are considered as due mainly to the co-ordination electrons around the metal atom, the electronic transitions occur much more readily with the electric vector along the direction binding the metal atom and the centres of the pentagonal rings than with the vector along the plane. In the previous reports on planar quadri-co-ordinate complexes[11], it was found that for the band, considered to be due to the co-ordinate linkages, the oscillator strength was much greater with the electric vector along the complex-plane in which co-ordinate linkages exist than with the vector perpendicular to the plane. Hence, the above rule (1) may be compatible with the previously derived relation[11], assuming that there should exist firm linkages between the metal atom and cyclopentadienyl-radicals. Furthermore, the remarkable difference in absorption coefficient between the *Z*- and *X*-absorption seems to indicate that the π-electrons of the cyclopentadienyl-radicals may be involved considerably in the linkages between the metal atom and the pentadienyl-rings.

Rule (2) is concerned with the specific band, which may be ascribed to transitions in the cyclopentadienyl-radicals in co-ordination with the metal atom. It may be expected that the compounds would exhibit similar dichroism to that of the benzene rings if the pentagonal rings in these compounds would hold their aromatic property. For the π-band of the benzene rings in such compounds as hexamethylbenzene, absorption with the

10) G. Wilkinson, *J. Am. Chem. Soc.*, **74**, 6148 (1952).

11) S. Yamada and R. Tsuchida, This Bulletin, **26**, 489 (1953). See also S. Yamada, *J. Am. Chem. Soc.*, **73**, 1182 (1951), etc.

electric vector along the benzene rings was found to be far more hyperchromic and slightly bathochromic to that with the electric vector perpendicular to the benzene rings[12], and for the specific bands of cupric complexes with β-diketones, such as tropolone, salicylaldehyde or acetyl-acetone, each involving π-electronic systems, absorption with the electric vector along the plane of π-electronic systems was found to be far more bathochromic to the absorption with the electric vector perpendicular to the plane[13]. It is seen that the above rule (2) on the specific band of the metallic dicyclopentadienyl-compounds is not compatible with the dichroism for the π-band of the benzene rings, nor with that for the specific band of π-electronic systems within ligands in co-ordination with the metal atoms. It is supposed, therefore, that *the electronic state of the cyclopentadienyl-radicals in the above compounds differs from that of the π-electronic systems in the metallic complexes of an ordinary type as well as from that of the benzene-derivatives. Thus, as far as dichroism is concerned, the cyclopentadienyl-raaicals in the metal-compounds exhibit little aromatic property.* The above relations on the dichroism with the present metal-compounds may be comprehensible, assuming that the π-electrons in the pentagonal rings may be greatly attracted toward the metal atom to form co-ordinate linkages with the metal atom[14].

Rules (1) and (2) can be elucidated also in terms of the group theory. The details of the quantum-theoretical treatment will be submitted later.

Electronic State of the Cyclopentadienyl-groups in the Metallic Complexes.—The electronic state of the cyclopentadienyl-groups in the metallic compounds of the above type may be judged also from the wave-length at the maxima of the specific band. When one metal atom in some compound of the above type is replaced by another, the electronic state of the cyclopentadienyl-radicals would change to a greater or less extent according to the change in the linkages between the metal atom and ligands. At the same time, as the π-electrons of the pentagonal rings are attracted toward the metal atom more strongly, π-bond character of the pentagonal rings would be lost more and more, the specific band being displaced hypsochromically corresponding to the change in the electronic state of the cyclopentadienyl-radicals. Thus it is seen from the data reported by former investigators that the Fe(II)- and Co(III)-comlexes exhibit their specific bands at a much shorter wave-length than the Ni(II) compound (Table IV). This fact suggests that the π-electrons

TABLE IV

MAXIMA OF SPECIFIC BANDS OF DICYCLOPENTADIENYL-COMPOUNDS IN SOLUTION

	ν, 10^{13}/sec.	$\log \varepsilon$
$Fe(C_5H_5)_2$(a)	120	3.08
$Co(C_5H_5)_2ClO_4$(b)	114.5	4.6
$Ni(C_5H_5)_2$(c)	97.5	4.0
$Ru(C_5H_5)_2$(d)	142.9	3.5

(a) Ref. 7. (b) Ref. 3.
(c) E. O. Fischer, *Z. Naturforsch.*, 8b, 217 (1953).
(d) G. Wilkinson, *J. Am. Chem. Soc.*, 74, 6146 (1952).

in the former two compounds would be attracted toward the metal atom more strongly than in the Ni(II)-compound. Such a presumption seems to be in good agreement with the order in stability of the compounds: the Fe(II)- and Co(III)-compounds are far more stable than the Ni(II)-compound. According to the same criterion, the π-electrons are supposed to be attracted rather firmly toward the metal atom in the Ru(II)-compound, which is known, as would be expected, to be very stable. It may be supposed from the above consideration that the electronic state of the cyclopentadienyl-radicals would change greatly from a compound of one metal to that of another. Moreover, there might be some possibility that the linkages or bonding orbitals in the compounds of the above type would change essentially with changing the central metal atom.

As described above, the pentagonal rings in the above compounds would involve a different electronic state from the benzene rings. Their electronic state, however, would not be quite identical with those of cycloparaffines either. Thus the fact that the metal compounds in question exhibit their specific bands in the region between 2500 and 3000 Å might be taken as indicating that the cyclopentadienyl-radicals in the above compound would involve some π-electronic character, since the ordinary cycloparaffines would show no such specific bands in the corresponding region. The dichroism, reverse to that of the ordinary benzene rings, was also observed with aromatic molecular compounds, in which π-π interaction is supposed to exist between benzene rings in the direc-

12) R. Tsuchida, M. Kobayashi and K. Nakamoto, *J. Chem. Soc. Japan*, 70, 12 (1949); K. Nakamoto, *J. Am. Chem. Soc.*, 74, 390 (1952), etc.; G. Scheibe, S. Hartwig and H. Müller, *Z. Elektrochem.*, 49, 372 (1943).

13) R. Tsuchida and S. Yamada, read before the sixth annual meeting of the Chemical Society of Japan, Kyoto, April, 1953; to be published soon.

14) S. Yamada, A. Nakahara and R. Tsuchida, *J. Chem. phys.*, 22, 1620 (1954).

tion perpendicular to the benzene plane[15]. By assuming a similar effect, the dichroism of the present compounds may be understood in the same way, if the π-electrons of the pentagonal rings would be attracted toward the metal atom.

It is interesting to note that the absorption spectra of dicyclopentadienyl-iron (II) and cobalt (III) bear a close resemblance to those of tris (acetylacetono) iron (III) and cobalt (III)[15] in which π-electrons of the ligands are supposed to be involved in the co-ordinate linkages with the metal atoms. This fact, which seems to indicate similarity in linkages between the metal atom and ligands in the complexes of the above two types, may be in harmony with the above presumption that the π-electrons of the cyclopentadienyl-radicals should be greatly involved in the metal-ligand linkages.

Summary

Dichroisms of dicyclopentadienyl-iron (II) and dicyclopentadienyl-cobalt (III) perchlorate in the crystalline state have been quantitatively determined. For the two compounds, the common rules on the dichroism have been obtained. (1) For the two bands at the longer wave-length, absorption perpendicular to the pentagonal rings is very hyperchromic to absorption parallel to the rings. (2) For the specific band, absorption perpendicular to the rings is slightly bathochromic to absorption parallel to the rings.

Consideration of the results has led us to the conclusion that the cyclopentadienyl-radicals in these compounds may be different from the π-electronic systems of ordinary benzene rings, suggesting that the π-electrons would be greatly attracted toward the metal atom to form co-ordinate linkages.

The authors wish to express their hearty thanks to Mr. C. Holstein of the Firm Holstein for a sample of dicyclopentadiene, and to Miss I. Föppl (Dipl. Chem.) for her kind interest and valuable help in the present work. This work was supported in part by a grant from the Ministry of Education.

Department of Chemistry, Faculty of Science, Osaka University, Osaka

15) R. Tsuchida, M. Kobayashi and K. Nakamoto, *Nature*, **167**, 726 (1951); K. Nakamoto, *J. Am. Chem. Soc.*, **74**, 1739 (1952), etc.

16) K. Sone, I. Miyake, K. Yamasaki and H. Kuroya, *J. Chem. Soc. Japan*, **69**, 70 (1948).

Sterols and Other Unsaponifiable Substances in the Lipids of Shell Fishes, Crustacea and Echinoderms. XVI. Reinvestigation of Hitodesterol and its Identity with α-Spinasterol

By Yoshiyuki TOYAMA and Toru TAKAGI

(Received April 11, 1955)

Hitodesterol[1], m.p. 167–168°C, was found first in *Asterina pectinifera* and subsequently in *Asterias amurensis* (formerly *Asterias rollestoni*) in this laboratory. The formula for this sterol was deemed at that time to be $C_{28}H_{42}O$ or $C_{29}H_{44}O$, its tetra-unsaturation being inferred mainly from its iodine value determined by the pyridine sulfate dibromide method. It became, however, known that Δ^7-sterols generally give abnormally high iodine values by halogen absorption methods, and after having had experienced such an abnormally high iodine value for corbisterol, a $\Delta^{5,7,22}$-sterol of the C_{29}-series, the authors came to believe that hitodesterol shouldbe a di-unsaturated $\Delta^{7,22}$-sterol of the formula $C_{29}H_{48}O$ or $C_{29}H_{46}O$ which has a close resemblance to spinasterol, stellasterol and chondrillasterol, and is possibly identical with one of them[2]. Matsumoto and Wainai[3] have recently come to a similar conclusion that hitodesterol is a $\Delta^{7,22}$-sterol of the C_{29}- or C_{28}-series, the derivatives of which have the closest resemblance to the corresponding derivatives of α-spinasterol. Although a di-unsaturated sterol, named stellasterol, of m.p. 149–150°C, was reported to occur in *Astropecten aurantiacus*[4], this sterol appears not to be a uniform com-

1) T. Matsumoto and Y. Toyama, *J. Chem. Soc. Japan*, **64**, 1069 (1943); T. Matsumoto, M. Yajima and Y. Toyama, ibid., **64**, 1203 (1943).

2) Y. Toyama and T. Takagi, This Bulletin, **27**, 39 (1954).

3) T. Matsumoto and T. Wainai, *J. Chem. Soc. Japan, Pure Chem. Sect.*, **75**, 1147 (1954).

4) A. Kossel and S. Edelbacher, *Z. physiol. Chem.*, **94**, 264 (1915).

pound. Bergmann and Stansbury[5] separated from *Asterias forbesi* a sterol mixture which was found to consist of $\Delta^{7,22}$- and Δ^{7}-sterols of the C_{28}-series, and they proposed to retain the name stellasterol for the former and assign the name stellastenol to the latter. Although a complete separation of these two sterols was not attained, ozonolysis of a mixture of stellasteryl and stellastenyl acetates yielded *d*-methylisopropylacetaldehyde which was identified as its 2, 4-dinitrophenylhydrazone of m.p. 119–120°C and $[\alpha]_D^{24}=+14.1°$. Hence these authors regarded stellasterol as a C–24 epimer of 5-dihydroergosterol.

The present paper records the results of our reinvestigation on hitodesterol. As for sterol components other than hitodesterol, such as mono-unsaturated sterols, in *Asterina pectinifera*, our investigation is now in progress, and the results will be reported in near future.

The crude sterol mixture of the star fish, *Asterina pectinifera*, was acetylated, and the acetylation product was subjected to repeated recrystallizations from acetone by which a steady rise of the melting point was brought about until finally a steryl acetate fraction (A) of m.p. 182–183°C was obtained. This fraction was found to be still contaminated with a minor amount of steryl acetate having a lower melting point, but the melting point and specific rotation of this fraction was not altered substantially by further recrystallizations. This fraction showed a saponification value which agrees with the calculated value for $C_{31}H_{50}O_2$ and an iodine value corresponding to 1.9 double bonds per molecule by the perbenzoic acid method, and was regarded as hitodesteryl acetate in the following. The melting points and specific rotations of hitodesterol and its derivatives are compared with the corresponding compounds of α-spinasterol, chondrillasterol and 5-dihydroergosterol in Table I.

The Liebermann-Burchard test for hitodesteryl acetate developed a blue coloration in which the change of absorption at 620 mμ with the reaction period was quite similar to that of the Δ^{7}-sterol type. A further evidence for the presence of double bond between C–7 and C–8 in hitodesterol was afforded by converting hitodesteryl acetate by the action of mercuric acetate to a product which showed the absorption characteristic to $\Delta^{7,9(11)}$-steryl acetates.

In order to obtain an insight into the structure of the side chain attached to C–17 of hitodesterol, its acetate was subjected to ozonolysis. Among the products of ozonolysis, *l*-ethylisopropylacetaldehyde was identified as its 2, 4-dinitrophenylhydrazone; m.p. 116–117°C and $[\alpha]_D^{14}=-4.6°$. Hence hitodesterol is established as a $\Delta^{7,22}$-sterol of the C_{29}-series and is identical with α-spinasterol, both having the same optical configuration at C–24.

Steryl acetate fractions having melting points between 171°C and 175°C were recovered from the mother liquors of the recrystallizations which were performed to obtain hitodesteryl acetate. These fractions were united, and the united fraction (B) was subjected to ozonolysis. 2, 4-Dinitrophenylhydrazones prepared from the products of ozonolysis were separated into several fractions, including a fraction of m.p. 115–116°C together with a small amount of a fraction of m.p. 124–126°C. The scarcity of the material did not permit us to determine the optical rotation. While the fraction of m.p. 115–116°C was regarded as 2, 4-dinitrophenylhydrazone of ethylisopropylacetaldehyde, the fraction of m.p. 124–126°C was considered to be 2, 4-dinitrophenylhydra-

TABLE I

COMPARISON OF HITODESTEROL AND SOME RELATED STEROLS

	Free sterol		Acetate		Benzoate		3, 5-Dinitrobenzoate	
	m.p. (°C)	$[\alpha]^{\circ}_D$	m.p. (°C)	$[\alpha]^{\circ}_D$	m.p. (°C)	$[\alpha]^{\circ}_D$	m.p. (°C)	$[\alpha]^{\circ}_D$
Hitodesterol	167–168	−3.0	182–183	−5.8	197–199	+3.8	195	±0
Hitodesterol[6]	167–168	±0	181–182	±0	—	—	—	—
Hitodesterol[7]	168–169	−2.6	182–183	−2.8	198.5	±0	195	±0
α-Spinasterol[8]	168–169	−3.6	186	−4.5	200	+1.8	—	—
α-Spinasterol[9]	167–168	−3	185	−5	201	+2	—	—
Chondrillasterol[10]	168–169	−1.1	175–176	−1	194–195	+4.0	—	—
5-Dihydroergosterol[9]	176	−19	181	−19	200	−10	—	—

5) W. Bergmann and H. A. Stansbury, Jr., *J. Org. Chem.*, **9**, 281 (1944).
6) l.c., 1).
7) l.c., 3).
8) L. F. Fieser, M. Fieser and R. N. Chakravarti, *J. Am. Chem. Soc.*, **71**, 2226 (1949).
9) D. H. R. Barton and J. D. Cox, *J. Chem. Soc.*, **1948**, 1354.
10) W. Bergmann and F. H. McTigue, *J. Org. Chem.*, **13**, 738 (1948).

zone of methylisopropylacetaldehyde. Accordingly the steryl acetate fraction (B) seems to contain a small proportion of the acetate of C_{28}-sterol, which gives methylisopropylacetaldehyde by ozonolysis, besides hitodesteryl acetate.

It is thus seen from the foregoing that the di-unsaturated sterol components of *Asterina pectinifera* consist mainly of hitodesterol, although C_{28}-sterol, possibly $\Delta^{7,22}$-sterol, seems to be present in a lesser amount. Whether this sterol of the C_{28}-series corresponds to stellasterol or not, remains undetermined in the present study. The fact that hitodesterol constitutes the main component of the di-unsaturated sterols of *Asterina pectinifera*, whereas the di-unsaturated sterol of *Asterias forbesi* was found by Bergmann and Stansbury to be stellasterol, is by no means difficultly explicable if it is taken into consideration that the content of some sterol components in the total sterol mixture of the same species of aquatic invertebrates often differs widely as has been found in the case of corbicula, chiton and *Asterias amurensis*[11]. It may also be worthy of mention that some sterols formerly found only in the vegetable kingdom have been found to occur not seldom in aquatic invertebrates too. Thus the occurrence of brassicasterol in oyster[12], mussel[13], corbicula[14] and clam[15], and β-sitosterol in *Spisula sachalinensis*[15] and *Ophiopholis aculeata*[17] has been reported in previous studies, and now the occurrence of α-spinasterol or hitodesterol in *Asterina pectinifera* has been demonstrated in the present study.

Experimental

Several lots of the sun-dried star fish, *Asterina pectinifera* (Müller et Troschel) were united. The united material, 15.7 kg. in total, was cut into small pieces and extracted with ether, yielding 268 g. (1.7%) of a dark reddish orange viscous lipid. On treating the lipid with 2.7 liters of acetone, an acetone-soluble oil (180 g.) with the following constants was obtained: d_4^{20} 0.9441, n_D^{20} 1.4906, acid value 92.0, saponification value 117.5, iodine value (Wijs method) 173.9, unsaponifiable matter 44.06%.

Recrystallization of steryl acetate mixture.—The unsaponifiable matter of the acetone-soluble oil was separated by saponification of the oil with alcoholic potash followed by extraction of the diluted soap solution with ether. It was a reddish orange mixture of solid and liquid, and contained 43.5% of sterol (digitonide method). The unsaponifiable matter (72 g.) was recrystallized from 200 cc. of acetone under cooling, and the solid material (49 g.) obtained was refluxed with acetic anhydride. The acetylated product was then recrystallized from 200 cc. of acetone-ether, yielding 26.5 g. of crystalline solid (crude steryl acetate mixture). Further recrystallization of this material from acetone brought about a steady rise of the melting point and iodine value as shown in Table II.

Table II

Recrystallization of steryl acetate mixture

No. of recrystallization	Steryl acetate crystallized out		Steryl acetate recovered from mother liquor	
	Yield (g.)	m.p. (°C)	m.p. (°C)	I.V. by the perbenzoic acid method
2	19.5	141–147	110–117	—
4	14.0	145–151	132–134	—
6	8.5	159–165	142–145	71.2
8	5.0	168–172	153–158	89.5
11	2.8	178–179	167–168	—
12	2.5	182–183	171–173	99.6
13	2.2	182–183	173–175	

The fraction (A) obtained after 13 recrystallizations had $[\alpha]_D^{12} = -6.0°$*. A portion (0.67 g.) of this fraction was subjected to further recrystallizations by which the melting point, 182–183°C, was unaltered, but the melting point of the material recovered from the mother liquor of recrystallization was raised until finally 0.1 g. of a uniform steryl acetate of m.p. 182–183°, $[\alpha]_D^{18} = -5.8°$ and iodine value by the perbenzoic acid method 108.1 was obtained. The fraction (A) had saponification value 124.6 which agrees with the calculated value (123.4) for $C_{31}H_{50}O_2$, and its iodine value (106.9) by the perbenzoic acid method corresponded to 1.9 double bonds per molecule (I.V. calcd. for $C_{31}H_{50}O_2$, 111.6).

Hitodesterol and its derivatives.—Saponification of the fraction (A) gave free sterol which showed m.p. 167–168°C and $[\alpha]_D^{12} = -3.0°$ after recrystallization from acetone. Benzoate prepared from the free sterol by using benzoyl chloride and pyridine had m.p. 197–199°C, $[\alpha]_D^{11} = +3.8°$ and saponification value 109.2 (calcd. for $C_{38}H_{52}O_2$, 108.6) after recrystallization from acetone. 3,5-Dinitrobenzoate prepared from the free sterol was light yellow laminae of m.p. 195°C and $[\alpha]_D^{11} = \pm 0$.

11) Cf. Y. Toyama and T. Takagi, This Bulletin, **27**, 421 (1954).
12) T. Matsumoto and Y. Toyama, *J. Chem. Soc. Japan*, **65**, 310 (1944).
13) W. Bergmann and R. C. Ottke, *J. Org. Chem.*, **14**, 1085 (1949).
14) T. Matsumoto and Y. Toyama, *J. Chem. Soc. Japan*, **65**, 258 (1944).
15) Y. Toyama, T. Takagi and T. Tanaka, This Bulletin, **26**, 154 (1953).
16) Y. Toyama and T. Takagi, *J. Chem. Soc. Japan, Pure Chem. Sect.*, **75**, 1238 (1954).
17) Y. Toyama and T. Takagi, *J. Chem. Soc. Japan, Pure Chem. Sect.*, **76**, 237 (1955).

*) Optical rotations were measured with the samples dissolved in chloroform.

Calcd. for $C_{35}H_{50}N_2O_6$: N, 4.62%. Found: N, 4.45%.

The change of color developed in the Liebermann-Burchard reaction for the fraction (A) with the period of reaction is shown in Fig. 1 in which the absorption at 620 mμ is plotted against the period of reaction. The curve for hitodesteryl acetate is quite similar to the curve for a typical Δ^7-sterol.

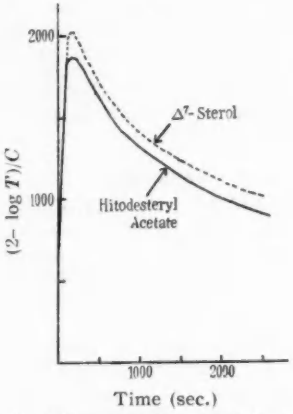

Fig. 1. Libermann-Burchard test for hitodesteryl acetate. T: Transmittance, C: Concentration (10^{-3} mole)

A solution of 0.1 g. of the fraction (A) was mixed with a solution of 0.3 g. of mercuric acetate in 10 cc. of glacial acetic acid, and the mixture was stirred for twelve hours. The product, after two recrystallizations from acetone, showed m.p. 168°C and $[\alpha]_D^{15}=+31.5°$. It exhibited an ultraviolet absorption in ethanol, as shown in Fig. 2, with the characteristic absorption maxima of $\Delta^{7,9(11)}$-sterol; $\log \varepsilon_{235}=4.02$, $\log \varepsilon_{243}=4.07$ and $\log \varepsilon_{250}=3.88$.

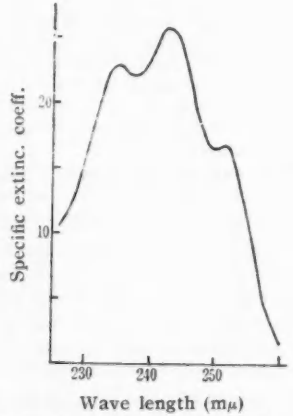

Fig. 2. Absorption curve of the conjugated product of hitodesteryl acetate.

Ozonolysis of hitodesteryl acetate and a fraction of lower melting point.—One g. of the fraction (A) was suspended in 20 cc. of glacial acetic acid, and a current of ozonized oxygen was passed through the suspension. After the suspension had become a clear solution, ozonization was continued for ten minutes more. One g. of zinc dust and a few drops of silver nitrate solution were then added, and the mixture was agitated for thirty minutes. Zinc was then removed by filtration. The liquid was diluted with water, and the solution was subjected to steam distillation. The distillate was collected in a trap containing 500 cc. of a 0.2% solution of 2,4-dinitrophenylhydrazine in 2 N hydrochloric acid. An orange yellow crystalline precipitate was formed in the trap, which was filtered after standing for twenty four hours. The precipitate (191 mg.) was dissolved in 10 cc. of chloroform, and the solution was passed through a 2 cm. x 22 cm. column of silica gel. The adsorption zone was then eluted with isohexane, yielding three eluates of 300 cc. each. Isohexane was distilled off from each eluate. The residues from the first, second and third eluates were 94 mg., 43 mg. and 15 mg. with m.p. 109–112°C, 108–111°C and 95–106°C, respectively. On recrystallizing the first and second fractions from ethanol, 118 mg. of orange yellow needles of m.p. 116–117°C and $[\alpha]_D^{14}=-4.6°$ were obtained. The melting point was unaltered by a further recrystallization. Its absorption curve in ethanol exhibited a maximum and a minimum characteristic to 2,4-dinitrophenylhydrazone of saturated aliphatic aldehyde as shown in Fig. 3 ($k_{350}=23.6$ and $k_{300}=1.6$).

Calcd. for $C_{13}H_{18}N_4O_4$: C, 53.05; H, 6.16; N, 19.04%. Calcd. for $C_{12}H_{16}N_4O_4$: C, 51.42; H, 5.76; N, 19.99%. Found: C, 53.03; H, 6.28; N, 18.48%.

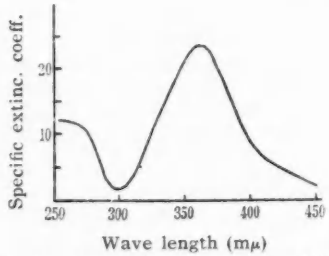

Fig. 3. Absorption curve of 2,4-dinitrophenylhydrazone.

Steryl acetate fractions, which were recovered from the mother liquors of recrystallizations in Table I and had melting points between 171°C and 175°C, were united. The united fraction (B), 0.7 g., was subjected to ozonolysis, and crystalline precipitates of 2,4-dinitrophenylhydrazone (90 mg.) were chromatographed in a similar way as described above, excepting that the adsorption zone was eluted first with isohexane and then with isohexane containing 1% of ether. The precipitates were thus separated into five fractions, the

fifth fraction being obtained by extraction of the silica gel with ethyl acetate. The first fraction (16 mg.) gave, on recrystallization from ethanol, orange yellow needles of m.p. 124–126°C. Calcd. for $C_{12}H_{16}N_4O_4$: N, 19.99%. Calcd. for $C_{12}H_{18}N_4O_4$: N, 19.04%. Found: N, 19.71%.

Recrystallization of the third, fourth and fifth fractions, 15 mg., 10 mg. and 25 mg., respectively, gave orange yellow needles of m.p. 115–116°C, 114–115°C and 114–115°C, respectively. These were united and once more recrystallized from ethanol giving orange yellow needles of m.p. 115–116°C. Calcd. for $C_{13}H_{18}N_4O_4$: N, 19.04%. Calcd. for $C_{12}H_{16}N_4O_4$: 19.99%. Found: N, 18.91%.

Summary

1. A fraction having m.p. 167–168°C and consisting mainly of hitodesteryl acetate was separated from the steryl acetate mixture of *Asterina pectinifera*. Hitodesterol was found to have an ethylenic linkage between C-7 and C-8. Among the products of ozonolysis of hitodesteryl acetate, *l*-ethylisopropylacetaldehyde was identified in the form of its 2,4-dinitrophenylhydrazone. Hence hitodesterol has been found to be a $\Delta^{7,22}$-sterol of the C_{29}-series and identical with α-spinasterol.

2. Among the products of ozonolysis of a lower melting steryl acetate fraction, the presence of a small amount of methylisopropylacetaldehyde besides ethylisopropylacetaldehyde was indicated. Hence it appears that a C_{28}-sterol having at least an ethylenic linkage between C-22 and C-23, possibly of $\Delta^{7,22}$-type, is also present in a lesser amount in the unsaturated sterol components of *Asterina pectinifera*.

Department of Applied Chemistry, Faculty of Engineering, Nagoya University, Nagoya

---

Studies on Dimethylglyoximato cobalt (III) Complexes. III. Direct Evidence for the Planar Coördination of Two Dimethylglyoximate Ions in Bis-(dimethylglyoximato)-cobalt (III) Complexes

By Akitsugu NAKAHARA

(Received April 16, 1955)

In the former papers[1),2)] the author discussed on the high stability of bis-(dimethylglyoximato)-cobalt (III) complexes. Then, an elucidation was suggested that the most important origin of the high stability is attributable to the O-H-O hydrogen bonds in the complex radical. However, the strong hydrogen bonds of this kind will be reasonably expected only when the two dimethylglyoximate ions coördinate to a cobalt atom with planar configuration. On the other hand, there has never been found any paper which dealt with the direct evidence for the planar coördination of two dimethylglyoximate ions in bis-(dimethylglyoximato)-cobalt (III) complexes. Thus, it seems to be desirable to afford not chemical but direct evidence for the above configuration. In this work, therefore, the author measured infrared absorption spectra of the so-called Feigl-Rubinstein's bis-(dimethylglyoximato)-cobalt (III)-derivative[3),4)] and the tris-(dimethylglyoximato)-cobalt (III)[1),5)], confirming the planar coördination of two dimethylglyoximate ions in the former compound.

Experimental

Materials

Hydrogen Dichloro-bis-(dimethylglyoximato)-cobaltate (III), (Feigl-Rubinstein's complex), $H[Co(DH^*)_2Cl_2]$[3),4)].— The method of Cambi et al.[4)] was applied in preparing the compound. To a concentrated aqueous solution of cobaltous acetate was added a slight excess of dimethylglyoxime, and the solution was oxidized by passing air through it. On adding concentrated hydrochloric acid, the compound was precipitated in dark green rhombs. It was recrystallized from aqueous solution by adding concentrated hydrochloric acid. For optical measurements the crystal had to be freed from accompanying moisture and hydrochloric acid.

Tris-(dimethylglyoximato)-cobalt (III), $[Co(DH)_3]$[1),5)].—The compound was prepared according to the previously described procedure[1),3)].

1) A. Nakahara, This Bulletin, **27**, 560 (1954).
2) A. Nakahara, This Bulletin, **28**, 207 (1955).
3) F. Feigl and H. Rubinstein, *Ann.*, **433**, 183 (1923).
4) L. Cambi and C. Coriselli, *Gazz. Chim. ital.*, **66**, 81 (1933).
5) A. Nakahara and R. Tsuchida, *J. Am. Chem. Soc.*, **76**, 3103 (1954).

* The following symbols are used: the ion of dimethylglyoxime (DH), $H_3CC(NO)C(NOH)CH_3$: the undissociated molecule of dimethylglyoxime (DH_2), $H_3CC(NOH)$-$C(NOH)CH_3$.

The pure product was heated on a water bath under reduced pressure in order to remove the water molecules of crystallization.

Dimethylglyoxime, DH_2.—The compound was recrystallized from 94%-ethanol, and dried in a vacuum desiccator over calcium chloride.

Measurements

The infrared absorption spectra were obtained with a Perkin-Elmer Model 21 Recording Spectrophotometer using sodium chloride prisms and a Nujol suspension of the compound in question.

Results

The results of the measurements are shown in Fig. 1 and Fig. 2. There is also inserted,

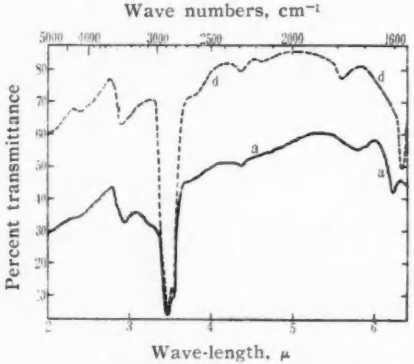

Fig. 1. Infrared absorption spectra of : (a), $H[Co(DH)_2Cl_2]$; (d), $[Ni(DH)_2]$.

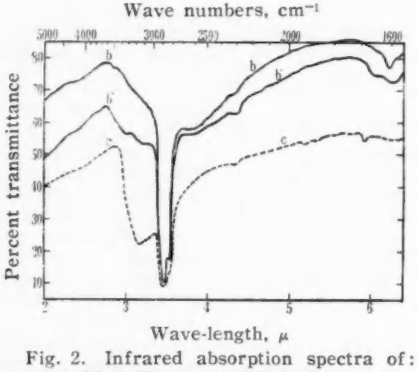

Fig. 2. Infrared absorption spectra of: (b), $[Co(DH)_3]$; (b'), $[Co(DH)_3]\cdot 2.5H_2O$; (c), Dimethylglyoxime.

in Fig. 1, the curve of bis-(dimethylglyoximato)-nickel (II), (d), which was obtained by Rundle and Parasol[6], for the purpose of comparison with the present results. As is clear from those Figures, the curve of bis-(dimethylglyoximato)-cobalt (III)-derivative, (a), is quite similar to that of the bis-(dimethylglyoximato)-nickel (II), (d). On the contrary, the curve of tris-(dimethylglyoximato)-cobalt (III), (b), differs to a considerable degree from those of (a) and (d). The difference between those two types of curves can be found, for instance, in the region from 3600 to 3300 cm^{-1} or from 1800 to 1670 cm^{-1}. Especially, the band found at 1725 cm^{-1} on the curve of (a) shows a very important meaning as discussed below.

Discussion

Recently Rundle and his co-workers[3,7,8] have presented trustworthy data concerning the crystal structure of bis-(dimethylglyoximato)-nickel (II).

According to their X-ray analysis, the complex molecule is planar and contains four five-membered rings as shown in Fig. 3. Of

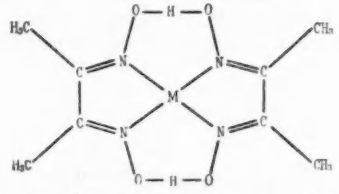

Fig. 3. The structure of planar bis-(dimethylglyoximato)-metal complex with O-H-O hydrogen bonds.

special interest was the very short O-H-O hydrogen bond, 2.44Å, shorter than any O-H-O hydrogen bond, heretofore reported. Furthermore, it was noteworthy that the O-H stretching frequency for this hydrogen bond is only 1775 cm^{-1}, about half the normal 3500 cm^{-1}, and that spectroscopic arguments have been presented indicating that the hydrogen lies symmetrically between the two oxygens in this case.

As can be seen in Fig. 1, the curve, (a), has a strong resemblance to the curve, (d), of the above bis-(dimethylglyoximato)-nickel (II) in the region from 5000 to 1670 cm^{-1}, suggesting the planar coördination of the two dimethylglyoximate ions about a cobalt atom in the bis-(dimethylglyoximato)-cobalt (III)-complex. This interpretation is supported by the fact that the curve, (b), of tris-(dimethylglyoximato)-cobalt (III) in which the planar coördination of two dimethylglyoximate ions could not be expected differs to a considerable extent from those of (a) and (d). In addition to that, the O-H stretching frequency for the above hydrogen bond can be found on (a) at 1725 cm^{-1}, and not on (b). This is

6) R. E. Rundle and M. Parasol, *J. Chem. Phys.*, **20**, 1487 (1952).
7) L. E. Godycki, R. E. Rundle, R. C. Voter and C. V. Banks, ibid., **19**, 1205 (1951).
8) L. E. Godycki and R. E. Rundle, *Acta Cryst.*, **6**, 487 (1953).

the direct evidence for the planar coördination of the two dimethylglyoximateions in the bis-(dimethylglyoximato)-cobalt(III)-derivative, since the existence of such a kind of hydrogen bond as described above could not be expected with any other configuration except the planar coördination. The appearance of the O-H stretching band on the curve, (a), is, however, somewhat broad and shifted a little towards a longer wave-length compared with the case of nickel (II)-complex, (d). This may be perfectly understandable by taking into consideration the action of an additional proton which is contained only in the Feigl-Rubinstein's bis-(dimethylglyoximato)-cobalt(III)-complex, $H^{*}[Co(DH)_2Cl_2]$, and not in the bis-(dimethylglyoximato)-nickel (II). It coincides also with Rundle's opinin[9] that there are indications that very broad bands, characteristic of strong hydrogen bonds, become sharper as the O-H-O bond becomes symmetric. But the difference between the ionic radii of nickelous- and cobaltic-ion may be also concerned with the above facts. At any rate, it can be said that the O-H-O hydrogen bond in bis-(dimethylglyoximato)-cobalt(III)-complexes has been proved to be the same kind of the nature as established in the bis-(dimethylglyoximato)-nickel(II).

Rundle and Parasol[5] have also discussed the relation between the bond length and the stretching frequency for O-H-O hydrogen bonds. If it be applied their investigation to the present O-H stretching frequency, 1725 cm^{-1}, the bond length of below 2.5 Å a very short hydrogen bond, will be forecasted.

As is seen in Fig. 1 and Fig. 2, some other differences between the curves of bis- and tris-(dimethylglyoximato)-complex can be also found. But the assignments of those bands are very difficult without more detailed research. The author is, at present, investigating the fruits which are obtained by the substitution of deuterium for hydrogen atom concerned with the above O-H-O hydrogen bond[9].

* Although the hydrogen atom has been written conventionally as the external cation of the comeplex anion, it is highly probable that the real structure of the complex should be considered to be "dichloro-dimethylglyoximato-dimethylglyoxime-cobalt (III)" molecule, $[Co(DH_2)(DH)Cl_2]$. If this proves to be the case, it seems to be most probable that the proton attaches to an oxygen atom.

9) To be submitted later.

Summary

Infrared absorption spectra of bis- and tris-(dimethylglyoximato)-cobalt(III)-complex were measured. Some discussions concerning the O-H stretching band of the former complex were given, and they reached the conclusion that the band at 1725 cm^{-1} corresponds to the band at 1775 cm^{-1} of the bis-(dimethylglyoximato)nickel (II) and is characteristic of the planar bis-(dimethylglyoximato)-complexes.

The author wishes to thank Professor R. Tsuchida for his kind guidance and encouragement throughout this work. Appreciation is also expressed to Mr. J. Fujita for his helpful discussions.

This work was supported in part by a grant from the Ministry of Education.

Department of Chemistry, Faculty of Science, Osaka University, Osaka

---

Magnetochemical Study of Violanthrene-iodine System

By Yoshio MATSUNAGA

(Received April 23, 1955)

Introduction

As reported in the preceding paper[1], it has been found that polycyclic aromatic hydrocarbons form molecular complexes with bromine or iodine, and these complexes behave as typical semiconductors with high conductivity. For instance, the electrical resistivity of perylene-bromine complex is as low as several ohm-cm. at room temperature with the energy gap for conductivity of 0.13 e.v., and that of violanthrene-iodine complex is about 40 ohm-cm. with the energy gap of 0.15 e.V.

In connection with the investigation for the electrical conductivity of these molecular

1) H. Akamatu, H. Inokuchi and Y. Matsunaga, *Nature*, **173**, 168 (1954), see also This Bulletin to be published.

complexes, we have studied the magnetic susceptibility of violanthrene-iodine complex as a function of iodine concentration in it. Included also are the following complexes, benzanthrone-bromine, perylene-bromine, perylene-iodine, and violanthrene-bromine.

Experimental

Materials

Benzanthrone-bromine.—Brass and Clar prepared this complex by addition of bromine to benzene solution of benzanthrone[2], but our sample was prepared by direct absorption of bromine vapor to a known quantity of crystalline powder of benzanthrone. The complex containing excess bromine was left in a desiccator, and its weight was measured from time to time. The change of composition with time shows that a complex is formed containing one molecule of benzanthrone and one atom of bromine (cf. Fig. 1). This result agrees well with that reported by Brass and Clar, though we prepared it by a different method.

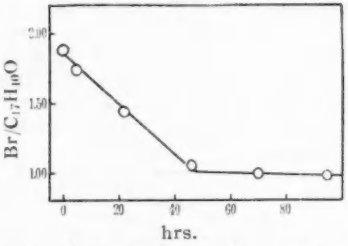

Fig. 1. Change of bromine content of benzanthrone-bromine complex by preservation in a desiccator.

Perylene-bromine.—The sample used in this study was prepared by direct absorption of bromine vapor[3]. The complex containing excess bromine was left over potassium hydroxide in a desiccator for a week. Therefore, the sample may be dibromoperylene-bromine complex with a little amount of free dibromoperylene[1].

Perylene-iodine.—This complex was prepared by addition of iodine to benzene solution of perylene[4]. To determine the composition of complex, we dissolved its known quantity in benzene, added potassium iodide and water, and titrated the liberated iodine with the standard solution of sodium thiosulfate.

Violanthrene-bromine.—This complex was also prepared by absorption of bromine vapor, and left in a desiccator until the change of weight due to the decomposition became so small that we could ignore it during the time required for the magnetic measurement. We have not yet prepared the complex which can be considered to have a definite composition. However, it is sure that a part of bromine which combines with violanthrene is used for substitution and the other part for the formation of molecular complex.

2) K. Brass and E. Clar, *Ber.*, **69**, 690 (1936).
3) A. Zinke and A. Pongratz, ibid., **69**, 1591 (1936).
4) K. Brass and E. Clar, ibid., **65**, 1660 (1932).

Violanthrene-iodine.—The crystalline powder of violanthrene was treated with benzene solution of iodine for some minutes at boiling point, or with carbon tetrachloride solution for a few days at room temperature. The precipitated complex was filtered and dried in vacuo at room temperature. The samples which have varied compositions were obtained by the change of iodine concentration of solution. Solubility of violanthrene and its complex to cold benzene and carbon tetrachloride is very small, so that in the calculation of its composition, we can leave out of consideration the loss of violanthrene during this treatment.

Magnetic measurement

The susceptibilities were measured using a Gouy balance as previously described[5]. The field was calibrated at two current strengths with distilled water. Fields of about 16 and 23 kilo-oersteds were used, and each sample was measured in two field strengths to detect any ferromagnetic impurities. The samples which exhibited field strength dependence of susceptibility were discarded.

Taking water as the standand substance (-0.720×10^{-6}), the susceptibility of a sample per gram (χ) is calculated by

$$-\chi\cdot10^{6}=0.749\times\frac{V}{M}\times\frac{F}{F_0}-\frac{0.029}{D}\qquad\text{(at 20°C)}$$

where F_0 and F are the resultant forces on water and the sample in g., respectively, V is the volume of water in cc. and the same volume is occupied by M g. of the sample, and D is the true density of the sample.

Results

The hydrocarbons and complexes under consideration together with the experimental molar susceptibilities are given in Table I

TABLE I

MOLAR SUSCEPTIBILITIES OF SOME MOLECULAR COMPLEXES AND RELATED COMPOUNDS

Substance	Formula	Molar suscept. ($-\chi_M\times10^6$) observed	estimated
benzanthrone	(1)	143	
benzanthrone-0.97 Br.		171	173
perylene	(2)	167	
dibromoperylene	(3)	216	215
perylene-3.87 Br.		62	286
perylene-2.67 I.		210	286
violanthrene	(4)	304*	
violanthrene-4.36 Br.		180	437
violanthrene-4.00 I.		308	482
bromine (1/2 Br_2 or Br)**		30.6	(Pascal's constants)
iodine (1/2 I_2 or I)**		44.6	(Pascal's constants)

* The previously reported value is 273, the new datum may be more correct.

** The constant for halogen is half the molar susceptibility.

5) H. Akamatu and Y. Matsunaga, This Bulletin, **26**, 364 (1953).

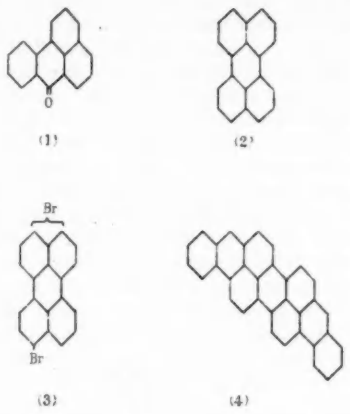

columns one and two. The molar susceptibilities of complexes estimated from the measurements on hydrocarbons and Pascal's constants for halogens by direct application of the additivity law are given in column three.

The experimental molar susceptibilities of benzanthrone-bromine complex and dibromoperylene are in accordance with the estimated ones within the errors of the experiments and the estimations. But, in the others, the estimated values are all in serious disagreement with the experimental ones.

Most of complexes which show such a large discrepancy are not stable, bromine complexes change spontaneously to brominated hydrocarbons evolving hydrogen bromide, and perylene-iodine complex loses iodine slowly and leaves the original hydrocarbon. Only violanthrene-iodine complex is so stable that we have no need to consider the change of composition with time. In Fig. 2, its susceptibility per gram is plotted against the concentration of iodine varied from 0 to 67.1 per cent in twelve steps. The dotted line shows the calculated susceptibility derived by the additivity law, and the susceptibility of iodine (-0.36×10^{-6}) is taken from "International Critical Tables"[6]. The actual susceptibility decreases lineary as a function of iodine concentration, but deviates remarkably from the dotted line. When iodine concentration exceeds 55 per cent, the susceptibility increases very slowly and approaches that of pure iodine. The maximum deviation amounting to over 35 per cent occurs at 55 per cent iodine, suggests that a complex is formed containing one molecule of violanthrene and two of iodine. The molecular complex which has this composition will show the most typical properties of this two-component system. If we assume merely the existence of the compound which has the above mentioned concentration of iodine, the linearity of susceptibility-composition curve below and above 55 per cent iodine will be explained. The linearity, whilst consistent with the assumption, can not be regarded as the evidence for non-existence of other complexes in this two-component system.

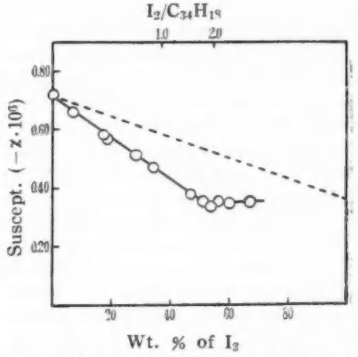

Fig. 2. Magnetic susceptibility of violanthrene-iodine complex as a function of iodine concentration.

Discussion

It is apparent that benzanthrone-bromine complex and the other complexes shown in Table I belong to different types of molecular complexes from each other. In the former case, the susceptibility follows the additivity law strictly, although stoichiometrical formula of this complex $C_{17}H_{10}O\cdot Br$ suggests the existence of unpaired electron, as Brass and Clar named these complexes "unpaarige Halogenide"[2,4]. For this reason, benzanthrone-bromine complex should be represented by doubled formula. The same conclusion had already been obtained by Müller and Wiesemann within the limits of their rather large experimental errors[7]. Schwab and Schwab-Agallidis applied the ortho-para conversion of hydrogen, and concluded also that this compound was not a radical[8].

On the other hand, the complexes between perylene or violanthrene and halogens, which are colored almost black and show surprisingly high electrical conductivities, are also very anomalous in magnetic behavior. In view of the peculiar and characteristic change of these properties, there can be little doubt

6) International Critical Tables, vol. 6, p. 355.

7) E. Müller and W. Wiesemann, *Ber.*, **69**, 2173 (1936).

8) G. M. Schwab and E. Schwab-Agallidis, *Z. physik. Chem.*, B, **49**, 196 (1941).

that in their complexes, hydrocarbons and halogens are present with very large changes in their electronic states. Dibromoperylene does not show such anomalies, and we can analyse perylene-iodine complex by titration with standard solution of sodium thiosulfate, so in these complexes, there is no doubt that halogens are not substituted in aromatic nuclei.

The decrease of molar susceptibility in these complexes is not explainable by the localization of π-electrons which have large orbital radii in aromatic molecules, as the contribution of these electrons to the susceptibilities of original hydrocarbons are no more than -65×10^{-6} in perylene and -137×10^{-6} in violanthrene. Therefore, these large decreases must be attributed to the occurrence of constituents or complex as a whole in the paramagnetic state, such as atomic halogen, hydrocarbon positive ion, triplet state or free electrons.

To make further examination of magnetic state, we estimate the depression of diamagnetism at the apparent composition containing one molecule of hydrocarbon and four atoms of halogen in each complex from the data shown in Table I, assuming that perylene-bromine, perylene-iodine and violanthrene-bromine behave like violanthrene-iodine in the susceptibility-composition curve. This assumption is not improbable in perylene-bromine and perylene-iodine, as the composition of the former complex is $C_{20}H_{12}\cdot2Br_2$ or $C_{20}H_{10}Br_2\cdot Br_2$ as described in the previous paper and that of the latter complex reported by Pestemer and Treiber is $C_{20}H_{12}\cdot2I_2$[9]. Violanthrene-bromine complex shown in Table I contains more halogen compared to the standard composition, so that the required value may be equal to the observed decrease. The estimated depressions are shown in Table II. In this Table, we regarded perylene-bromine complex as pure dibromoperylene-bromine complex, so the depression was estimated for $C_{20}H_{10}Br_2\cdot Br_2$.

TABLE II

THE ESTIMATED DEPRESSION OF MOLAR SUSCEPTIBILITY OF COMPLEX AT THE APPARENT COMPOSITION OF ArH-4X

Substance	Estimated depression of molar suscept.
perylene-bromine	240×10^{-6}
perylene-iodine	110×10^{-6}
violanthrene-bromine	260×10^{-6}
violanthrene-iodine	170×10^{-6}

We can find from Table II that bromine is more effective to the depression of diamagnetism than iodine, and violanthrene is affected more than perylene by these two halogens. Consequently, it is not probable that the occurrence of paramagnetism is due to the dissociation of halogen molecule, as the bond energy of bromine is larger than that of iodine, and if so, iodine should be more effective. The order of depression of diamagnetism is not compatible with that of the electronegativity of halogen and besides probably with that of the ionization potential of aromatic molecule. The partial ionization of constituents may be sufficient to explain the above data. But this explanation is inconsistent with the data on the electronic conduction described in the previous paper.

Nowadays, it is well known that aromatic hydrocarbons as benzene[10], naphthalene[11], and phenanthrene[12] form complexes with halogens. The bonding power in these complexes is named by Mulliken as "intermolecular charge-transfer force"[13]. He showed also that the theory predicts the possibility of highly intense absorption even for very loose complexes. Benzene, naphthalene and their derivatives form only loose complexes in solutions, so that the charge-transfer may be limited in one complex molecule. If the complex molecules are packed together closely as in our solid complexes, the charge-transfer will not be limited in one complex molecule, but spread out more widely and strongly. In such a case, the complexes have to be extremely deeply colored and show very intense absorption. The occurrence of the excited form with unpaired electrons by thermal excitation may be plausible. The order of difference between observed and estimated molar susceptibilities seems to be consistent with this theory We are not yet ready to state whether the electrical conductivity is explainable by triplet state or not, but we can conclude confidently that the excited state relates to the electrical conductivity of these complexes from its temperature dependence.

If we assume that the difference between observed and estimated molar susceptibilities is equal to the paramagnetic contribution of unpaired electrons and all unpaired electrons behave as free electrons, the excitation energy 0.17 e.V. for violanthrene-iodine complex ($C_{34}H_{18}\cdot2I_2$) is anticipated from it[14].

9) M. Pestemer and E. Treiber, *Ber.*, **74**, 964 (1941).

10) H. A. Benesi and J. H. Hildebrand, *J. Am. Chem. Soc.*, **71**, 2703 (1949).

11) N. W. Blake, H. Winston and J. A. Putterson, ibid., **73**, 4437 (1951).

12) L. J. Andrews and R. M. Keefer, ibid., **74**, 4500 (1952).

13) R. S. Mulliken, ibid., **74**, 811 (1952), *J. Phys. Chem.*, **56**, 801 (1952).

14) Assuming that the paramagnetic contribution of one mole of free electron is equal to 1270×10^{-6}, the relation between the depression of molar susceptibility ($\Delta\chi_M$ and the excitation energy ($\Delta\varepsilon$) is approximated by $\Delta\chi_M 2\times1270\times10^{-6}=2\cdot\exp(-\Delta\varepsilon/2kT)$.

This is in good accordance with that obtained from the temperature dependence of electrical conductivity.

Bhatnagar and Lakra[15], and Rao and Govindarajan[16] studied the magnetic susceptibility of benzene solution of iodine. Both of them found that the susceptibility of solution is more diamagnetic than expected from the additivity law. The apparent susceptibility per gram of iodine reported by the former investigators is -0.51×10^{-6}. This increase of apparent susceptibility is not inconsistent with the above explanation, as, in this case, the interaction between complex molecules may be negligibly small and the charge-transfer in a complex molecule will bring about only the expansion of the orbital radii of π-electrons, namely, the increase of diamagnetism, and not the occurrence of a paramagnetic state.

If we take into consideration the expansion of the orbital radii of π-electrons in our complexes, the contribution of paramagnetism to molar susceptibility will increase and the excitation energy will decrease to a little extent. For example, if we take the apparent susceptibility of iodine in violanthrene-iodine complex for -0.60×10^{-6}, calculated from the apparent susceptibility in benzene solution and the formation constant of benzene-iodine complex[10], assuming that the susceptibility of iodine not tied up as complex is equal to -0.36×10^{-6}, the magnitude of paramagnetism will be 300×10^{-6}, and the excitation energy 0.15 e.V. The agreement between the final estimated value of excitation energy and that obtained from the temperature dependence of electrical conductivity is surprisingly good.

15) S. S. Bhatnagar and C. L. Lakra, *Indian J. Phys.*, 8, 43 (1933).
16) S. R. Rao and S. R. Govindarajan, *Proc. Indian Acad., Sci.*, 15, A. 35, (1942).

Summary

The magnetic susceptibility of violanthrene-iodine complex was measured as a function of iodine concentration. This complex shows the large discrepancy between the observed susceptibility and the estimated one which was derived by direct application of the additivity law. Perylene-bromine, perylene-iodine, and violanthrene-bromine show a similar behavior also. The susceptibility-composition curve in violanthrene-iodine system suggests the existence of molecular complex containing one molecule of violanthrene and two of iodine. At that composition, the discrepancy exceeds 35 per cent. This depression of diamagnetism is so large that we can not explain it by the localization of π-electrons in aromatic molecule. The occurrence of paramagnetic state is taken into consideration, and the nature of this state is discussed. The large difference between observed and estimated susceptibilities is attributed to the partial cancellation of diamagnetism by the paramagnetic contribution of free electrons produced by the intermolecular charge-transfer force which spreads out widely and strongly in this solid complex.

The author expresses his hearty thanks to Prof H. Akamatu for his kind direction of this study. The cost of this research has been defrayed from the Grant in Aid for Fundamental Scientific Research from the Ministry of Education, to which the author's thanks are due.

Department of Chemistry,
Faculty of Science,
Tokyo University,
Tokyo

The Selenium Dioxide Oxidation of Substituted Acetophenones

By Tadashi SATO and Masaki OHTA

(Received April 26, 1955)

It is widely known that the methyl group adjacent to the carbonyl group can conveniently be oxidized to aldehyde group by selenium dioxide. In this way many arylglyoxals (I) have been obtained from substituted acetophenones (II).

$$\underset{\text{(I)}}{ArCOCHO} \qquad \underset{\text{(II)}}{ArCOCH_3}$$

As we came to the need of *o*-nitro- and *o*-acetamino-phenylglyoxal for further synthesis in our study, we carried out the oxidation of *o*-nitro- and *o*-acetamino-acetophenone. It has been reported[1] that the oxidation of *p*-nitro- and *p*-acetamino-acetophenone gives corresponding phenylglyoxal derivatives. We found, however, that the oxidation of the *o*-acetaminoacetophenon did not give *o*-acetaminophenylglyoxal, while that of *o*-nitroacetophenone gave *o*-nitrophenylglyoxal. In the case of the oxidation of *o*-acetaminoacetophenon, its methyl group was oxidized to the carboxylic group, and the product was a mixture of almost equal amount of *o*-acetaminophenylglyoxylic acid (III) and isatin (IV). The presence of (IV) is considered to be the result of deacetylation of (III) and ensuing cyclization. Isatin was, in fact, formed by heating (III) in 10% hydrochloric acid.

(III) reacted with 2,4-dinitrophenylhydrazine, semicarbazide, and thiosemicarbazide to give crystalline products. But they were not the ordinary condensation products (V) at all, though their structures have not been confirmed here.

o-Nitrophenylglyoxal was also identified by analysis, of its 2,4-dinitrophenylhydrazone and thiosemicarbazone.

o-Nitrophenylglyoxal gave the condensation product, *o*-nitrobenzoylacrylic acid (VI), on treatment with malonic acid in acetic acid solution containing a small amount of sulfuric acid, while in pyridine solution, only a small amount of crystals could be obtained, which melted at 233–4°, and had the empirical formula of $C_{15}H_{10}N_2O_5$.

Experimental

***o*-Nitrophenylglyoxal.**—Fourteen grams of selenium dioxide were dissolved in the mixture of 70 cc. of dioxane and 3 cc. of water with heating. To this warm solution, 19 g. of *o*-nitroacetophenone was added at one time and refluxed for seven hours with constant stirring. After the metallic selenium was filtered off, the most part of dioxane was evaporated, water was added and extracted with ether. After drying over anhydrous sodium salfate, ether was evaporated. From the residue a deep yellow oil distilled at 124-4.5° at a pressure of 3.5 mmHg, yield 13 g. Found: N, 8.24. Calculated for $C_8H_5NO_4$: N, 7.82%.

***o*-Nitrophenylglyoxal thiosemicarbazone.**—The thiosemicarbazone was prepared from *o*-nitrophenylglyoxal (1 g.) and thiosemicarbazide (0.6 g) in dilute ethanol by refluxing for one hour. Recrystallization from ethanol gave light needles, m.p. 172°. Found: N, 22.11. Calculated for $C_9H_8N_4O_3S$: N, 22.2%.

1) C. Musante et al., *Gazz. Chim. Ital.*, **81**. 451 (1951). C. A. **46**, 5549 (1952).

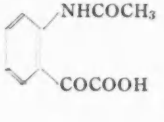

(III)

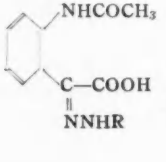

(V)

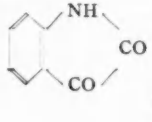

(IV)

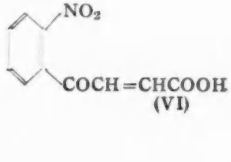

(VI)

o-Nitrophenylglyoxal 2,4-dinitrophenylhydrazone.—Small amounts of *o*-nitrophenylglyoxal and 2,4-dinitrophenylhydrazine were heated in ethanol for thirty minutes. Upon recrystallization from ethanol, this hydrazone melted at 186–8°. Found: N, 19.82. Calculated for $C_{14}H_9N_5O_7$: N, 19.6%.

The oxidation of *o*-acetaminoacetophenone.—Thirty five grams of *o*-acetaminoacetophenone were oxidized with 22 g. of selenium dioxide in dilute dioxane (120 cc. of dioxane and 4 cc. of water) and extracted with ether in the same way as described above in the case of *o*-nitro derivative. After evaporating ether, a red oily substance remained which soon solidified. This was washed with benzene and added to the aqueous sodium carbonate solution. The insoluble substance was filtered (filtrate A), washed with water and recrystallized from acetone-benzene. The red needles of isatin were obtained., m.p. 200°C. Found: C, 64.88; H, 3.51; N, 10.16. Calculated for $C_8H_5NO_2$: C, 65.3; H, 3.40; N, 9.54%. Filtrate A, when acidfied with hydrochloric acid, gave white crystals. Recrystallization from water gave white needles of *o*-acetaminophenylglyoxylic acid, m.p. 162°C. Found: N, 7.09. Calculated for $C_{10}H_9NO_4$: N, 7.78%.

The change of *o*-acetaminophenylglyoxylic acid into isatin.—*o*-Acetaminophenylglyoxylic acid, when heated with 10% hydrochloric acid, went gradually into solution. The hot solution was filtered off from a small amount of insoluble matter and cooled. Red needles were obtained. The mixed melting point with isatin showed no depression.

The reaction of *o*-nitrophenylglyoxal with malonic acid.—To a solution of 12 g. of *o*-nitrophenylglyoxal in 24 cc. of gracial acetic acid, 10 g. of malonic acid and 5 drops of concentrated sulfuric acid were added. The mixture was heated at 70°C for thirty minutes and then refluxed for ten minutes, water was then added and extracted several times with saturated sodium carbonate solution. The acidification of the combined water layer with hydrochloric acid gave white crystal accompanied by resinous matter. This was washed with dilute ethanol and recrystallized from dilute ethanol, yield 3 g., m.p. 170°C. Found: C, 53.85; H, 3.48; N, 6.27. Calculated for $C_{10}H_7NO_5$: C, 54.3; H, 3.16; N, 6.33%.

Laboratory of Organic Chemistry,
Tokyo Institute of Technology

The Estimation of the Thioethoxyl Group of a Sugar Diethylmercaptal

By Susumu HIRASE and Choji ARAKI

(Received April 26, 1955)

In the course of our investigation on the mercaptolysis[1,2] of a polysaccharide, it has become necessary to estimate the thioethoxyl group of a sugar diethylmercaptal. This group has been usually estimated by the conversion to a sulfate group by the nitric acid oxidation according to the Carius' method. But the Carius' method is somewhat time-consuming, and in addition, it can not be applied to the mercaptolysates of such polysaccharides as those of sea weeds, which contain the sulfate group in their molecules. The present paper offers a convenient method, by which the direct estimation of the thioethoxyl group of a sugar diethylmercaptal and its acetylated and methylated derivatives has been made without any possibility of the interference of the originally present sulfate group.

The method involves the acid hydrolysis[3] of the mercaptal followed by the distillation and the subsequent iodometrical titration of the liberated ethylmercaptan, as shown by the equations (1) and (2)[4].

$$R-CH(SC_2H_5)_2+H_2O=R-CHO+2C_2H_5SH \quad (1)$$

$$2C_2H_5SH+I_2=C_2H_5-S-S-C_2H_5+2HI \quad (2)$$

Experimental

Materials.—Sugar diethylmercaptals and their derivatives used in this study were prepared according to original papers. Melting point or boiling point of each compound used is included in Tables I and II.

1) C. Araki and S. Hirase, This Bulletin, **26**, 463 (1953).
2) S. Hirase and C. Araki, This Bulletin, **27**, 109 (1954).
3) E. Fischer, *Ber.*, **27**, 673 (1894).
4) P. Klason and J. Carlson, *Ber.*, **39**, 738 (1906); J. W. Kimball, R. L. Kramer and E. E. Reid. *J. Am. Chem. Soc.*, **43**, 1199 (1921).

Apparatus and General Procedure.—The apparatus (Fig. 1) was essentially the same as that used for the estimation of the ordinary methoxyl or ethoxyl group. The trap (B) was charged with distilled water (about 20 cc.), to keep

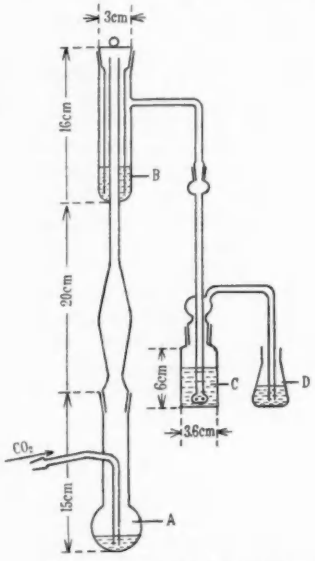

Fig. 1. The apparatus for the thioethoxyl estimation.

any hydrolysing agent from getting into the receiver. The receiver (C) and the sub-receiver (D), in which the reaction shown by the equation (2) occurred, were charged with an excess 0.1N-potassium iodide-iodine solution (20 cc. and 5 cc., respectively), and equal volumes of ethanol were respectively added to each receiver to increase the solubility of ethylmercaptan. An exactly weighed sample (0.1~0.2 g.) to be analysed was placed in the reaction flask (A), and hydrolysing agent, aqueous N-hydrochloric acid (10 cc.) was added.

Then the apparatus was immediately assembled as shown in Fig. 1, all ground joints being moistened with distilled water. A slow stream of carbon dioxide free from any hydrogen sulfide was bubbled through the solution at a rate of about two bubbles a second. The reaction flask was gradually heated in a glycerol bath during thirty minutes to a gentle boiling (bath temperature 115~120°C). After keeping a gentle boiling for two hours, the excess iodine remaining in the receiver and the sub-receiver was individually titrated with a 0.1N-sodium thiosulfite solution without using a starch indicator, which is no use in the high concentration of ethanol. In most cases ethylmercaptan was perfectly absorbed in the receiver C. The quantity of the thioethoxyl group was calculated from the iodine consumed: SC_2H_5 g. = 0.06113 × 0.1N-I_2 cc. consumed.

Results

Sugar Diethylmercaptals.—The analysis of several sugar diethylmercaptals, carried out by the above method, gave satisfactory results as shown in Table I. Considerable lite-

TABLE I

THE ESTIMATION OF THIOETHOXYL GROUPS OF SUGAR DIETHYLMERCAPTAL

Diethylmercaptal of	Sample g.	0.1N-I_2 cc. consumed	SC_2H_5% found	Error
D-Galactose[3]	0.1394	9.75	42.75	+0.06
[141~143°]	0.1384	9.71	42.89	+0.20
	0.1293	9.07	42.88	+0.19
D-Glucose[3]	0.1471	10.30	42.80	+0.11
[127~128°]	0.1246	8.70	42.68	−0.01
	0.1247	8.73	42.79	+0.10
D-Mannose[3]	0.1207	8.42	42.64	−0.05
[131~133°]	0.1776	12.32	42.41	−0.28
	0.1338	9.31	42.53	−0.16
L-Arabinose[3]	0.1377	10.69	47.46	−0.18
[124~126°]	0.1165	9.10	47.75	+0.11
	0.1300	10.10	47.49	−0.15
L-Rhamnose[3]	0.1173	8.68	45.23	+0.02
[135~137°]	0.1184	8.80	45.43	+0.22
	0.1421	10.57	45.47	+0.26
3,6-Anhydro-	0.1557	11.65	45.74	+0.19
L-galactose[1]	0.1046	7.83	45.76	+0.21
[110~111°]	0.1378	10.29	45.65	+0.10
Agarobiose[2]	0.1234	5.75	28.49	+0.09
[171~172°]	0.1517	7.01	28.25	−0.14
	0.1524	7.04	28.24	−0.15

[ ]: m.p. of the sample used for the analysis.

rature[5] has recorded the difficult hydrolytic cleavage of the carbon-sulfur bonds of mercaptals. This may be due to the incomplete elimination of the liberated ethylmercaptan by distillation[5].

Acetylated and Methylated Sugar Diethylmercaptals.—Pentaacetyl and pentamethyl D-galactose diethylmercaptal were tentatively analysed by the same method as above mentioned, but analytical figures obtained were 14.7% and 30.6% (theoretical values 24.6% and 34.3%) respectively. This may be attributed to the low solubility of the sample in the hydrolysing agent, and to the resistance of

5) E. Stuffer, *Ber.*, 23, 3241 (1890); E. Fisher and K. Delbrück, *Ber.*, 42, 1476 (1909); W. Schneider, J. Sepp and O. Stiehler, *Ber.*, 51, 220 (1918); E. Pacsu, *Ber.*, 58, 509 (1925).

6) D. S. Tarbell and D. P. Harnish, *Chem., Rev.*, 49, 1~90 (1951).

TABLE II

THE ESTIMATION OF THIOETHOXYL GROUPS OF FULLY ACETYLATED AND METHYLATED SUGAR DIETHYLMERCAPTALS

Diethylmercaptal of	Sample g.	0.1N-I_2 cc. consumed	SC_2H_5% found	Error
Pentaacetyl	0.1404	5.63	24.51	−0.10
D-galactose[7]	0.1505	6.01	24.41	−0.20
[77～79°]	0.1446	5.80	24.53	−0.10
Pentaacetyl	0.1326	5.30	24.45	−0.16
D-glucose[8]	0.1148	4.61	24.55	−0.06
[46～48°]	0.1774	7.07	24.36	−0.25
Tetraacetyl	0.1324	6.18	28.53	−0.26
L-arabinose[9]	0.1608	7.54	28.66	−0.13
[78～80°]	0.1473	6.89	28.59	−0.20
Pentamethyl	0.2022	11.30	34.16	−0.11
D-galactose[10]	0.1591	8.93	34.31	+0.04
(175～180°/4mm.)	0.1187	6.62	34.09	−0.18
Pentamethyl	0.1368	7.65	34.18	−0.09
D-glucose[10]	0.1421	7.95	34.20	−0.07
(175～180°/4mm.)	0.1244	6.94	34.10	−0.17
Hexaacetyl	0.1258	3.71	18.03	+0.09
agarobiose[2]	0.1456	4.42	18.01	+0.07
[101～103.5°]	0.1361	4.04	18.15	+0.21

[ ]: m.p., ( ): b.p. of the sample used for the analysis.

7) M. L. Wolfrom, *J. Am. Chem. Soc.*, **52**, 2464 (1930).
8) M. L. Wolfrom, *J. Am. Chem. Soc.*, **51**, 2188 (1929).
9) M. L. Wolfrom and M. R. Newlin, *J. Am. Chem. Soc.*, **52**, 3619 (1930).
10) P. A. Levene and G. M. Meyer, *J. Biol. Chem.*, **69**, 175 (1926).

the sample against hydrolysis. These difficulties, however, have been overcome by putting glacial acetic acid (2 cc.) into the hydrolysing agent to increase the solubility and prolonging the heating period up to four hours. The analysis by this modified method gave good results as shown in Table II.

Institute of Chemistry, Faculty of Industrial Arts, Kyoto Technical University, Matsugasaki, Kyoto

On the Color-reactions of the Condensed Polycyclic Aromatic Hydrocarbons and their Related Quinones in the Solutions of the Concentrated Sulfuric Acid

By Takashi HANDA

(Received April, 12, 1955)

Introduction

The condensed polycyclic aromatic hydrocarbons and their related quinones develop deep beautiful color from yellow to green in the concentrated sulfuric acid. It is understood that these reactions are ascribed to the interaction between the π-electrons of these compounds and the protons in the sulfuric acid, and with the under-standing that these reactions are those of the so-called "between acids and bases" in the sense of Brönsted, the basicity of these compound is evaluated in terms of Hammett's pK_B-values by varying the acidity of the sulfuric acid, and measuring the adsorption-spectrum of these compounds at various concentrations of the acid after the method of L. P. Hammett, with the assumption that the equilibria are obtained between bases and their complexes with protons in the sulfuric acid.

Experimental

The measurement of the absorption-spectra was done with Beckmanntype spectrophotometer, with quartz-cell of which dimensions were 1.0×1.0×3.0 cm^3, at room temperature. The evaluation of pK-value was done after the method of L. P. Hammett[1], and reasonably the same result was obtained with anthraquinone, of which value was described on the Table V. On this account, this method of measurement is extended to the longer side of the visible region of spectrum, although, owing to the low dispersion of spectrum in this region, the accuracy of the measurement was not so good. The concentrated sulfuric acid used in this measurement was the commercially chemical pure product, not having any traces of peroxides, or nitric acid, or any impurities in the visible region of spectrum in which the measurement had been carried out. The specimens used in this measurement were as follows: perinaphthoindenone (I), benzoanthrone (II), *p*-naphthoquinone (III), anthraquinone (IV), naphthacene-

1) Leo. A. Flexser, Louis P. Hammett and Andrew Dingwall, *J. Am. Chem Soc.*, **57**, 2103 (1935).

buinone (V), mesonaphthodianthrone (VI), 3, 10-perylenequinone (VII), 1, 2-benzoperylene-3, 10-quinone, (VIII), helianthrone (IX), 1, 2, 7, 8-dibenzoperylene-3, 9-quinone (X), dianthrone (XI), diphenoquinone (XII), *p*-benzoquinone (XIII), dibenzopyrenequinone (XIV), isodibenzopyrenequinone (XV), pyranthrone (XVI), violanthrone (XVII), isoviolanthrone (XVIII), flavanthrone (XIX), anthanthrone (XX) hexamethylbenzene (XXI), pyrene (XXII), dibenzopyrenee (XXIII), isodibenzopyrene (XXIV), pyranthrene (XXV), anthanthrene (XXVI), dibenzocoronene (XXVII), ovalene (XXVIII), benzoperylene (XXIX) tetracene (XXX), violanthrene (XXXI), isoviolanthrene (XXXII), perylene (XXXIII), mesonaphthodianthrene (XXXIV), thianthrene (XXXV), zethrene (XXXVI)[2]. The structual formula of these compounds is illustrated on the Table I. These compounds are synthesized after the usual manner described in the literature of this subject. They were recrystallised from preferable sorts of solvents, for instance, 1-methylnaphthalene and were further purified by the repeated sublimation in *vacuo* at 10^{-3}–10^{-4} mm Hg[3]. Each of these compounds was extremely fine, even from the viewpoint of spectroscopy. The solutions of these compounds used in this measurement were prepared, at first, by dissolving from 4 mg. to 7 mg. of specimens in the concentrated sulfuric acid of which concentration was known, and after that, by diluting the original standard solutions with sulfuric acid of the same quality to the appropriate concentration of both specimens and acidity for the measurement. Beer's law was held for these kinds of specimens and for this method of the preparation of the solutions. It is not necessary to consider the effect of sulfonation at room temperature during the time of measurement after certifying the fact that the filtrate of the diluent of the original solution with aquo., is clear, having no extinction of light in the visible region, and the effect of the influence of peroxides is eliminated with the fact that the evidence for the non-existence of peroxides is certificated by iodometry and the color of the solutions are quite different from those of the corresponding quinones in the cases of hydrocarbons.

TABLE I

STRUCTURAL FORMURA OF SPECIMEN USED IN THIS EXPERIMENT

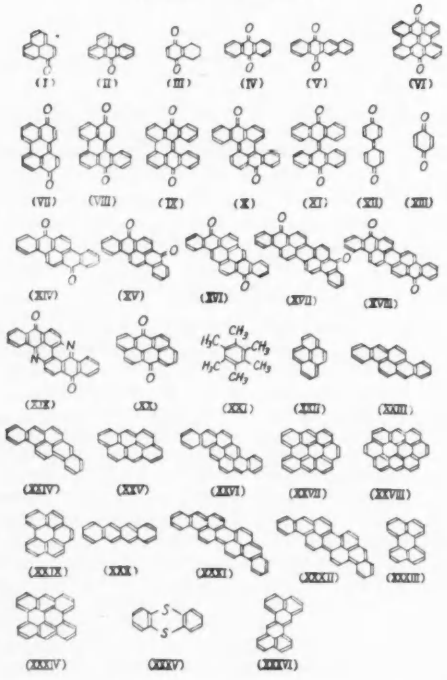

The state of the existence of these complexes may be considered to be the following form, that, with ketones or quinones each proton (H^+) is attached to the carbonyl group and forms hybride resonance between $(\rangle C{=}OH)^+$ and $(\rangle C{-}\ddot{O}{-}H)^+$. It was partially supported by the cryoscopic method to measure the depression of the freezing point of the 100% sulfuric acid by L. P. Hammett and J. Dyrup[4]. It was partially supported by the fact that there exists equilibrium between bases and their complexes in the sulfuric acid, which is shown in Fig. 1 and Fig. 2, and it also exists between complexes and their reduced forms with chromous ion (Cr^{++}). Some of the shapes of the absorption-spectra of the fully reduced forms of the complexes are similar to those of the vatted forms of the original compounds ($\rangle C{-}O{-}H$), which are shown in Fig. 3, with flavathrone.

For the state of the existence of the complexes between condensed polynuclear aromatic hydrocarbons and the protons (H^+) in the sulfuric acid, it may be reasonable to consider that there exist equilibria between hydrocarbons (bases) and their complexes. It will be supported empirically from the shapes of the absorption-spectra in various degrees of the acidity of the sulfuric acid, which meet nearly at one definite wavelength with a little correction, considering the solvent effect and which vary regularly showing the so-called existence of equilibria between bases and their complexes, as is shown in the cases of quinones, which are illustrated in Fig. 5 and Fig. 6 and Fig. 7. The absorption-spectra of these compounds in the concentrated sulfuric acid shift towards the longer side of the visible region compared with those of the original ones taken in the non-polar solvents, for instance, 1-methylnaphthalene. For these reasons above mentioned, it may be reasonable to consider the existence of equi-

2) see E. Clar. "Aromatishe Kohlenwasserstoff," Springer Verlag, Berlin, (1952), p. 387. This substance was not used in this experiment. It was previously reported in this paper that it was very basic.

3) Purification of specimens was done by H. Inokuchi in our laboratory, to which the author's sincere thanks are due. H. Inokuchi, This Bulletin, 24, 222 (1951).

4) L. P. Hammett and J. Dyrup, *J. Am. Chem. Soc.*, 54, 2721 (1932); ibid., 55, 1900 (1933).

libria between these compounds and their complexes with protons in the sulfuric acid, and estimate the basicity as the function of pK_B from the absorption curves after L. P. Hammett, putting that;

$$C = C_B + C_{BH^+} \quad (1)$$

$$\varepsilon = \log I_0/I/dc \quad (2)$$

$$C_{BH^+}/C_B = \frac{\varepsilon_{BH^+} - \varepsilon}{\varepsilon - \varepsilon_B} \quad (3)$$

$$pK_B = -\log \frac{a_{H^+} a_B}{a_{BH^+}} \quad (4)$$

$$H_0 = -\log (a_{H^+}) \quad (5)$$

$$H_0 = pK_B - \log C_{BH^+}/C_B \quad (6)$$

C; Molar concentration of specimen, suffix B means unprotonated base, BH^+ means protonated base.

ε; Molar extinction-coefficient of specimen.

a; Molar activity coefficient of each component.

H_0; Logarithm of the activity of the hydrogen ion.

H_0 being the Kolthoff's acidity-function which really means the value of $\log a_{H^+}$. Equation (2) means that Beer's law is held. K is the dissociation constant of the ionized base. So from the equation from (1) to (6), the base-strength pK_B is defined. The pK_B of each of these compounds have been estimated in this manner. Among the results obtained, for instance, the result for anthraquinone was in good agreement with that of L. P. Hammett. The former value is -7.5, the latter is -8.0. In this case the absorption curves are corrected approximately against the influence of the solvent-effect by the lateral shift of spectrograph with the isobestic-point or the sharp peak of the absorption-curve as standards after L. P. Hammet. The small difference of pK_B to that of L. P. Hammett was found, when the Kolthoff's table was used unlike in the case of him, who had used his own table. In this sense the result obtained agreed well with that of L. P. Hammett. The absorption-spectra of anthraquinone in various acidity of sulfuric acid is illustrated in Fig. 1.

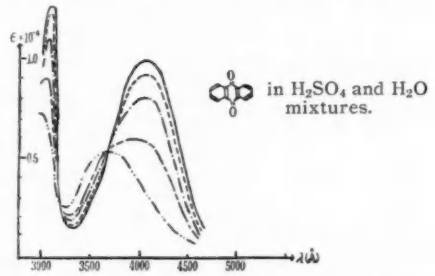

Fig. 1. The absorption spectrum of anthraquinone in H_2SO_4 and H_2O mixtures (corrected by the lateral schift).

Another example in the longer side of the visible region is illustrated with anthanthrone of which pK_B is estimated on the Table II, and of which absorption-curves are shown in Fig. 2. The state of existence of equilibrium between the complex and it's reduced form with chromous ion (Cr^{++}), which suggests the nature of this type of complex, is shown in Fig. 3, with flavanthrone in which protons (H^+) may be assumed to be attached to both the carbonyl group and nitrogen atoms. In Fig. 3, curve (I) shows that of the completely

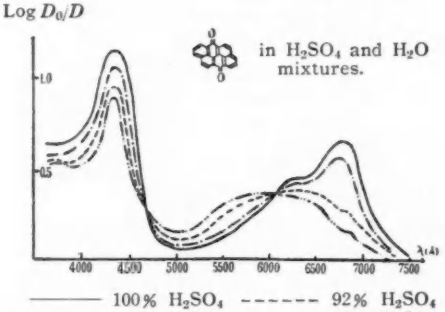

Fig. 2. The absorption spectrum of anthanthrene in H_2SO_4 and H_2O mixtures (corrected by the lateral schift).

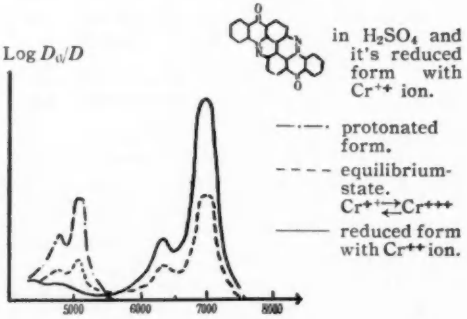

Fig. 3. The absorption spectrum of flavanthrone in H_2SO_4 and it's reduced form with chromous ion.

reduced form, curve (II) shows that of the complex-form which may be called the oxidized form, With other complexes of quinones, they may be said to be similar to those of the vatted states, which are shown in Fig. 4. With mere hydrocarbons in this series, the same may be said as those of quinones. However, in these cases, it will be necessary to consider how many numbers of protons are attached to the hydrocarbon molecule and to what positions in the molecule they are attached. In this report, we have as-

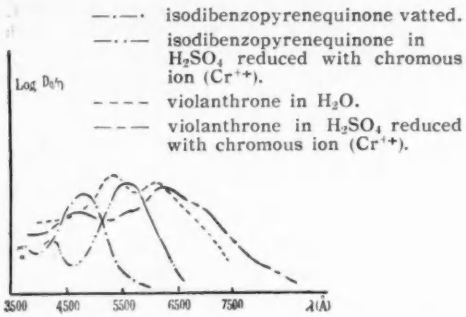
—·—· isodibenzopyrenequinone vatted.
—··— isodibenzopyrenequinone in H_2SO_4 reduced with chromous ion (Cr^{++}).
- - - - violanthrone in H_2O.
— — — violanthrone in H_2SO_4 reduced with chromous ion (Cr^{++}).
Log D_0/I
3500 4500 5500 6500 7500 λ(Å)

Fig. 4. The absorption spectra of isodibenzoquinone and violanthrone vatted in H_2O, and reduced with chromous ion (Cr^{++}) in H_2SO_4.

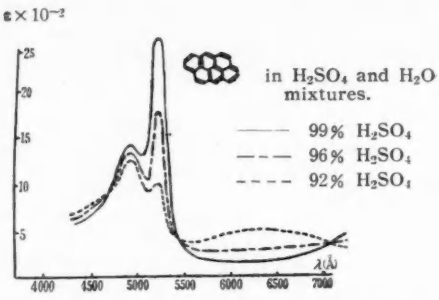

Fig. 5. The absorption spectrum of anthanthrene in H_2SO_4 and H_2O mixtures (corrected by the lateral schift).

TABLE II

pK_B VALUES FOR ANTHANTHRONE BY ISOBESTIC-POINT METHOD

Wave-lenghth	Optical density in H_2SO_4 and H_2O mixtures				pK_B*	pK_B**
(Å)	100%	96%	92%	85%		
6500	0.50	0.45	0.36	0.31	−7.6	−7.5
6600	0.56	0.51	0.34	0.25	−7.5	−7.7
6700	0.63	0.55	0.30	0.20	−7.7	−8.0
6800	0.66	0.55	0.26	0.15	−7.8	−8.1
6900	0.58	0.44	0.22	0.12	−8.0	−8.1
7000	0.38	0.28	0.17	0.09	−8.1	−8.0
				average	−7.8	−7.9
				Total average	−7.8	

* means the pK_B values from the absorption-curves observed in 96% H_2SO_4 and 100% H_2SO_4. It is assumed that in 100% H_2SO_4 the specimen is completely protonated.

** means the pK_B values from the absorption-curves observed in 92% H_2SO_4 and 100% H_2SO_4.

sumed the numbers of protons attached or dispatched from the hydrocarbon molecule reversibly, empirically from the shapes of the absorption-curves of the complexes in the acid, as is shown in Fig. 5 and Fig. 6 and Fig. 7, which are considered to be in equilibria with the original hydrocarbons. These are usually one, and in several cases two protons which contribute to pK or basicity. The problem, to what positions in the molecule the protons are attached can not be discussed in this method of measurement. Even, it may be inferred from the whole result of this report as follows; they may be attached to the positions in the molecule where the π-electrons are localized. In Fig. 5 which is the case of anthanthrene molecule, it is shown from it's shapes of absorption-curves as in the case of quinones, that there exist equilibrium between hydrocarbon and its complex. There exist three isobestic-points above 4000Å which support the existence of equilibrium-state and in this case in one definite range of wave-length between the isobestic-points, there is only mere increase or decrease of extinction of light with the elevation of the concentration of the acid. In this case, it is assumed that there is only one proton which takes parts in the complex-formation, or in other words, there is only one phase of substance or complex. In Fig. 6 which is the case of dibenzopyrene (XXIII), there are also isobestic-points, but in this case in one definite range of wavelength from 5000 to 6000 Å, there are both increase and decrease of extinction of light with the elevation of the degrees of acidity. In this case, it is assumed that there exist two final states of complexes (one-proton-complex, and two-proton-complex in the sense mentioned above.). The complex-formation proceeds by two steps in this case. On the Table III, the evaluation of pK is shown

TABLE III

pK_B VALUES FOR VIOLANTHRENE BY ISOVESTIC-POINT METHOD

Wave-lenghth	Extinction-coefficient in H_2SO_4 and H_2O mixtures ($\varepsilon\times10^{-4}$)				pK_B
(Å)	99.5%	96%	92%	85%	
6500	27.5	26.5	25.5	18.0	
6600	27.0	26.0	25.0	18.0	
6700	26.3	25.5	24.5	17.6	−7.0
6800	33.0	30.0	26.0	16.3	−7.4
6900	44.0	40.0	34.0	18.0	−7.4
7000	62.0	56.0	45.0	21.0	−7.4
7100	74.0	66.0	56.0	23.0	−7.4
7200	60.0	52.0	41.0	21.0	−7.3
7300	32.0	30.0	26.0	16.0	−7.1
7400	21.0	20.0	18.0	13.0	−7.0
				average	−7.2

with violanthrene. In every case, when we add very small amounts of chromous ion (Cr^{++}), the shape of the absorption-curve changes, there stands another peak towards the shorter side of the spectrum, which seems to be in equilibrium with the former one, and the solution be comes to possess fluorescence. But, it is not studied quantitatively here. In this report, the color-change of a specimen is described, when Cr^{++} ion is added, on the Table IV. This color-change is reversible, when hydrogenperoxide or free radical is added

TABLE IV

THE COLOR-REACTIONS OF CONDENSED POLYNUCLEAR AROMATIC HYDROCARBONS AND THEIR RELATED QUINONES IN THE CONCENTRATED SULFURIC ACID

Index No. of structural formula of specimen	Name of specimens	Color-change in H_2SO_4 ($+H_2O_2$) $\rightleftarrows$ (Cr^{++})	
XX	anthanthrene	green	red brown
VI	mesonaphthodianthrene	red viollet	colorless
XIV	dibenzopyrenequinone	viollet	pale brown
IX	helianthrone	orange	greenish yellow
XVIII	violanthrone	red viollet	green
XVIII	isoviolanthrone	green	blue
XVI	pyranthrone	blue	orange-red
XV	isodibenzopyrenequinone	dark orange	red-viollet
XIX	flavanthrone	orange	green
	indanthrone	dark brown	pale brown
	perylene-tetracerboxylic acid	scarlet	green
XXXI	violanthrene	blue green	sky blue
XXXIII	perylene	green red viollet	blue green
XXVIII	ovalene	green	red viollet
XXVII	dibenzocoronene	dark green	red viollet
XXXV	thianthrene	red	colorless
XXIII	dibenzopyrene	blue-green	red violet
II	benzanthrone	red	red (No Change)

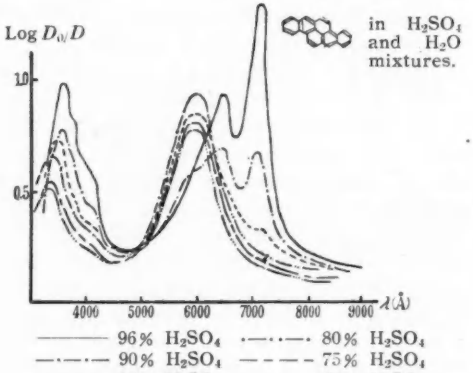

Fig. 6. The absorption spectrum of dibenzopyrene in H_2SO_4 and H_2O mixtures.

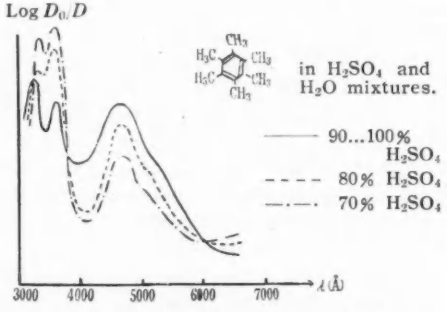

Fig. 7. The absorptionspectrum of hexamethylbenzene in H_2SO_4 and H_2O mixtures (corrected by the lateral schift).

Results and Discussions

The estimated pK_R with various condensed polynuclear aromatic hydrocarbons and their related quinones are shown on the Table V. It seems from that table that pK_R becomes smaller as the molecular-weight becomes larger. However, as in the case of dibenzopyrene, there exist two values of pK_R which means that two protons actually take parts in the complex-formation. The smaller value is -7.4, which is comparatively equivalent to that of anthanthrene, ovalene, dibenzocoronene, etc. The relatively larger value is -5.1, which is equivalent to hexamethylbenzene, pyrene, tetracene. To explain the contradiction between the experimental results, and the general understanding which suggests that the basicity or freee energy of complex-formation becomes larger as the molecular weight increases, it may be reasonable to think that the smaller value of anthanthrene, ovalen, dibenzocoronene, which are found in the experiment is the smaller one of the two pK_R values, the larger one not being able to be found in this measurement, perpaps owing to the low solubility or unstability of these compounds in the sulfuric acid. In the case of smaller molecules such as hexamethylbenzen, or tetracene, it may be considered that one proton takes part in the complex-formation. In the case of larger molecules such as anthanthrene,

TABLE V

pK_B VALUES FOR CONDENSED POLYNUCLEAR AROMATIC HYDROCARBONS AND THEIR RELATED QUINONES BY ISOBESTIC-POINT METHOD

Index No. of structural formura of specimens	Name of speciment	pK_B
I	peri-naphthoindanone	−0.4
II	benzanthrone	−3.2
III	*p*-naphthoquinone	−7.2
IV	anthraquinone	−7.5
V	naphthacenequinone	−8.4
VI	mesonaphthodianthrone	−6.0
VII	perylenequinone	−5.5
VIII	1.2-benzoperylene-3.10-quinone	−4.7
IX	helianthrone	−5.2
X	1.2.7.8.-dibenzo-3.9.-quinone	−5.1
XI	dianthrone	*
XII	diphenoquinone	**
XIII	*p*-benzoquinone	***
XIV	dibenzopyrenequinone	−7.4
XVI	pyranthrone	−6.0
XVII	violanthrone	−7.6
XX	anthanthrone	−7.9
XXI	hexamethylbenzene	−5.0
XII	pyrene	−4.7
XXIII	dibenzopyrene	−5.1 −7.4
XXV	anthantrene	−7.4
XXVI	pyranthrene	−8.2
XXVII	dibenzocoronene	−8.7
XXVIII	ovalene	−8.9
XXX	tetracene	−6.6
XXIX	benzoperylene	−8.3
XXXI	violanthrene	−7.3
XXXIII	perylene	−5.2****
XXXIV	mesonaphthodianthrene	−6.0*****

*, **, ***. It is not yet possible to measure the value owing to the destruction of specimens in the concentrated sulfuric acid.

****, *****. New trials are being attempted with other appropriate solvents and at low temperature.

ovalene, violanthrene, dibenzopyrene, it may be considered that two protones take part in the complex-formation. It may be thought that there is a relatively small difference of pK_B value with the shape of the molecule in such smaller molecules as hexamethylbenzene, tetracene etc., as in the cases of aza-aromatic hydrocarbons such as pyridine, quinoline, and acridine. When one proton is added to the molecule, the aromaticity for the rest of the molecule is reasonably destroyed and so the basicity corresponding to the next proton becomes much smaller than that corresponding to the first one, as in the case of diazine such as pyrimidine, pyrazine, cinnoline etc[5]. It may be possible, on the same way of consideration, to explain the difference of pK_B value, or the basicity between the monoketones such as perinaphhtoindenone, benzoanthrone, and quinones such as anthraquinone, violanthrone etc. In the cases of quinones, it seems unreasonable to consider that there exist two values of pK_B from the cryoscopic data of L. P. Hammett and J. Dyrup, who had determined the number of protons attached to the anthraquinone molecule from the depression of the freezingpoint of the sulfuric acid. However, in the present measurement, one value (−7.5) is found, which seems to be considerably smaller compared with that of benzoanthrone of which pK_B value is −3.2. To explain the considerably large difference, it may be considered that in the present measurement it is unable to find the larger one of two pK owing to the stability of one-proton-complex, or the low-solubility of that in the sulfuric acid. The relatively small difference between the pK values of various quinones may be ascribed to the molecular structure of each molecule. The relatively larger pK_B observed in violanthrene, mesonaphthodianthrene molecule compared with that observed in ovalene, anthanthrene molecule, suggests that the proton is easily attached to the molecule which is more or less easily excited, or which seems to have localized π-electron. Such sorts of molecules are known to have more or less localized π-electron from the magnetic study by H. Akamatu and Y. Matunaga in our laboratory[6]. It is reported by E. Clar that zethrene is easily soluble in the glacial acetic acid to be protonated by it, which means its pK_B is relatively very large, or it is relatively very basic compared with other hydrocarbons of this sort. It is explained that zethrene possesses localized π-electron from the standpoint of organic chemistry and may be a little para-magnetic, if measured. From this standpoint pentacene, and hexacene may be more basic than tetra-

5) A. Albert, R. Goldacre and J. Phillips., *J. Chem. Soc.*, **1948**, 2240.

6) H. Akamatu and Y. Matsunaga, This Bulletin **26**, 364 (1953).

cene, if they are measured. In addition, the molecular extinction-coefficient of violanthrene in the sulfuric acid is about twenty times larger than that taken in non-polar solvent.

Summary

The basicity of the condensed polynuclear aromatic hydrocarbons and their related quinones with higher molecular weight have been measured after the method of L. P. Hammett and J. Dyrup, and it is approximately estimated in terms of pK_R. In dibenzopyrene molecule two values of pK_R have been found. The larger seems to correspond to that of the smaller molecules such as hexamethylbenzene, tetracene. The smaller one seems to be equivalent to that of ovalene, anthanthrene etc. approximately, with which molecules the larger pK_R value seems to be unable to be found, owing to the unstability or the low-solubility of them in the sulfuric acid in the present method of measurement. The relatively large difference of pK_R between monoketones and quinones seems to be explained on the same considerations as above. The relatively small difference of pK_R seems to be dependent on the molecular structure as in the case of azaaromatic hydrocarbons such as pyridine, quinoline and acridine. From the results of such series of molecules as violanthrene, mesonaphhtodianthrene, zethrene, compared with the series of circulartype of molecules such as ovalene, anthanthrene, it is suggested that the proton is more easily attached to the molecule which seems to have localized π-electron in some sense.

The author expresses his hearty thanks to Prof. H. Akamatu, who has directed him throughout this study and to Dr. Inokuchi and M. Kobayashi and to Mr. Matsunaga for their collaboration and advice in this study. The cost of this study was defrayed from the grant of the Ministry of Education, to which the author's thanks are due.

Department of Chemistry, Faculty of Science, Tokyo University, Tokyo

---

A Note on the Measurement of the Absorption Coefficient in Infra-red Region. Influence of the Thickness of Layer on the Measurement of Absorption Coefficient

By Masasi YASUMI

(Received November 30, 1954)

Introduction

In order to determine the absorption coefficient k (or absorption index κ) in infra-red region, the transmission method is usually used. In the most of the researches, it is assumed that the Beer's rule holds strictly. For the gases and dilute solutions, this assumption may be valid, but inadequate to the liquids and solids which are highly absorbing. The invalidity of the Beer's law is due to the boundary reflexion and to the multiple reflexion of the substance layer whose thickness is comparable to the wavelength.

Recently, Simon[1] has investigated the surface reflexion of the highly absorbing substances including carbon tetrachloride and has obtained the values of refractive indices and of the absorption indices from the reflexion coefficients.

We have calculated the transmission coefficient of the infra-red beam passing through a thin layer of liquid carbon tetrachloride according to the correct formula using Simon's data, and have compared this with the value calculated from simple Beer's law.

The effect of the thickness of the layer is very marked, and it is concluded that we cannot obtain the correct value of the absorption coefficient for the highly absorbing materials by the simple transmission method usually used.

The Formula of Transmission Coefficient for the Single Plane Layer

A plane electromagnetic wave of the wavelength λ is considered to be linearly polarized and to be propagated in the medium 1. An absorbing dielectric layer with plane boundary surface is placed as shown in Fig. 1.

1) I. Simon, *J. Opt. Soc. Am.*, **41**, 336 (1951).

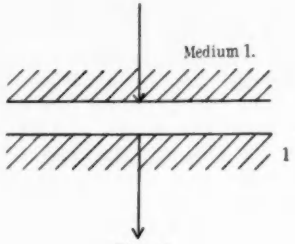

Fig. 1.

The direction of the propagation of incident wave is considered to be normal to the boundary surface. A part of the wave will be transmitted through the sheet characterized by refractive index n, absorption coefficient k ($=n\kappa$, where κ is absorption index) and thickness d. The medium 1 is considered to be non-absorbing and to be characterized by refractive index n_1.

The transmission coefficient of the sheet D^2 is expressed as follows[2]:

$$D^2=e^{-\frac{4\pi kd}{\lambda}}\times\frac{1+R_{12}^4-2R_{12}^2\cos 2\tau}{1+R_{12}^4e^{-\frac{8\pi kd}{\lambda}}-2R_{12}^2e^{-\frac{4\pi kd}{\lambda}}\cos\left(\frac{4\pi nd}{\lambda}+2\tau\right)}$$

$$=\frac{\sin h^2(-\ln R_{12})+\sin^2\tau}{\sinh^2\left(\frac{2\pi kd}{\lambda}-\ln R_{12}\right)+\sin^2\left(\frac{2\pi nd}{\lambda}+\tau\right)} \qquad (1)$$

where

$$R_{12}^2=\frac{(n-n_1)^2+k^2}{(n+n_1)^2+k^2} \qquad (2)$$

$$\tan\tau=\frac{2n_1k}{(n^2-n_1^2)+k^2} \qquad (3)$$

Transmission Coefficient for the Thin Layer of Liquid Carbon Tetrachloride

The calculation is made for the thin layer of carbon tetrachloride placed between rock salt plates.

The refractive indices and the absorption coefficients of carbon tetrachloride for the infra-red waves in the wave number 760–815 cm^{-1} region are tabulated in Table I. The data are taken from Simon's paper[1]. Using these values, the values of R_{12}, and $\tan\tau$ are calculated. In this calculation, n_1 is taken to be 1.52. The calculated values are tabulated also in Table I.

Carbon tetrachloride shows marked absorption and dispersion in the region 760–815 cm^{-1} [1]. The suitable thickness of the layer for the measurement of the absorption coefficients by transmission method in this region would be, therefore, very small and would be comparable to the wave-length. We have calculated the transmission coefficients D^2 for the layer of the thickness $d=2.5\times10^{-5}$ cm., 5×10^{-5} cm. and 10^{-4} cm. respectively. On the other hand, the values of hypothetical transmission coefficient $T^2=\exp(-4\pi kd/\lambda)$, are also calculated. These values are tabulated in Tables II, III, and IV. The values of $(-\ln D^2)$ and $4\pi kd/\lambda$ are also given in Tables II, III and IV.

TABLE I

REFRACTIVE INDICES, ABSORPTION COEFFICIENTS AND RELATED CONSTANTS OF CARBONTETRACHLORIDE IN INFRA-RED REGION

$\tilde{\nu}$($cm.^{-1}$)	n	k	R_{12}	$\tan\tau$
760	1.30	1.20	0.40	−21.5
765	1.30	1.25	0.41	−76.1
770	1.30	1.25	0.41	−76.1
775	1.45	1.30	0.41	+ 2.65
780	1.85	1.75	0.51	+ 1.29
785	2.15	3.10	0.66	+ 0.79
790	1.70	3.50	0.74	+ 0.78
795	1.20	2.00	0.60	+ 1.94
800	0.80	0.80	0.44	− 2.38
805	0.85	0.45	0.34	− 0.99
810	0.95	0.25	0.25	− 0.52
815	1.05	0.15	0.16	− 0.41

The value of refractive index of rock salt is taken as $n_1=1.52$.

TABLE II

TRANSMISSION COEFFICIENTS AND RELATED QUANTITIES FOR THE LAYER OF CARBON TETRACHLORIDE

$d=2.5\times10^{-5}$ cm.

$\tilde{\nu}$(cm^{-1})	D^2	$\exp(-4\pi kd/\lambda)$	$-\ln D^2$	$4\pi kd/\lambda$
760	0.818	0.751	0.201	0.287
765	0.796	0.740	0.228	0.301
770	0.796	0.740	0.228	0.303
775	0.740	0.728	0.301	0.317
780	0.635	0.674	0.454	0.395
785	0.394	0.465	0.931	0.766
790	0.377	0.418	0.976	0.873
795	0.624	0.605	0.471	0.502
800	0.884	0.812	0.123	0.208
805	0.935	0.892	0.067	0.114
810	0.955	0.938	0.046	0.064
815	0.964	0.963	0.037	0.038

2) M. Yasumi, This Bulletin. 24, 54 (1951).

TABLE III

$d=5\times10^{-5}$ cm.

$\tilde{\nu}$(cm^{-1})	D^2	exp$(-4\pi kd/\lambda)$	$-\ln D^2$	$4\pi kd/\lambda$
760	0.663	0.563	0.411	0.575
765	0.639	0.547	0.448	0.603
770	0.635	0.546	0.454	0.606
775	0.565	0.530	0.571	0.634
780	0.442	0.452	0.892	0.792
785	0.182	0.217	1.70	1.53
790	0.160	0.174	1.83	1.75
795	0.444	0.367	0.812	1.00
800	0.761	0.657	0.273	0.417
805	0.886	0.799	0.121	0.224
810	0.902	0.880	0.103	0.127
815	0.936	0.927	0.066	0.076

TABLE IV

$d=10^{-4}$ cm.

$\tilde{\nu}$(cm^{-1})	D^2	exp$(-4\pi kd/\lambda)$	$-\ln D^2$	$4\pi kd/\lambda$
760	0.415	0.317	0.879	1.15
765	0.391	0.301	0.939	1.20
770	0.390	0.298	0.942	1.21
775	0.348	0.281	1.06	1.27
780	0.224	0.206	1.50	1.58
785	0.044	0.047	3.12	3.06
790	0.030	0.030	3.51	3.50
795	0.187	0.135	1.68	2.00
800	0.553	0.434	0.592	0.834
805	0.725	0.639	0.322	0.448
810	0.797	0.776	0.227	0.254
815	0.866	0.858	0.144	0.153

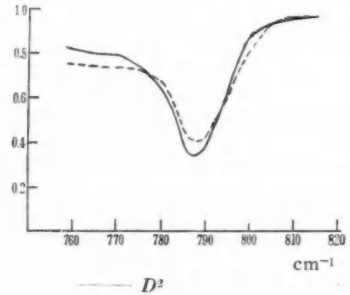

——— D^2
- - - - T^2

Fig. 2.

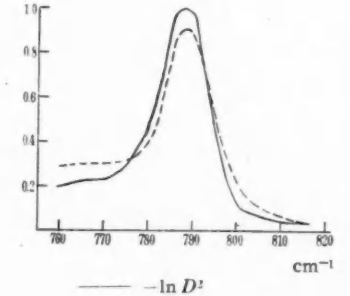

——— $-\ln D^2$
- - - - $4\pi kd/\lambda$

Fig. 3.

The values of D^2 and T^2 versus wave numbers for the thickness of $d=2.5\times10^{-4}$ cm. are illustrated in Fig. 2. The behavior of $(-\ln D^2)$ and $4\pi kd/\lambda$ versus wave numbers are shown in Fig. 3.

Discussion

As shown in Tables I—III, and Figs. 2—3, it is concluded that the values of the transmission coefficients for the thin layer of carbon tetrachloride calculated with the exact formula are markedly different from the hypothetical transmission coefficient calculated with simple Beer's law. In the case of $d=10^{-4}$ cm., the maximum deviation amounts about 30%.

If we calculate the absorption coefficients from the values of D^2, which will be identical with the experimental transmission coefficients in ideal cases, according to simple Beer's law, the obtained values would be $-\ln D^2/(4\pi d/\lambda)$. As shown in Table I—III, the values of $(-\ln D^2)$ are markedly different from $4\pi kd/\lambda$.

The situation will be more serious when the relative absorption coefficient is concerned, for the deviation will have plus sign in one wave-length region and minus sign in another region.

It can be said that the transmission method based upon the simple Beer's law cannot be applied for the highly absorbing substances and an erroneous conclusion would be drawn if we calculate absorption coefficient according to Beer's law.

It may not be unexpected that the absorption coefficient is dependent on the thickness of the layer and that the unexisting lines appear in some case or existing lines disappear in another case[3].

For the less absorbing materials the effect of the thickness will be less important, but for the lines whose absorption coefficient is about 0.5[4] the effect is not negligible[5].

Summary

The transmission coefficient of a thin layer of carbon tetrachloride is calculated according to the exact formula and compared with the

3) Earle K. Plyer and Nicola Aquista, *J. Opt. Soc. Am.*, 44, 505 (1954).

4) e. g. k is ca. 0.6 for 8.90 μ of ethyl ether, 0.5 for 5.8 μ of ethyl acetate.

5) This conclusion is drawn from the calculation made by K. Kuratani.

value calculated by simple Beer's rule.

The usual transmission method which is based upon the Beer's law is inadequate to the determination of the absorption coefficient of highly absorbing substances such as carbon tetrachloride.

We are grateful to Prof. San-ichiro Mizushima for his kind advice and the encouragement throughout this work, and to Dr. Kenji Kuratani for his valuable advice.

Our thanks are also due to the Ministry of Education for a grant in aid of this research.

Institute of Science and Technology,
Tokyo University,
Tokyo

A Rapid Colorimetric Determination of Vanadium in Carbon Materials

By Ken SUGAWARA, Motoharu TANAKA and Akiya KOZAWA*

(Received February 9, 1955)

Introduction

Among heavy metal impurities found in the "electrolyte" (a concentrated sodium chloride solution), the undesirable effect of vanadium upon the chlorine-caustic electrolysis is particularly marked even at a low concentration.[1] Hence, the establishment of a reliable and rapid method of vanadium determination is desirable to estimate the quality of anode carbon and its raw materials and to improve upon it. Indeed, there have been many method tested and others proposed by various investigators. Some, however, are unsatisfactory because insufficient attention was paid to the possible escape of vanadium in the ashing process[2], while others involve some tedious processes unsuitable for use in industrial laboratories.

By overcoming these difficulties, the authors devised a new method having the following characteristics.

(1) Addition of sodium carbonate to the sample accelerates the ashing and guards against the escape of vanadium during the process.

(2) The use of ferric hydroxide gives a simple method for separation of vanadium which replaces E.B. Sandell's tedious processes of leaching the sodium carbonate cake and extracting the vanadium oxinate in the original phospho-tungstate method[3].

Procedure

Pulverize a 0.5–1.0 g. sample so that it can pass through a 100 mesh sieve. Grind the sieved sample in an agate mortar with 2 g. of sodium carbonate for a few minutes and transfer it into a quartz dish so as to make a thin layer. Place it in an electric furnace at 650–750°C and reduce it to ash. After complete ashing, dissolve the ash in sulfuric acid and boil for about five minutes.

Add 5 mg. of ferric iron and 50 ml. of distilled water to the solution thus obtained. Neutralize the solution roughly with sodium hydroxide (3N) while stirring constantly. The neutralization is completed by using six drops or less of ammonia (3N) to B. C. P. or *p*-nitrophenol as indicator. Filter and dissolve the precipitate into 20 ml. of a hot phosphoric acid (1 : 3). Add one ml. of sodium tungstate reagent (0.5M) and keep the solution boiling for about five minutes. After cooling to room temperature, transfer the solution into a 25 ml. measuring flask and fill it with distilled water to the 25 ml. mark. Then the optical density is measured spectrophotometrically at the wavelength of 410 mμ to determine the vanadium, using the working curve described by one of the authors.[4]

When the vanadium content of the sample is below 30 μg., it is advisable to prepare a standard solution of a concentration approximate to that of the sample, and to compare the color of the sample with the standard, using ordinary Nessler tubes of 8 mm. caliber and 35 cm. height. In this way even 5 μg. of vanadium can be determined.

* Department of Applied Chemistry, Faculty of Engineering, Nagoya University.

1) G. Angel and T. Lundén, *J. Electrochem, Soc.*, **99**, 435 (1952).

2) I. Iwasaki and I. Ukimoto, *J. Chem. Soc. Japan*, **63**, 1678 (1942).

3) E. B. Sandell, *Ind. Eng. Chem.*, Anal. Ed., **8**, 336 (1936).

4) M. Tanaka, This Bulletin, **27**, 10 (1954).

Discussion

1) **Ashing.**—As shown in Table I, the presence of sodium carbonate hinders the escape of vanadium in the ashing process, which is considerable when it is absent. At the same time the carbonate accelerates ashing. Thus, in the presence of the salt, the ashing process which would otherwise require a full hour, is completed within twenty minutes at 650–750°C.

TABLE I

ANALYSES OF SEVERAL SAMPLES

Sample	Sample taken g.	V added μg.	V found μg.	V found* μg.
Coke No. 1	0.50	0	8	8.5
〃	0.50	23	30	—
Coke No. 2	0.50	0	226	230
Coke No. 2†	0.50	0	158	—
Coke No. 2†	0.50	0	181	—
Coke No. 3	1.00	0	18	16
〃	0.50	46	57	—
Graphite No. 4	0.50	0	128	133
〃	0.50	46	176	—
〃	0.50	92	224	—
Grrphite No. 4†	0.50	0	100	—
Graphite No. 4†	0.50	0	119	—
Graphite No. 5	0.50	0	8	9
Cathode of "AD" cell (containing Mn)	0.50	0	10	12
〃	0.50	23	34	—
〃	0.50	46	57	—

* Determined after the ashed mixture was once put to fusion.
† Ashed without sodium carbonate.

The process of ashing, here mentioned, is sufficient to bring the vanadium in the sample completely into a soluble form. As shown in the same table, the vanadium values do not increase after the ashed sample is once put to fusion. Consequently, fusion is dispensable in the present procedure.

Also it must be added that the wet method of combustion using sodium iodate[5] can successfully replace the ashing. The sieved sample (0.5 g.) is put into 10 ml. of concentrated sulfuric acid contained in a 100 ml. beaker. While the beaker is kept slightly heated, 8—9 g. of sodium iodate powder is added. A violent reaction occurs with a considerable sublimation of iodine, giving a yellowish color to the solution. Diluted with 30 ml. of distilled water, the solution is kept boiling until the iodine is completely expelled. Then the solution is ready for the procedure described above from the point of addition of ferric salt.

The iodate method may be recommended because of its rapidity, but it must be noted that it requires iodate which is expensive and considerable skill for the manipulation.

2) **Ferric Hydroxide as Vanadium Collector**[6].—In the present method, vanadium is collected and separated by ferric hydroxied from the ions of ammonium and potassium which may interfere with the final colorimetry. The following experiment shows that the vanadium collection is complete when it is conducted under the conditions prescribed in the procedure. A series of sulfuric acid solutions was prepared containing various amounts of vanadium, tetra- and quinquevalent in addition to 5 mg. iron. These solutions were processed according to the directions given in the procedure. Table II shows that the result is quite satisfactory. Also it is noticeable that during the process the tetravalent vanadium is completely oxidized into quinque-valent.

TABLE II

COLLECTION OF VANADIUM BY FERRIC HYDROXIDE

No. of experiment	V taken μg.	Valency	V found μg.	Recovery %
1	50	IV	50	100
2	125	IV	123	97
3	250	IV	248	99
4	200	V	201	100
5	300	V	295	98

3) **Interference by Large Amounts of Iron and/or Manganese and its Avoidance.**—When more than one mg. of manganese is present in the sulfuric acid solution, it is partly coprecipitated with ferric hydroxide and oxidized by the air into the tri-valent state, forming pink colored manganic phosphate by later treatment with phosphoric acid. Further, the color is intensified by the addition of sodium tungstate, causing remarkable error in the colorimetry. Also more than 10 mg. of iron cause a considerable error. E.B. Sandell avoided such interferences by sodium carbonate fusion and leaching of the cake obtained. In our procedure, the interfering manganese and iron can be separated as given in the following example: a series of 60 ml. of sulfuric acid solution (0.5N) was prepared in which various amounts of vanadium are contained in addition to 5 mg. each of iron and manganese. After the addition of one ml. of 30% hydrogen peroxide, the

5) T. Kiba, S. Ohashi, T. Takagi and Y. Hirota, *Japan Analyst* **2**, No. 5, 446 (1953).

6) K. Sugawara, M. Tanaka and H. Naito, This Bulletin, **26**, 417 (1953).

solutions were neutralized with sodium hydroxide solution (3N) and 3—5 ml. of the same reagent were added in excess. After being stirred well, they were left standing at 70°C for about ten minutes until the decomposition of the hydrogen peroxide was complete. The precipitate was filtered off through a glass filter and the filtrate was processed according to the direction in the procedure. Table III proves that the separation was successful.

TABLE III
SEPARATION OF VANADIUM FROM MANGANESE AND IRON

No. of experiment	V taken μg.	V found μg.	Recovery %
1	0	0	—
2	11.5	12	104
3	23	23	100
4	115	118	103
5	230	237	103

4) **Other Interfering Elements.**—Ti, Zr, Bi, Sb, and Sn are considered possible as other interfering elements. Their contents in anode samples, however, are negligible so that a discussion on them can be dispensed with.

5) Table I shows some results of the application of the proposed method to coke and graphite samples and particularly a cathode sample of air depolarized cell. The latter was remarkably contamined with manganese. Consequently their analyses were carried out under the special directions given in the preceding article.

Faculty of Science, Nagoya University, Nagoya

A New Method of Spectrophotometric Determination of Iodine in Natural Waters

By Ken SUGAWARA, Tadashiro KOYAMA and Kikuo TERADA

(Received February 16, 1955)

Introduction

Because no appropriate method is available for the determination of a small amount of iodine found in ordinary natural waters, the determination of this element has been limited to special kinds of water which are iodine-rich. In order to fill this lack, the present method was established.

The characteristics of this method are the following:

1) By the use of silver nitrate solution, together with a large amount of silver chloride, iodide ions are precipitated as silver iodide and are completely gathered into the chloride precipitate.

2) The precipitated iodide is converted into iodate by bromine. Then the reaction between the iodate and cadmium iodide liberates the iodine, in a quantity six times that of the original sample. Thus the minimum amount of determinable iodide is lowered to one-sixth.

3) Finally, the liberated iodine is determined spectrophotometrically as starch-iodine-chromogen. Thus 0.2 μg. of iodine can be determined with an error of only ±5%.

Analytical Method

Reagents

1) Sodium chloride solution, about 0.1 N, free from iodine.

The addition of a small amount of silver nitrate solution can remove any trace of iodine in the form of silver iodide involved in a large amount of silver chloride.

2) Silver nitrate solution, about 0.1 N.

3) Sulfuric acid, about 3 N.

4) 1/2 M acetate buffer with pH 2.8 saturated with bromine.

1000 parts of 1/2 M acetic acid are mixed with 20 parts of 1/2 M sodium acetate. A suitable amount of bromine is added.

5) Cadmium iodide solution, about 5%.

Cadmium iodide crystals are dissolved in distilled water and boiled for five minutes before they are stored in a brown glass bottle.

6) Starch solution, about 0.5%.

After being prepared in the usual way, the solution is put to centrifuge at 3000 r.p.m. for ten minutes. Then it is filtered through a filter paper of fine texture.

7) Sodium acetate solution, about 25%.

8) Sodium sulfite solution, about 1%.

Procedure

1) Take a suitable amount of sample, usually

3—5 litres, depending upon the iodine content, filter it through a piece of absorbent cotton previously washed with 3 N hot hydrochloric acid and distilled water. And a sufficient amount of 0.1 N sodium chloride solution to the filtrate to adjust the chloride concentration to about 15 mg. per litre. While vigorously stirring, add an amount of silver nitrate solution equivalent to the chloride. After the silver chloride is completely precipitated, add 3 N sulfuric acid in the proportion of 1 ml. to 1 litre of the solution. Allow the solution to stand in a dark place for about twenty hours. After the precipitate has completely settled, the supernatant is siphoned off and the remaining precipitate is transferred to a small beaker (50 ml.). Rinse the precipitate with distilled water several times and pour the washings on a filter paper so that any suspended precipitate will be collected on it. Transfer the collected precipitate with a small amount of water back into the original beaker.

2) To the content of the beaker, add 2 ml. of 0.1 N sodium chloride solution and then and 10 ml. of 1/2 M acetate buffer previously saturated with bromine. Dilute the total volume with distilled water to about 25 ml. Stir and allow it to stand for one hour at a temperature below 20°C with occasional stirring. At this step, the iodine is completely oxidized into iodate.

3) Warm the beaker on a boiling water bath until excess bromine is expelled and the solution turns pale yellow. After cooling by tap water, filter the liquid through a small filter paper of fine texture. Wash the residue on the filter paper three times with small portions of distilled water. Gather the filtrate and washings into a 50 ml. beaker.

4) Warm the beaker on a boiling water bath until all trace of bromine is expelled and the solution is colorless. Leaving it to cool to room temperature, add 0.2 ml. of 1% sodium sulfite solution to remove any bromous acid which might have been formed during the above oxidation process.

5) Add 10 ml. of 1/2 M acetate buffer and keep the solution at a temperature below 20°C. Oxidation is complete within thirty minutes. Evaporate the solution on a boiling water bath to a volume of about 10 ml.

6) Cool and transfer the solution into a 25 ml. measuring flask of brown glass. Dilute the solution to about 20 ml. And 1 ml. of 0.5% starch solution and cool by tap water for five minutes. Then add 1 ml. of cadmium iodide solution, shake vigorously, and allow it to stand for fifteen minutes until a deep blue color fully develops. Adjust the pH to 4.2 by the addition of 0.3 ml. of 25% sodium acetate solution. After filling distilled water to the mark, the contents of the flask is mixed well.

The optical density of the solution is determined spectrophotometrically, using a wavelength of 580 mμ.

Discussion

1) The usual evaporation method[1] for iodine enrichment has many tedious dfficulties which are accompanied by unavoidable loss in iodine and by contamination with other interfering elements. The proposed silver iodide method is absolutely free from such difficulties and moreover, gives a result of 100% accuracy for a tenth mg. of iodine from a sample of 3–5 litres as will be shown later. The addition of sulfuric acid perfects the coagulation of silver iodide.

2) The idea introducing the iodide-bromine reaction for minimizing the least determinable iodine to one-sixth, originally occurred to H. Ballczo[2] who recommended that the oxidation of iodide by bromine be carried out at pH 4.3. The authors obtained a satisfactory result when steps from the iodide oxidation by bromine up to the addition of starch solution and cadmium iodide are processed at pH 2.8 and then the pH is adjusted to 4.2 for colorimetry.

3) In some cases samples are left for a long time without further treatment after silver nitrate solution was added, when some amount of metallic silver may be produced due to photochemical decomposition. This silver reacts with bromine at a later step by the following equation

$$Ag^+ + Br_2 + H_2O = HBrO + AgBr + H^+$$

with the production of hypobromous acid. This hypobromous acid liberates iodine in the cadmium iodide treatment, causing a considerable error in the final colorimetry. The treatment by sodium sulfite is naturally given whereby hypobromous acid and iodate are reduced to bromide and iodide. Thus in the second oxidative treatment by bromine, iodate alone is produced.

4) For the liberation of iodine, cadmium iodide was preferred to the potassium iodide currently used[3,4] because the latter compound tends in an acid medium to liberate iodine even in the absence of iodate, thus causing a considerable error in the precise determination at which the authors are aiming.

Cadmium iodide solution keeps for at least two months without any liberation of iodine when it is stored in a brown glass bottle after being boiled for five minutes.

1) American Public Health Association, "Standard Methods for the Examination of Water and Sewage", New York, (1946), 9th Ed., p. 47.
2) H. Ballczo und G. Mondl, *Mikrochem. ver. Mikrochim. Acta*, **39**, 247 (1952).
3) W. G. Gross, L. K. Wood and J. S. McHargue, *Anal. Chem.*, **20**, 900 (1948).
4) F. G. Houston, *Anal. Chem.*, **22**, 493 (1950).

5) Starch-iodine-chromogen gives a maximum absorption at a wave length of 580 mμ. (See Fig. 1) and strictly obeys the Beer's law covering a range of 0.00–120 μg. of iodine.

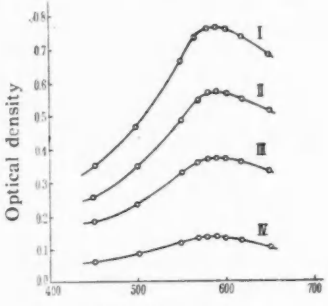

Fig. 1. Absorption curves.
I: 100 μg. of I in 25 cc.
II: 75 μg. of I in 25 cc.
III: 50 μg. of I in 25 cc.
IV: 20 μg. of I in 25 cc.

When the authors use Coleman Model 14 Universal Spectrophotometer with an accessory "round cuvette" of an effective cell thickness 13.06 mm., the following relation holds:

$$X = \frac{E - 0.006}{0.0074},$$

where X is the amount of iodine in 25 ml. and E is the optical density for 580 mμ.

The amount of iodine in the original sample can be calculated by dividing X by 6[5].

Starch species and temperature affect somewhat the standard curve. Therefore, the curve sometimes should be constructed for several starch species and at various temperatures (See Fig. 2).

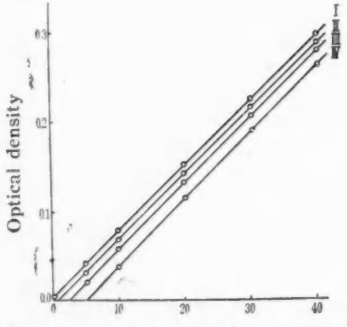

Fig. 2. Effect of temperature on color intensity at a wavelength of 580 mμ.
I: at 10–20°C III: at 25°C
II: at 23°C IV: at 28°C

5) L.W. Andrews, *J. Am. Chem. Soc.*, 25, 756 (1903).

The color undergoes no measurable change for at least two hours if the pH of the solution is adjusted to 4.2 after the color developed at pH 2.8. Fig. 3 shows the effect of pH on the rate of color development.

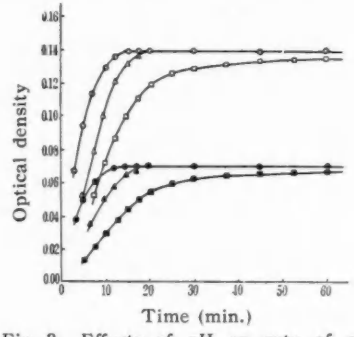

Fig. 3. Fffects of pH on rate of color development at a wave length of 580 mμ.
—○— pH: 2.8 —○— 20 μg. of I in 25 cc.
—△— pH: 3.6
—□— pH: 4.2 —●— 10 μg. of I in 25 cc.

6) Among common elements in ordinary natural waters, chloride, bromide, nitrate and sulfate cause interference which at least is not up to the concentrations 200, 10, 30 and 30 mg., respectively.

TABLE I
ACCURACY OF THE METHOD

Cl added mg.	I used μg.	I found μg.	Error %
17.5	0.00	0.00	—
17.5	0.20	0.19	−5.0
17.5	0.20	0.20	0.0
17.5	0.20	0.21	+5.0
17.5	0.99	0.95	−4.0
17.5	0.99	0.96	−3.0
17.5	0.99	1.03	+4.0
17.5	1.98	1.95	−1.5
17.5	1.98	1.91	−3.5
17.5	1.98	1.99	+0.9
17.5	4.95	4.99	+0.8
17.5	4.95	4.92	−0.6
17.5	4.95	4.98	+0.6

7) The accuracy of the proposed method was tested using various amounts of a standard solution of potassium iodide. Table I gives the result.

The fact that the oxidation of silver iodide is complete was also shown by the following experiment: Various amounts of the standard solution of potassium iodide were similarly processed and the iodine liberated at pH 2.8

was determined using standard solution of thiosulfate. Table II shows the result.

TABLE II

OXIDATION OF SILVER IODIDE BY BROMINE*

Cl added mg.	I used mg.	I found mg.	Recovered %
35.5	0.00	0.00	—
35.5	0.19	0.19_2	101.0
35.5	0.19	0.19	100.0
35.5	0.19	0.19_1	100.5
35.5	0.39	0.39	100.0
35.5	0.39	0.38_9	99.7
35.5	0.39	0.38_9	99.7
35.5	0.49	0.49_1	100.0
35.5	0.49	0.48_6	99.2
35.5	0.49	0.48_5	99.2
35.5	0.49	0.48_9	100.0

* Determination was carried out volumetrically.

Table III shows examples of the result from natural waters to which the present method was applied.

TABLE III

EXAMPLES OF ANALYSIS

Description	Sample taken l.	I found μg./l.	Cl found mg./l.
Rain water collected at Higashiyama area, Nagoya City (June, 1954)	4.0	0.9_0	0·18
	4.0	1.3_1	0.89
	2.0	1.1_5	0.58
	2.0	1.0_5	0.36
Ground water from a well in the campus of Nagoya University (June, 1953)	5.0	0.8_5	3.83
Surface water of Lake Biwa-ko, Shiga Prefe- (Oct., 1953)	5.0	1.3	4.69
Surface water of Lake Gongen-ike, Mt. Norikura, Gifu Prefecture (Sept., 1953)	10.0	0.2	0.13
A spring water from Higashiyama area, Nagoya City (Aug., 1954)	3.0	2.2	5.58

The present study was accomplished by using Coleman Model 14 Universal Spectrophotometer supplied by the Elizabeth Thompson Science Fund. The authors express their appreciation to the Trustees of that fund.

Chemical Institute, Faculty of Science, Nagoya University, Nagoya

---

Electron Transfer Spectra in the Crystals of Hexamminecobalt(III) Salts

By Yukio KONDO

(Received April 25, 1955)

Introduction

The formation of the ion-pairs of hexammine and tris-(ethylenediamine) complex cations of cobalt(III) and chromium(III) with various anions in aqueous solutions and the consequent appearance of a new absorption band in the ultraviolet were first observed by Linhard[1], and the thermodynamical study of the ion-pair formation was spectrophotometrically done by him[1], Evans and Hancollas[2] and Kubota[3]; this so-called association band has been attributed to the transfer of an electron from an anion to a complex ion[2,3,4]. It will be natural to suppose that in crystals in which a complex ion is closely surrounded by anions, this absorption band will acquire more intensity than in solutions, and indeed Linhard and Weigel[4] suggested in their paper that the deepening in the color of the crystals of hexamminecobalt(III) chloride, bromide and iodide in this order is attributable to the presence of this band. Actually, in 1936, in the study of the absorption spectra of cobalt(III) ammine salt crystals, Kobayashi[5] observed the new absorption band which was absent in solutions. But he attributed it to the transition of an electron from a ligand to the central atom.

On the other hand, studying theoretically the absorption spectra of the first transition metal complexes by the crystalline field ap-

1) M. Linhard, *Z. Elektrochem.*, **50**, 224 (1944).
2) M.G. Evans and G.H. Hancollas, *Trans. Faraday Soc.*, **49**, 363 (1953).
3) T. Kubota, *J. Chem. Soc. Japan (Pure Chem. Sec.)*, **75**, 552 (1954).
4) M. Linhard and M. Weigel, *Z. anorg. Chem.*, **266**, 49 (1951).
5) R. Tsuchida and M. Kobayashi, *J. Chem. Soc. Japan (Pure Chem. Sec.)*, **64**, 1268 (1943); "The Colors and the Structures of Metallic Compounds", Zoshindo Co., Osaka, Japan (1944), p. 180.

proximation, Tanabe and Sugano[6] have recently suggested the possibility of the appearance of the absorption band due to the two-electron jump within a metal ion in the case of nickel(II), cobalt(III) and chromium(III) complexes. Thus, concerning the origin of the new absorption band appearing in crystals, there are three different possibilities, namely, the transitions of electrons of the central atom, a ligand and an anion.

The present study was undertaken for the purpose of confirming the existence of this band in the spectra of various hexamminecobalt(III) salt crystals, as only the chloride was investigated by Kobayashi, and also to determine which of the above mentioned theories is correct.

Experimental

Materials.—Hexamminecobalt(III) salts investigated in the present study are listed in Table I. The chloride was prepared by the air oxidation of the ammonical solution of cobalt(II) chloride and ammonium chloride using activated charcoal as a catalyst according to the method of Bjerrum and McReynolds[7]. The iodide selenate was prepared by the oxidation of the ammoniacal solution of cobalt(II) selenate and ammonium selenate with iodine after Hassel and Bödtker Naess[8]. The others were derived from the chloride by the method described briefly in the table[9-17]. These were, in general, recrystallized from slightly acidic, hot aqueous solutions.

Apparatus and Procedure.—The optical system of the microscope used is shown in Fig. 1, in

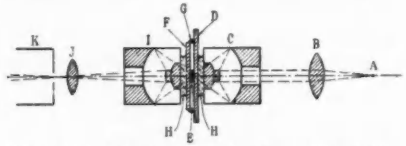

Fig. 1. Optical system (schematic) of the reflecting microscope used for measuring the absorption spectra of microscopic crystals.

which A, B, C, I and J are fixed to the body of a usual microscope. As a light source A, a hot cathode hydrogen discharge tube was used except in the case of the iodide in which a tungsten lump was used. A fused quartz lens B of a focal distance 8 cm. was used to parallelize the light from the source. A reflecting condenser*1C has the similar abilities with a reflecting objective*1I with the exceptions of having some aberrations and providing an iris diaphragm and centering screws. The reflecting objective has the abilities of numerical aperture max. 1.0, magnification 100×, and working distance 1 mm. In addition to the merit of having no color aberration, the reflecting objective has practically neither spherical aberration nor coma by means of making its surface non spherical[18].

TABLE I

Crystal	Thickness (mm.)	Exposure time (min.)	Wave length of the 2nd band max. (mμ)	Wave length of absorption edge (mμ)	Method for preparation
$[Co(NH_3)_6](ClO_4)_3$	0.058	60	332	254	chloride+$HClO_4$, Ref. 8
$[Co(NH_3)_6]_2(SO_4)_3 5H_2O$	0.076	60	336	265	chloride+H_2SO_4, Ref. 9
$[Co(NH_3)_6]_2(HPO_4)_3 4H_2O$	0.032	30	336	274	chloride+Na_2HPO_4, Ref. 10
$[Co(NH_3)_6]Cl_3$	0.021	30	330	299	Ref. 7
$[Co(NH_3)_6]Br_3$	0.01	30	—	357	chloride+HBr, Ref. 11
$[Co(NH_3)_6]I_3$	0.038	5	—	505	chloride+KI, Ref. 12
$[Co(NH_3)_6]Cl(ClO_4)_2$	0.040	20	331	259	chloride+NH_4ClO_4, Ref. 13
$[Co(NH_3)_6]Cl(SO_4)3H_2O$	0.045	30	334	265	chloride+Na_2SO_4, Ref. 14
$[Co(NH_3)_6]Br(SO_4)$	0.040	30	336	287	bromide+H_2SO_4, Ref. 10
$[Co(NH_3)_6]I(SO_4)$	0.056	30	—	354	sulfate+KI, Ref. 15
$[Co(NH_3)_6]I(SeO_4)$	0.035	30	—	364	Ref. 8
$[Co(NH_3)_6]_2(C_2O_4)_3 4H_2O$	0.041	30	332	292	chloride+$(NH_4)_2C_2O_4$, Ref. 16
$[Co(NH_3)_6](NO_3)_3$	0.048	30	—	—	chloride+HNO_3, Ref. 9
$[Co(NH_3)_6](NO_2)_3$	0.022	30	—	—	chloride+$NaNO_2$, Ref. 17

6) Y. Tanabe and S. Sugano, *J. Phys. Soc. Japan*, **9**, 753, 766 (1954).
7) J. Bjerrum and J. P. McReynolds, "Inorganic Syntheses", Vol. II, p. 217.
8) O. Hassel and G. Bödtker Naess, *Z. anorg. Chem.*, **174**, 25 (1928).
9) S. M. Jörgensen, *Z. anorg. Chem.*, **17**, 457 (1898).
10) S. M. Jörgensen, *J. prakt. Chem.*, (2) **35**, 431 (1887).
11) W. Biltz, *Z. anorg. Chem.*, **83**, 178 (1914).
12) E. Fremy, *Ann.* **83**, 290 (1892).
13) H. Alvisi, *Gazz. chim. ital.*, **31**, II, 291 (1901).
14) T. Klobb, *Bull. soc. chim. France*, (3) **25**, 1025 (1901).
15) F. Ephraim and W. Flügel, *Helv. chim. Acta*, **7**, 739 (1924).
16) E. Birk and W. Biltz, *Z. anorg. Chem.*, **153**, 124 (1926).
17) E. Birk, *Z. anorg. Chem.*, **164**, 243 (1927).
*1 Made by Olympus Optical Co, Ltd., Tokyo.
18) S. Miyata, S. Yanagawa and N. Noma, *J. Optical Soc. Am.*, **42**, 431 (1952).

A crystal E is chosen from a sample and its thickness is determined under a travelling microscope. This is placed on a fused quartz slide glass D and is covered with a fused quartz cover glass F and then the latter is sealed with paraffin G to the former. These are brought into the apparatus. As the microscope is a liquid immersion type, the space between C and I is filled with the glycerin water mixture H whose glycerin content is about 90% and the refractivity of which is identical with that of quartz, $n_d=1.458$. Focusing is carried out by inspecting through a glass eyepiece J, which is then removed. The image of the crystal magnified by the microscope is projected on the slit of a Jobin-Yvon medium type quartz spectrograph K and an absorption spectrum is photographed on a dry plate together with a wave length scale, the slit width being fixed at 0.2 mm. throughout this study. A qualitative absorption curve is obtained by tracing the plate photographed with a recording microphotometer. The thicknesses of the crystals used and the time exposed are shown in Table I. As our condenser has the numerical aperture of 1.0, its condensed light falls on the samples, not parallel, but with the angles of max. 43°18′ to the center line. Therefore, the thicknesses shown in the table do not indicate the actual thicknesses of the crystals passed by the light, the true values being a little larger than those reported.

Schwarzschild-Villiger Effect.—Although the reflecting objective is stated to have less Schwarzschild-Villiger (S-V) effect[19] which is very important in microspectrophotometry, than the usual transmission microscope, the stray light entering the objective from the exterior of a sample may still produce a large error in the result obtained. To avoid this, crystals which had larger areas than 0.1 mm.×0.1 mm. were used throughout this study with a few exceptions, considering the image of the light source projected on the crystals was the circle whose diameter was about 0.03 mm. It was proved that the stray light had no effect on the spectra obtained, since the highly absorbed part of the dry plate photographed was perfectly blank after long exposure.

Results

From the smooth microphotometer traces of blanks shown in Fig. 2, it will be apparent

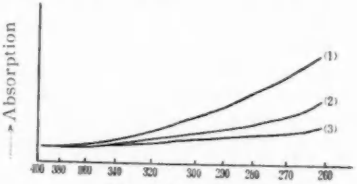

Fig. 2. Microphotometer traces of blanks; exposure time: 10 min. (1), 30 min. (2). 60 min. (3).

19) See for example: H. Naora, *Science*, **114**, 279 (1951); **115**, 248 (1952); *Biochim. Biophys. Acta*, **9**, 582 (1952).

that the light source, the optical system and the dry plate give no selective absorption on the spectra obtained, and that our qualitative method is satisfactory for the detection of absorption bands. In the spectra of the perchlorate, the sulfate and the hydrogen phosphate shown in Fig. 3*2, the second

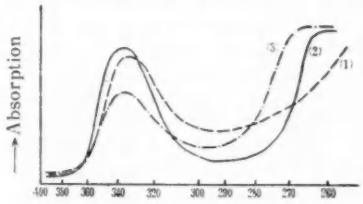

Fig. 3. Absorption spectra of the crystals of hexamminecobalt(III) perchlorate (1), sulfate (2) and hydrogen phosphate (3).

absorption band due to a *d* electron appears clearly, the position of which is about the same in these salts and is almost identical with that in aqueous solutions. There is practically no absorption in the range between the second band and the intense absorption edges*3 found at shorter wave lengths. It is apparent that these absorption edges are not due to the anions, since these disply no absorption down to 220 mμ[20].

In the spectra of the halogenides shown in Fig. 4, the edge absorption moves to

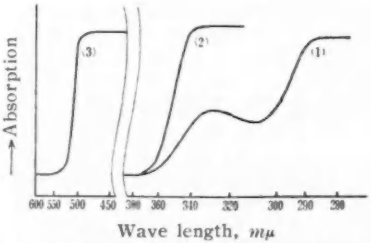

Fig. 4. Absorption spectra of the crystals of hexamminecobalt(III) chloride (1), bromide (2) and iodide (3).

longer wave lengths in the following order: iodide > bromide > chloride, thus covering

*2 The flattened upper and lower parts of the spectra indicate the perfect absorption and transmission of light, respectively.

*3 The term, edge absorption or absorption edge, is used, for convenience, throughout this study to designate our band in question, since it is beyond the ability of our apparatus to determine the stronger part of the spectra using thinner crystals than those used here, because thin crystals usually are attended with smaller sizes, which result in the increase of the S-V effect as stated above. To avoid this, the use of the microscope having much larger magnifying power than the one used here is necessary.

20) S. Kato, *Sci. Papers Inst. Phys. Research*, Tokyo, **13**, 7 (1950).

perfectly the second band in the bromide and the iodide. This red shift is the feature of the spectra in crystals, as the second band appears clearly in dilute aqueous solution even in the case of the iodide. In the series of the chloride perchlorate, the chloride sulfate, the bromide sulfate, the iodide sulfate and the iodide selenate shown in Fig. 5, the

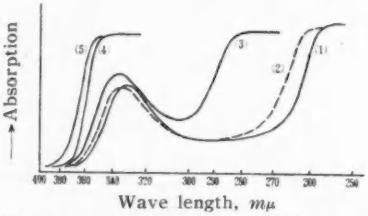

Fig. 5. Absorption spectra of the crystals of hexamminecobalt(III) chloride perchlorate (1), chloride sulfate (2), bromide sulfate (3), iodide sulfate (4) and iodide selenate (5).

absorption edge behaves like the simple halogenides, but is shifted to a shorter wave length as compared with that of the corresponding halogenide. The absorption spectrum of the oxalate shown in Fig. 6 resembles

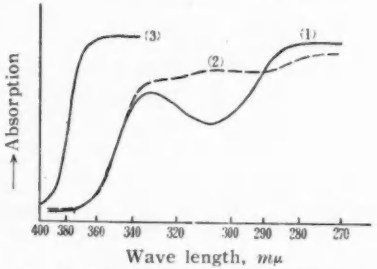

Fig. 6. Absorption spectra of the crystals of hexamminecobalt(III) oxalate (1), nitrate (2) and nitrite (3).

that of the chloride. Here again, it is apparent that the edge absorption is not attributable to the anion, as it absorbs at a shorter wave length (ca. 270 mμ)[21]. In the spectra of the nitrate and the nitrite shown in the same figure, the absorption bands due to the anions make it impossible for one to determine exactly the positions of the absorption edges.

The positions[*4] of the absorption edges are listed in Table I. The results obtained are summarized as follows; in the absorption spectra of the crystals of hexamminecobalt (III) salts, there are strong edge absorptions, the positions of which are shifted to longer wave lengths as compared with those in aqueous solutions and are largely affected by anions.

Discussion

Comparison of the Present Results with Kobayashi's.—In the spectrum of the crystal of hexamminecobalt(III) chloride, Kobayashi[5] found the distinct absorption maximum at 282 mμ which had a little lower intensity than that of the second band. In the present study, however, this absorption peak which had been called by Tsuchida and Kobayashi the third band was not found not only in the chloride, but was also absent in the mixed chlorides with the perchlorate or the sulfate, in which the content of the chloride ions was diminished to one-third of the pure chloride. In place of absorption peaks we have obtained absorption edges which indicate the existence of much stronger absorption bands than the second band.

This discrepancy will be interpreted by considering the S-V effect in the apparatus used by Kobayashi, in which the condenser having small magnifying power and the transmission microscope, which are both apt to produce stray light, are employed Since the stray light increases as the wave length becomes shorter, it is expected that the sum of the light really transmitted and the stray light may produce a spurious maximum at a given wave length. It should also be pointed out that the error due to the S-V effect gets greater as the optical density of a sample becomes larger, and according to Naora[19], in some extreme cases, a sample having the transmittance of 1% indicated the erroneous value of 20%.

The above statement will also apply to the spectra of other cobalt(III) ammine in which Kobayashi found either no absorption bands or weak ones in crystals, even in the case where complexes showed strong absorption in aqueous solutions. In fact, the discrepancy has been found recently in the crystals of dinitrotetramminecobalt(III) salts investigated by Faust and Quagliano[22]. In place of only one broad weak band reported by Kobayashi, they obtained the strong absorption bands corresponding to those in aqueous solutions using a potassium bromide disk method.

21) H. Ley and B. Arends, *Z. physik. Chem.*, **B17**, 177 (1932).

*4 These were obtained by subtracting a corresponding blank curve from each absorption spectrum, and taking, for convenience, the wave length of the edge absorption which had the same intensity as that of the maximum of the second band. Where the latter was unknown, it was calculated from another salt assuming Lambert's law to be valid.

22) J. P. Faust and J. V. Quagliano, *J. Am. Chem. Soc.*, **76**, 5346 (1954).

Origin of the Edge Absorption.— The dependence of the edge absorption on anions is understood only by considering the strong interaction between a complex ion and an anion in a crystal. We shall first consider the possibility of interpreting the edge absorption by the transitions of the electrons within a complex ion.

According to Tanabe and Sugano[6], a possible transition responsible for the third band in cobalt(III) complexes is a two-electron excitation, $(d\varepsilon^5)^1A_1 \rightarrow (d\varepsilon^4 d\gamma^2)^1F_2$. The degree of the energy change in the upper level, $^1F_2$, by the change in a crystalline field is, though a little larger, not so different from those in the levels, $(d\varepsilon^5 d\gamma)^1F_1$ and $(d\varepsilon^5 d\gamma)^1F_2$, which are responsible for the first and the second bands, respectively, in so far as we assume that, even in crystals, the field acting on the cobalt ion is of cubic symmetry as a first approximation. Therefore, the fact that the edge absorption is remarkably affected by anions, in contrast to the almost unchanged second band, suggests that the former is not due to the above transition. Moreover, the intensity criterion made by Tanabe and Sugano that as the mixing with another configuration may be small, the third band must have a much lower intensity than those of the first two bands, makes the two-electron jump hypothesis more inadequate for the origin of the edge absorption. Further evidence substantiating the above conclusion will be given in the last section of the discussion.

Tsuchida and Kobayashi[5] proposed the idea that the ammonias in ammine complexes dissociated into amino radicals and protons as a result of the hydrogen bonds with anions, and that the transition of the electron of the amino radical thus formed to the central atom was the very one responsible for the third band in crystals. Actually, in the crystals of metal complexes the possibility of hydrogen bonding is very large. For example, we can find it in trinitrotriamminecobalt(III) and chlorodinitrotriamminecobalt (III) for which the hydrogen bonds between ammonias of one molecule and oxygens of the others were suggested by Tanito et al.[23], and in dichlorotetrammineplatinum(IV) chloride and chloropentammineplatinum(IV) chloride monohydrate in which the hydrogen bonds between nitrogens and anionic chlorines were found by Bokij et al.[24]. On the other hand, the partially dissociated character of strongly hydrogen bonded NH and OH groups, which results in the formation of non-bonding electrons, has recently been shown by Tsuboi[25]. The effect of an anion on the electron of the hydrogen bonded NH bond will be larger than on *d* electrons and largely determined by the hydrogen bonding power or the electro-negativity of the anion. Therefore if the edge absorption were due to the electron of the dissociated ammonia, it should shift to longer wave lengths and increase its intensity in the following order: chloride>bromide>iodide, since the approach of the anion will facilitate the transition and increase its probability. As the order in the shifts is contrary to the results obtained, the dissociation hypothesis must be abandoned.

The explanation of the far ultraviolet intense edge absorption of the hexamminecobalt(III) ion in aqueous solutions ($\log\varepsilon=4$) by the transition of the bonding electron of a Co-N bond proposed by Linhard[1] is interesting because of the facts that our band in question also absorbs strongly, and that the transition of bonding electrons usually produces intense absorptions. However, it is easy to show that if the edge absorption in crystals were due to the red shift of the one in aqueous solution, it should shift to longer wave lengths in the following order: bromide sulfate> iodide sulfate>iodide selenate>iodide>perchlorate, since the potential energy of an hexamminecobalt(III) ion in a crystal, $A'''e^2/r_a$, increases in this order (see Table II). Here again, this order is inconsistent with our results. Therefore, all the possible transitions within the complex ion stated above are inadequate to account for the edge absorption.

Secondly, we must consider the possibility of the red shift of the absorption band due to an anion which was taken up by Linhard[1] in an early stage and by Yoneda[26] recently to explain the association band in solutions. In oxy-acidic anions, sulfate, hydrogen phosphate, perchlorate, oxalate, nitrate and nitrite ions, there are the non-bonding electrons which were shown, in some cases, to be rather strongly affected by an outer field. For example, according to Schaumann[27], the weak band of nitrate ion in aqueous solutions at 302 mμ with $\varepsilon=7$ which is said to arise from an $n\rightarrow\pi$ transition[28,29], suffers in the crystal a large shift in its position, the

23) Y. Tanito, Y. Saito and H. Kuroya, This Bulletin, 25, 188 (1952); 26, 420 (1953).
24) G. B. Bokij and M. A. Poraj-Koshits, *Doklady Akad. Nauk S.S.S.R.*, 64, 337 (1949); G. B. Bokij and L. A. Popova, ibid., 67, 73 (1949).
25) M. Tsuboi, This Bulletin, 25, 385 (1952).
26) H. Yoneda, This Bulletin, 28, 125 (1955).
27) H. Schaumann, *Z. Physik*, 76, 106 (1932).
28) H. McConnell, *J. Chem. Phys.*, 20, 700 (1952).
29) W. G. Trawick and W. H. Eberhardt, ibid., 22, 1462 (1954).

values of which are 304 mμ for potassium nitrate, 291 mμ for sodium nitrate and 278 mμ for barium nitrate. Another example is the weak band of sodium nitrite at 350 mμ which is said to arise from the transition of the non-bonding electron of nitrogen to an anti-bonding orbital[29]. It was shown that the crystal of silver nitrite lacked this band on account of probable existence of the weak covalent binding between the nitrogen and the silver[29]. But, the present measurements on the crystals of hexamminecobalt(III) nitrate and nitrite suggest that the shift of the absorption band of the anions due to the complex ion is not sufficiently large to explain the remarkable shift of the edge absorption. The same is also observed in the absorption bands of chromate and permanganate ions which are both said to arise from $n \rightarrow \pi$ transitions[30] and are almost equal in aqueous solution and in mixed crystals[31].

Although we can not draw any definite conclusion as to whether the red shift of the absorption band of an anion can explain the edge absorption from the above discussion, the situation is simpler in the halogendies than in the oxy-acidic salts, as will be seen in the following paragraphs.

Absorption spectra of alkali halogenides in gaseous molecules, aqueous solution and crystals were studied extensively by many workers[32], and the results showed that there was no evidence of the transition within an anion and the absorption spectra were due to the transfer of an electron from an anion to a cation or water. That this is also true in our crystals containing halogen ion is shown by the following consideration: if the edge absorption of the iodide sulfate and the iodide were the absorption band of the iodide ion perturbed by a crystalline field, the former should be more bathochromic than the latter, since the potential energy of the iodide ion in the crystals, $A'e^2/r_\alpha$, is larger in the iodide sulfate than in the iodide as is seen from Table II. As this is contrary to the experimental results, the possibility of the red shift of the absorption band of an anion must be excluded at least in the halogenides and the edge absorption must be interpreted by the transfer of an electron from an anion to the complex ion, as in the association band in aqueous solution.

Such an electron transfer is also expected in the oxy-acidic anions, since the far ultraviolet intense absorption bands of nitrate, nitrite, chlorate ions etc. have been attributed to the transfer of an electron from an anion to its hydration sphere[33], although the alternative interpretation which assigned $\pi \rightarrow \pi$ transitions to them also exists[29].

Calculations of the Differences Between the Wave Lengths of the Absorption Edges by the Energy Cycle Method.—If the edge absorption is an electron transfer spectrum, it should correspond to the first absorption band of ionic crystals due to an exciton, the wave length of which can be calculated by the energy cycle method as is usually performed. We shall do this below to the bands of the iodide, the iodide selenate, the iodide sulfate and the bromide sulfate.

We perform the following cycle[34,35,36].

1) Remove a halogen ion[*5] from a crystal; the work necessary is $A'e^2/r_\alpha$, where A' is the crystal potential constant at the lattice point of the halogen ion and r_α the lattice constant of the crystal.

2) Remove an electron from the halogen ion; the work necessary is E, the electron affinity of the corresponding halogen atom.

3) Replace the halogen atom; the work necessary is zero.

4) Remove a neighbouring hexamminecobalt(III) ion from the crystal; the work necessary is $(A'''-B)e^2/r_\alpha$, where A''' is the crystal potential constant at the lattice point of the hexamminecobalt(III) ion and B the potential constant at that point due to a neighbouring halogen ion.

5) Add the electron to the hexamminecobalt(III) ion; the work necessary is $-I$, where I is the ionization potential of an hexamminecobalt(II) ion.

6) Replace the hexamminecobalt(II) ion; the work necessary is $-2(A'''-B)e^2/3r_\alpha$.

7) The movement of the electron from the halogen ion to the hexamminecobalt(III) ion will polarize the surrounding medium; the polarization energy is denoted by $-\omega$.

8) It will also polarize the halogen atom and the hexamminecobalt(II) ion; we denote the polarization energy of the former by $-\Omega_X$ and that of the latter, plus the decrease in the energy due to the dipole formed in the latter, by $-\Omega_L$.

Adding the contributions of covalent binding, the van der Waals force and hydrogen bonding designated by ΔU, the total energy $h\nu$ of an edge absorption is thus given by

30) M. Wolfsberg and L. Helmholz, *J. Chem. Phys.*, **20**, 837 (1952).
31) J. Teltow, *Z. physik. Chem.*, **B43**, 198 (1939).
32) E. Rabinowitch, *Revs. Modern Phys.*, **14**, 112 (1942).
33) H.L. Friedman, *J. Chem. Phys.*, **21**, 319 (1953); see also Ref. 32.
34) W. Klemm, *Z. Physik*, **82**, 529 (1933).
35) N.F. Mott, *Trans. Faraday Soc.*, **34**, 500 (1938).
36) Y. Uehara, *J. Chem. Soc. Japan (Pure Chem. Sec.)*, **63**, 597 (1942).

$$h\nu = \psi + E - I - \omega - \Omega_X - \Omega_L + \Delta U, \qquad (1)$$

where $\psi = A'e^2/r_a + (A''' - B)e^2/3r_a$.

Unfortunately, even the approximate calculations of $h\nu$'s are impossible for the reason that the values of I and ΔU are unknown, and also the estimations of ω and Ω_L are impossible since the estimation of the former requires the unknown polarizabilities of hexaminecobalt(III) and sulfate or selenate ions and that of the latter requires the unknown polarizability of hexamminecobalt(II) ion, according to the method of Klemm[34].

Thus, we must content ourselves only with calculating the differences of the $h\nu$'s between those salts. Taking into account the fact that the sum of ω and Ω_L are a few eV in alkali halogenides, the differences between the halogenides of a same cation being much smaller[34,35], the values of Ω_X are less than 0.1 e.V. in our crystals*3, and the values of ΔU are also a few eV, even in the silver halogenides[37] which have considerable covalent character, we neglect these terms in Eq. 1, which then becomes

$$h\nu = \psi + E - I \qquad (2)$$

Then, we have only to calculate the crystal potential constants. The crystal structures of hexamminecobalt(III) iodide and perchlorate were determined by Meisel and Tiedje[38], et al. being an anti- $(NH_4)_3FeF_6$ type (see Fig. 7). On the other hand, the iodide selenate, iodide sulfate and bromide sulfate have an anti- K_2PtCl_6 type structure according to Hassel and Bödtker Naess[8], et al. (Fig. 8).

Now, we assume that the +3 charges on the hexamminecobalt(III) ion are concentrated on the cobalt. The assumption is justified in so far as potential constants are concerned, since the calculation based on the assumption that the charge is zero on the cobalt, therefore +1/2 on each nitrogen atom, according to Pauling's neutrality principle[39], gives the potential constant of 6.88 which is very close to that of 6.93 calculated on the former assumption, even for the nearest

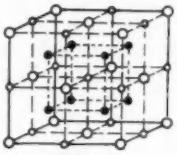

Fig. 7.

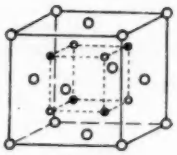

Fig. 8.

Fig. 7. Crystal structure of hexamminecobalt(III) iodide and perchlorate; the large circles are the hexamminecobalt (III) ions, and the small ones, open and solid, are the iodide or perchlorate ions.

Fig. 8. Crystal structure of hexamminecobalt(III) iodide sulfate, iodide selenate and bromide sulfate; the large circles are the hexamminecobalt(III) ions, the small open circles are the halogen ions and the small solid ones the sulfate or selenate ions.

halogens. Thus, we are justified for treating our crystals as having a BiF_3 or a CaF_2 type structure. Their crystal potential constants can easily be obtained using the potential data calculated for the cubic lattice by the method of Ewald. The potential, $a\psi(xyz)$, at the lattice point (000) due to the simple cubic lattice situated on lattice points $a(xyz)$ are given as follows[40]:

$$a\psi(000) = \varphi_0 = -2.83729$$
$$a\psi(00\tfrac{1}{2}) - \varphi_0 = \varphi_1 = 2.7414$$
$$a\psi(0\tfrac{1}{2}\tfrac{1}{2}) - \varphi_0 = \varphi_2 = 2.2548$$
$$a\psi(\tfrac{1}{2}\tfrac{1}{2}\tfrac{1}{2}) - \varphi_0 = \varphi_3 = 2.0354$$
$$a\psi(\tfrac{1}{4}\tfrac{1}{4}\tfrac{1}{4}) - \varphi_0 = \varphi_4 = 2.6368.$$

From Figs. 7 and 8 and taking into consideration the +3 charges on the hexamminecobalt(III) ions and the −2 charges on the sulfate and selenate ions, our expressions for the crystal potential constants are given as follows:

for the iodide and the perchlorate,

$$A' = -3\varphi_1 - 3\varphi_2 - \varphi_3 + 8\varphi_4$$
$$A''' = 9\varphi_1 - 27\varphi_2 + 3\varphi_3 + 24\varphi_4;$$

for the iodide selenate, the iodide sulfate and the bromide sulfate,

$$A' = -6\varphi_1 - 3\varphi_2 - 2\varphi_3 + 12\varphi_4$$
$$A''' = -27\varphi_2 + 36\varphi_4.$$

B is easily calculated to be 6.9282. The values of A' and A''' are listed in Table II, together with r_a, ψ and E. The differences of the $h\nu$'s calculated between four salts are also given as well as the observed values.

Table II indicates that there is fairly good agreement between the $\Delta h\nu$'s calculated and

*5 In the crystal of hexamminecobalt (III) iodide, there are two kinds of iodide ions, whose distances from the complex ion are not the same (see Fig. 7). We assume that the edge absorption in this crystal is due to the transition of the electron of the iodide ion nearer to the complex ion.

37) Y. Uehara, *J. Chem. Soc. Japan (Pure Chem. Sec.)*, **63**, 1041 (1942); S. Kikuchi and S. Umano, ibid., **70**, 94 (1949).

*6 According to Klemm, Ω_X is represented by $\Omega_X = e^2\alpha_X/2r_0^4$, where α_X is the polarizability of a halogen atom which is assumed to be 70% of that of the corresponding ion, and r_0 is the shortest cation-anion distance.

38) K. Meisel and W. Tiedje, *Z. anorg. Chem.*, **164**, 223 (1927).

39) L. Pauling, *J. Chem. Soc.*, **1948**, 1461.

40) T. Nagamiya and T. Matsubara, "The Theory of Solids", Vol. I, Kyoritsu Shuppan Co., Tokyo (1951), p. 234.

TABLE II

Crystal	A'	A'''	r_α(A)	ϕ(e.V.)	E(e.V.)	$\Delta h\nu_{calc.}$	$\Delta h\nu_{obs.}$
$[Co(NH_3)_6](ClO_4)_3$	4.0704	33.1824	11.38	16.20			
$[Co(NH_3)_6]I_3$	4.0704	33.1824	10.91	16.90	3.12	>0.96	0.96
$[Co(NH_3)_6]I(SeO_4)$	4.3580	34.0452	10.79	17.86	3.12	>0.13	0.09
$[Co(NH_3)_6]I(SO_4)$	4.3580	34.0452	10.71	17.99	3.12	>0.74	0.82
$[Co(NH_3)_6]Br(SO_4)$	4.3580	34.0452	10.51	18.33	3.52		

observed. Thus, the red shift of the edge absorption in the order listed in the table could be interpreted using the theory of the exciton. Unfortunately, the lattice structures of the chloride, the bromide and the chloride sulfate are unknown*7. The complete explanation of the observed order in $h\nu$ is, therefore, impossible, but it will be suggested that the increase in E and the probable decrease in r_α will be the major factors determining the increasing tendency of $h\nu$, though potential constants are necessarily different from that of a cubic lattice in the monoclinic lattice of the chloride and the rhombic one of the bromide.

As was stated previously, in the crystals containing oxy-acidic anions, the possibility of interpreting the edge absorption by the red shift of the anion's absorption was not excluded. However, it must be pointed out here that the fact that the edge absorptions exist at shorter wave lengths in those salts shown in Fig. 3 than those of the halogenides will be interpreted by the electron transfer theory, since the large ionization potential of oxygen (10 e.V. in perchlorate ion[30]) may be the principal factor determining the increase in $h\nu$.

Effect of a Crystaline Field on the Second Absorption Band.—In the preceding paragraphs, we neglected to discuss the behavior of the second band in crystals. Now, we shall briefly consider below the effect of a crystalline field on this band. The crystalline field theory mentioned above tells us that the stronger the crystalline field becomes, the larger the splitting of a d level, say in our case, the difference between the excited level, $(d\varepsilon^5 d\gamma)^1F_2$, which is responsible for the second band and the ground one, $(d\varepsilon^6)^1A_1$, becomes. The expectation is attained in our crystals, as the second band exists at shorter wave lengths in crystals (330–336 mμ) than in aqueous solutions (339 mμ). This is also true for the larger shifts of the second band in the chloride and the chloride perchlorate than that of the others, since the crystalline field in these complexes is expected to be stronger than in the others.

It is of interest to note here that if the edge absorption were of similar origin with the second band, it must shift to shorter wave lengths as compared with the one in aqueous solutions, contrary to our results. This is another reason why the two-electron jump hypothesis must be discarded.

*7 In the famous W. Hückel's "Anorganische Strukturchemie", Ferdinand Enke Verlag, Stuttgart (1948), p. 548, Fig. 68b, hexamminecobalt(III) chloride is illustrated as having a cubic lattice. This is incorrect, since its crystal form is monoclinic. It seems to the present author that its lattice structure has not so far been analysed as well as that of the bromide.

Summary

(1) The ultraviolet absorption spectra of the crystals of fourteen hexamminecobalt(III) salts were qualitatively measured using a reflecting microscope (magnification 100×), a quartz spectrograph and a recording microphotometer.

(2) All the crystals investigated showed, besides the weak absorption bands due to the complex ion, the strong absorption edges which were situated at longer wave lengths than those in aqueous solutions, and the positions of which were largely affected by anions. The most remarkable example was the iodide, the absorption edge of which extended to the visible region.

(3) It is concluded that, at least in the case of the halogenides, all the possible transitions within the complex ion and an anion are inadequate explanations and the electron transfer from an anion to the complex ion is most statisfactory for the origin of these strong absorption bands.

(4) The differences between the wave lengths of the absorption edges of hexamminecobalt(III) iodide, iodide selenate, iodide sulfate and the bromide sulfate were calculated by the energy cycle method and the results agreed fairly well with the experimental values, thus showing that these bands corresponded to the excition bands in ionic crystals.

Special acknowledgment is due to M. Linhard, R. Tsuchida and M. Kobayashi whose works stimulated this investigation. The author wishes to express his sincere thanks to Prof. T. Uemura and Prof. Y. Inamura for their kind encouragement and advice. The author's thanks are also due to Prof. K. Kozima who gave him a chance to use the recording microphotometer, and to Mr. W. Suetaka and Mr. M. Nakahara for their kind help in the microphotometer tracing.

Laboratory of Inorganic Chemistry,
Tokyo Institute of Technology,
Tokyo

Studies on Molecular Structure by the Measurement of the Dielectric Constants of Gases. III. The Dipole Moment and the Structure of Alkyl Nitrites

By Takehiko CHIBA

(Received April 18, 1955)

Studies on molecular structure concerning the internal rotation have been made on many compounds such as ethane derivatives[1] but in these compounds both ends of internal axis have three atoms or groups which contribute to the forces determining the structure of these compounds. In alkyl nitrites both ends of the internal axis N-O have only an oxygen atom and a group R respectively, which will make the treatment easier. Recently Tarte made infrared investigation on alkyl nitrites[2] and found that there are two rotational isomers in these compounds.

This paper reports the results of the dipole moment measurement on some of the alkyl nitrites: ethyl, isopropyl, and tertiarybutyl nitrites in the gaseous state at various temperatures.

Preparation of the Materials

The samples were prepared by dropping concentrated hydrochloric acid in the mixture of corresponding alcohol and 35% aqueous solution of sodium nitrite in cooling. The raw products of the *i*-propyl and *t*-butyl nitrites seemed to decompose when washed with water; they were therefore first dried over calcium chloride and distilled, and then dry air was passed though them to exile the remaining NO and NO_2 gases, and finally redistilled. Ethyl nitrite was washed with sodium carbonate solution and distilled over calcium chloride. Ethyl nitrite b.p. 17°C, *i*-propyl nitrite b.p. 39.2–.4°C, *t*-butyl nitrite b.p. 63.0°C.

The Procedure and the Results of the Measurement

Because of the instability of the alkyl nitrites the measurement was made at temperatures below about 60°C. The electric part of the apparatus is that described in the previous paper[3], but some improvements were made on the thermostat, the gas cell, and the gas filling devices. A Dewar-vessel filled with insulating oil was used for the thermostat at low temperature (down to −20°C). Ethyl and propyl nitrites have vapor pressures high enough for the measurement of dielectric constant at these temperatures. The dimensions of the gas cell are the same as the cell "D" of the previous paper, but in order to keep the lead from contact with oil in the bath, a new cell was constructed which is shown in Fig. 1. To reduce the

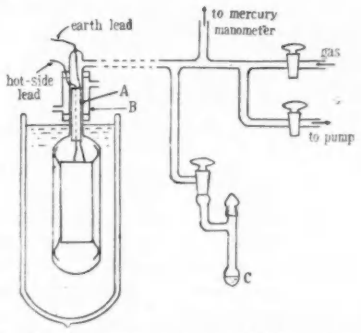

Fig. 1. Gas cell and vapor filling system.

stray field the hot-side lead was covered with a nickel cylinder (A) of earth-side which itself formed a part of the earth lead. The part (A) was covered with a glass mantle (B) through which dry air was allowed to flow to avoid the condensation of moisture on it.

The cell constant was calibrated many times by measuring the dielectric constant of carbon dioxide, and further checked with carbon tetrachloride and benzene. The correction due to the capacity of the part (A) was computed as a coaxial cylinder. Samples were introduced into the reservoir (C) by vacuum distillation. After each run of observations of $\Delta\varepsilon$ and Δp, the cell was pumped out, and a fresh sample was used for each observation to avoid the errors due to the decomposition of the sample.

The results of the observations are summarized in Table I, Though these compounds are appreciably yellow colored, the extrapolation of the refractive index in visible region to infinite wave length shows no

1) S. Mizushima, "Molecular Structure and Internal Rotation", (1954).
2) P. Tarte, *J. Chem. Phys.*, 20, 1570 (1952).
3) T. Chiba, This Bulletin, 28, 19 (1955).

TABLE I

OBSERVED POLARIZATIONS AND DIPOLE MOMENTS OF ETHYL, *i*-PROPYL AND *t*-BUTYL NITRITES

Ethyl nitrite

$P_E+P_A=1.05MR_D$(assumed)$=18.5$ cc.

T(°K)	n	p(mmHg)	P(cc.)	ΔP(cc.)	μ(D)
253.3	8	64–85	158.1	0.4	2.40_9
266.7	6	70–82	151.8	0.2	2.41_4
295.9	7	85–131	139.0	0.4	2.41_7
298.0	6	69–90	138.2	0.3	2.41_8
316.1	6	70–104	130.5	0.4	2.41_0
333.8	8	70–97	124.8	0.4	2.41_2

i-Propyl nitrite

$P_E+P_A=1.05MR_D$(assumed)$=23.3$ cc

T	n	p	P	ΔP	μ
256.1	7	33–52	181.6	0.6	2.57_8
267.4	8	25–56	174.9	0.3	2.57_8
284.2	7	46–63	164.7	0.5	2.56_8
300.3	8	51–74	157.2	0.2	2.56_8
314.3	8	54–70	151.2	0.5	2.56_8
332.4	7	56–83	143.8	0.4	2.56_2

t-Butyl nitrite

$P_E+P_A=1.05MR_D$(assumed)$=28.1$ cc.

T	n	p	P	ΔP	μ
288.8	5	45–51	183.2	0.6	2.71_1
291.0	6	41–63	181.1	0.7	2.70_1
301.4	4	51–63	175.1	0.4	2.69^5
313.2	5	65–77	169.2	0.4	2.69_1
330.1	5	57–67	161.2	0.3	2.68_4

n: number of the observations.
p: pressure range of the observations.
ΔP: average deviation of P.

abnormality; for instance, for ethyl nitrite, $MR_D=17.60$ cc., $MR_\infty=17.32$ cc. (extrapolated), and a sum of atomic refractions $\Sigma AR_D=16.9$ cc. Therefore, P_E+P_A is taken as $1.05MR_D$ as in the usual cases.

The moment of ethyl nitrite in the gaseous phase was given by Czerlinsky[4] to be 2.38D at 17°C, and the dielectric constant of ethyl nitrite at 15°C and 760 mmHg given by Cordonier[5] is 1.0182, which corresponds to the dipole moment of 2.43D. The present results are in good agreement with these two.

Discussion

According to the infrared study of Tarte[2] the absorption lines assigned to $\nu_{N=O}$, ν_{N-O}, ν_{C-O}, and δ_{ONO} have doublet structure, the ratio of the intensity of each doublet line depending on alkyl radical, as well as on temperature. This phenomenon was explained adequately by the existence of the rotational isomers. It is, however, difficult to attribute the effect of giving two isomers to the forces such as steric or dipole one, since these forces should vary monotonously from the *cis* to the *trans* position. The possible explanation of this is to take into account resonances such as

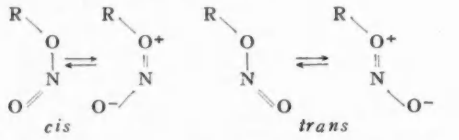

which stabilizes the planar structure, i.e., the *trans* and the *cis*. A calculation of resonance energy was made by a simple MO method to estimate barrier height at 90°C position. This calculation was made for a four-electron system of the skeleton of $-O^{++}-N^{+}-O^{+}$ and for the corresponding localized system, and the potential barrier is taken as a difference in resonance energy between them. This was made after the procedure employed by Kurita and Kubo[6] for the case of tropolone except exchange integral β_{ij} between atoms i and j, i.e., β_{ij} was taken as $\beta_{ij}=\beta\cdot s_{ij}/s$, where β is an exchange integral of benzene π-electron, s_{ij} and s are corresponding overlap integrals. Bond distances used were those given by Rogowski[7] for methyl nitrite: that is N-O: 1.37Å, N=O: 1.22Å. From this calculation the barrier height of 0.34β can be obtained; therefore if we assume 30 kcal./mole for β, this barrier is as high as about 10 kcal./mole. This is only an approximate value, but as shown later, it is a reasonable order of magnitude compared with the case of HONO, and therefore, it can be said that the resonance force is large enough to separate these molecules into two isomers.

Since there is a small temperature dependence of the moments of *i*-propyl and *t*-butyl nitrite (see Table I), it must be concluded that an energy difference exists between the *cis* and the *trans* forms. The energy difference can be calculated by use of the well-known formula of the average moment μ at the temperature T:

$$\bar{\mu}^2=\frac{\mu_c^2+\mu_t^2 s e^{\Delta E/RT}}{1+s e^{\Delta E/RT}}, \qquad (1)$$

where s denotes the ratio of the entropy factor of the *trans* form to that of the *cis* form. Its value cannot be computed since the curvatures at the potential minima are not known. Therefore, it is left as an un-

4) E. Czerlinsky, *Z. Physik*, **88**, 515 (1934).
5) Cordonier and Guinchaut, *Compt. rend.*, **185**, 1449 (1927).
6) Y. Kurita and M. Kubo, This Bulletin, **24**, 13 (1951).
7) F. Rogowski, *Ber.*, **75B**, 244 (1942).

known parameter which should be determined by the experiments.

Now, if the temperature dependence of the moment is small and $d\bar{\mu}/dT$ is constant in the range of the observation, then from Eq. (1) it is easily seen that

$$\Delta E = -2RT^2 \frac{(\mu_t^2 - \mu_c^2)\bar{\mu}}{(\bar{\mu}^2 - \mu_c^2)(\mu_t^2 - \bar{\mu}^2)} \cdot \frac{d\bar{\mu}}{dT}. \quad (2)$$

Thus the energy difference can be evaluated if we know the values of μ_c and μ_t without the knowledge of s. The value of s is calculated from Eq. (1), using the value of ΔE thus obtained[8].

The diple moments of the *cis* and the *trans* forms are calculated to be $\mu_c = 1.27$D, and $\mu_t = 2.97$D respectively, using $\mu_{N=O} = 2.0$D, $\mu_{N-O} = 0.3$D, $\mu_{R-O} = 1.1$D, and $\angle$RON = tetrahedral and $\angle$ONO = 120°.[9] The values of ΔE and s which give the best fit with the observed temperature dependence of the dipole moments using μ_c and μ_t obtained above are given in Table II. As mentioned above, the μ_t, it can safely be said that ΔE of *i*-propyl nitrite is estimated to be less than about 140 cal., and that of *t*-butyl nitrite to be less than 340 cal. Thus ΔE increases in the order of methyl, ethyl, *i*-propyl and *t*-butyl nitrites, although ΔE is not great in the last two compounds.

Tarte[11] obtained ΔE from the measurements of the temperature dependence of the intensity of absorption lines assigned to both isomers. His result is −350 cal. for methyl nitrite and nearly equal to zero for ethyl and *i*-butyl nitrites, and $\Delta E \geqslant 0$ in *t*-butyl nitrite. In the last case accurate value was not obtained since the *cis* absorption line is very weak. The constant moment of ethyl nitrite in the present work agrees well with his result.

We shall next consider these ΔE values from the theoretical considerations. First of all, it should be mentioned that the resonance effect is not a main cause of the energy difference between the isomers because the

Table II

ΔE and s values of alkyl nitrites estimated from the observed data of dipole moment

	$\mu_t = 2.97$D, $\mu_c = 1.27$D,		$\mu_c = 1.40$D, $\mu_t = 3.27$D.	
	s	ΔE cal./mol.	s	ΔE cal./mol.
CH_3ONO	1.5[a]	(−350)	0.9[a]	(−350)
C_2H_5ONO	1.4	0	0.8	0
$(CH_3)_2CHONO$	1.8	140	1.0	100
$(CH_3)_3CONO$	2.1	340	1.1	200

a: These values are estimated using dielectric constant data for methyl nitrite given by Cordonier (Ref. 5).

contribution of the resonance forms is considerable in these molecules. Hence in calculating μ_c and μ_t it will be more reasonable to take into account the polar structures[10]. However, the simple MO calculation does not provide a reliable estimate to the augmentation of the moments, since it has usually a trend to give considerably high values. In Table II there are also shown the values obtained by assuming 10% higher values for μ_c and μ_t. It is seen from this table that, if we take higher values for μ_c and μ_t, ΔE's of *i*-propyl and *t*-butyl nitrites becomes smaller. Hence, although there are some ambiguities in the values of μ_c and

effect of alkyl radical R on the resonance is that of a higher order. Therefore we have to look for the origin of the energy difference in some other effect. It is seen that the dipole-dipole interaction between R-O and O-N stabilizes the *cis* position whereas the steric force between the radical R and the end O atom has an opposite effect. Since dipole interaction energy does not vary so much by replacing R, the difference obtained for different radicals may be mainly due to the steric effect. It can easily be understood that ΔE of steric nature is higher in (Et..... O) than in (Me.....O) because in the former a hydrogen atom of a methyl radical is replaced by another methyl and, in the same way ΔE in (*i*-Propyl,.....O) is higher than in (Et.....O), and in (*t*-Butyl.....O) higher than in (*i*-Propyl.....O). If we replace one hydrogen atom of a methyl radical by another methyl or by other alkyl radical with longer chain, the steric energy may remain nearly

8) ΔE is taken here to be positive when the *trans* form is more stable than the *cis* one.

9) $\mu_{N=O} = 2.0$D was given by Smyth from the value 2.5D of *t*-nitrosobutyl (Smyth, *J. Am. Chem. Soc.*, **60**, 183 (1938)). The moment of N=O bond presumably varies with the extent of resononce, but on account of the lack of other available data, the above value is tentatively used.

10) There is a possibility of larger μ_c and μ_t in higher alkyl nitrites by induction effect.

11) P. Tarte, unpublished.

the same, because the atoms in the radical are far apart from the oxygen atom and the steric energy is probably determined by the interaction between the end oxygen atom and the atoms in α, β-position of R. Really a similar situation has already been found in ethane derivative hydrocarbons. The hindering barrier against the internal rotation around C-C axis in propane is considerably higher than that in ethane, but the difference does not increase so much in *n*-butane, or *n*-pentane[12]. By these considerations, the observed change in ΔE by replacing R and the spectroscopic result of nearly equal ΔE in ethyl and in *i*-butyl nitrite can be adequately explained.

A peculiar feature of the spectrum of alkyl nitrites is that the ratio of the extinction coefficients ($\ln I_t/\ln I_c$) of the $\nu_{N=O}$ band in the *cis* and the *trans* isomers is constant in esters of same α-carbon class of R, but differs appreciably in different classes[2]. Now the ratio of the extinction coefficients is given by a product of the ratio of the number of molecules N_t/N_c and the square of the ratio of the change of the dipole moments with the normal mode of vibration:

$$\ln I_t/\ln I_c=(N_t/N_c)\,|(d\mu/dQ)_t/(d\mu/dQ)_c|^2. \quad (3)$$

It is easily seen that the change of the ratio N_t/N_c is small, because it is given by the expression $s\cdot\exp(\Delta E/RT)$ and the difference of ΔE is small. Therefore the large change of the extinction coefficients must be attributed to a large change of the ratio $(d\mu/dQ)_t/(d\mu/dQ)_c$. However, from the ordinary concept of the normal vibration, such a large change cannot be expected at all, since the inner vibration of the N=O group is hardly affected by the structure of the outer part of that group. One explanation is the change of the amount of resonance, but this must bring about a considerable change of ΔE, contrary to the observed result. Thus the explanation of the above fact requires further study.

Lastly a few words should be added with regards to HONO molecule. This molecule is too unstable for the measurement of the dipole moment, but several authors reported the infrared spectrum. It is interesting to compare these results with those of RONO. According to the studies of Jones[13] and of D'Or[14] the characteristic frequencies of this molecule $\nu_{N=O}$, and ν_{N-O}, and δ_{ONO} have doublet structure, from which the molecule is considered to have also two rotational isomers, the *trans* and the *cis* forms. From the measurement of the temperature dependence of band intensity, Jones concluded that the *trans* form is about 500 cal. more stable than the *cis* form. This conclusion seems to be unlikely at first sight, since the steric force between O and H in the *cis* position is smaller than that between O and R. Actually, however, in the spectrum of HONO there are several points different from that of RONO; namely, $\nu_{N=O}$ of RONO is lower than that of HONO, on the contrary, ν_{N-O} of the former is higher than that of the latter. From these results, Jones suggested that in HONO the central N-O bond is much weaker than in RONO, which is a result of a contribution of the resonance form (III) besides (I) and (II).

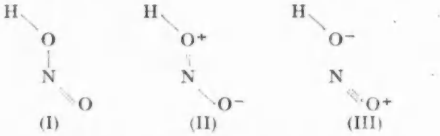

The potential barrier of internal rotation of HONO is found to be 9-10 kcal., using the torsional frequencies given by these authors, and assuming the cosine type potential ($V=\frac{1}{2}V_0(1-\cos\varphi)$). In RONO this frequency is not observed, but it is very interesting to compare the value 9-10 kcal. of HONO with the value 10 kcal. of RONO derived from the MO calculation described earlier.

Summary

The dipole moment measurement was made at various temperatures on ethyl, *i*-propyl and *t*-butyl nitrites. Observed moments are 2.41D for ethyl, 2.57D for *i*-propyl, 2.70D for *t*-butyl nitrite at room temperature. The moment of the latter two compounds decrease slightly with temperature while ethyl compound remains constant. These esters are considered to consist of two isomers: the *trans* and the *cis* separated by a barrier of several kcal. due to a resonance effect. The energy difference ΔE between the two isomers is found to be zero in ethyl, <140 cal. in *i*-propyl, and <340 cal. in *t*-butyl nitrite; in the latter two the trans from being more stable.

This change in ΔE with replacing R is satisfactorily explained as due to the steric energy between R and the end oxygen atom.

12) K. S. Pitzer, *Faraday Soc. Disc.*, **10**, 66 (1951); G. Herzberg, "Infrared and Raman Spectra", (1945), p. 520.
13) I.H. Jones et al., *J. Chem. Phys.*, **19**, 1599 (1951).
14) L. D'Or and P. Tarte, *Bull. soc. roy. sci. Liege*, **1951**, 478.

The author wishes to express his sincere thanks to Prof. Y. Morino and to Dr. Miyagawa for the kind guidance and valuable advice through this study and to Dr. P. Tarte of the University of Liège, who kindly informed the author of his spectroscopic results including some of the unpublished data. The cost of this research has been defrayed from the Grant in Aid for Fundamental Scientific Research from the Ministry of Education to which the author's thanks are also due.

Department of Chemistry, Faculty of Science, Tokyo University, Tokyo

---

Estimation of the Geologic Age of Radioactive Sediment Containing Radium Isotopes

By Hitoshi SAKAI

(Received February 18, 1955)

Introduction

The determination of the geologic age of sediment is one of the important and very difficult problems in geochemistry. Generally the complex conditions governing the sedimentation process present many difficulties for researchers.

So far as radioactive sediments are concerned, however, it is sometimes possible to estimate their geologic age. The ionium-radium method[1] proposed for the determination of the geologic age of deep-sea sediments is the best known example of this. But this method is only applicable to appreciably old sediments of several hundred years. Recently, Koczy[2] estimated the sedimentation intensities[3] of some sorts of clay by statistical calculations using the content of radium, manganese and titanium in these samples. In this case, however, it is obvious that the degree of accuracy is limited by the number of samples analyzed.

When a fairly young sediment contains isotopes of radium which are not supported by their long-lived parents, the abundance ratios of these isotopes should vary with the age of the sediment. Based upon this relation, three new methods are proposed for the estimation of sedimentation rate and intensity of young sediments which are approximately one to two hundred years old.

1) C. S. Piggot and W. D. Urry, *Ameri. J. Sci.*, 240, 1 and 93 (1942).
2) F. F. Koczy, *Geochim. et Cosmochim. Acta*, 1, 73-85 (1951).
3) Sedimentation intensity means the sedimentation velocity in gram per unit area per unit time, see koczy loc. cit.

Assumptions

In our methods, the following conditions are assumed to persist during the period of sedimentation.

(1) The abundance ratios of radium isotopes keep constant in the water precipitating sediments.

(2) There is no way for the elements once precipitated in the sediments to be lost by any process.

(3) Within the sediments, no migration of elements occurs.

(4) Sedimentation intensity of an element keeps constant and consequently the intensity is uniform at least in that part of the sediments which we examine.

The conditions (1) to (4) are necessary to develop the following methods (a) and (b), while in the method (c), the condition (3) is not necessary.

In this paper the following values are used as the decay constants of radioactive elements: 4.3×10^{-4}, 68.7, 3.1×10^{-2}, 0.10, 0.36 and 69.3 per year for Ra^{223}, Ra^{222}, Pb^{210}, Ra^{228}, Th^{228} and Ra^{224}, respectively. These values are calculated on the basis of nuclear data which appeared in the Table of Isotopes by Hollander, Perlman and Seaborg.

Principle of the Methods

(a) The Method Based on the Vertical Variation of the Ratios of Radium Isotopes.—Let us consider an infinitely thin layer in a sediment perpendicular to the direction of growth. The number of atoms of radium isotopes present in the layer at the time t

from the beginning ($t=0$) of sedimentation can be represented by the following equations.

$$[Ra^{226}]' = [Ra^{226}]\, e^{-\lambda_1 t}, \tag{1}$$

$$[Ra^{228}]' = [Ra^{228}]\, e^{-\lambda_2 t}, \tag{2}$$

$$[Ra^{224}]' = [Ra^{224}]\, e^{-\lambda_4 t} + \lambda_2\lambda_3/\lambda_4(\lambda_3-\lambda_2), [Ra^{228}]\,(e^{-\lambda_2 t} - e^{-\lambda_3 t}), \tag{3}$$

where $[Ra]'$ and $[Ra]$ stand for the number of atoms of radium in the layer at $t=t$ and $t=0$, respectively, λ_1, λ_2, λ_3 and λ_4 being the decay constants of Ra^{226}, Ra^{228}, Th^{228} and Ra^{224}, respectively. Deriving the above equations the contributions by Th^{228} and other long-lived parents are neglected because, as will be given later, the Th^{228} content in the water precipitating the sediment is negligibly small and because the effect by other long-lived parents is also negligibly small so far as a short period of from 100 to 200 years is concerned. In addition, the first term of the equation (3) can be neglected if t is longer than about thirty days as in our samples described later.

From equations (1) and (3), equation (4)′ is obtained.

$$[Ra^{224}/Ra^{226}]' = [Ra^{224}/Ra^{226}]\, e^{(\lambda_1-\lambda_4)t} + \lambda_2\lambda_3/\lambda_4(\lambda_3-\lambda_2)[Ra^{228}/Ra^{226}]\,(e^{-\lambda_2 t} - e^{-\lambda_3 t})/e^{-\lambda_1 t} \tag{4}'$$

where the first term can be neglected because it is much smaller than other terms when t is longer than about thirty days. Then by introducing numerical values for constants, equation (4) is obtained.

$$[Ra^{224}/Ra^{226}]' = 2\times10^{-3}[Ra^{228}/Ra^{226}]' (e^{-0.10t} - e^{-0.36t})/e^{-0.43\times10^{-4}t} \tag{4}$$

Here, according to condition (1), the ratio $[Ra^{228}/Ra^{226}]'$ can be represented by the corresponding ratio in the water at the present time, which can be determined experimentally. Also the ratio Ra^{224}/Ra^{226} in the layer now in qnestion can be determined. Thus the time elapsed after the layer was formed and consequently the rate of sedimentation for the sediment laying above the layer are calculated.

(b) The Method Based on the Vertical Variation of the Beta-activity of the Daughter Nuclides from Radium Isotopes.—The equation for the beta-activity in the same layer as considered in the method (a) can be similarly derived. Here, the contributions by short-lived nuclides originally precipitated from the water are neglected, and only the secondarily produced activities from Ra^{226}, Pb^{210} and Ra^{228} are taken into consideration. The activity due to beta particles from Pb^{210} can also be neglected because of their extremely low maximum energy. Then the beta activity of a layer is given by the following equations at the time t,

$$[\Sigma Ra^{226}]^t = 3\lambda_1[Ra^{226}]'e^{-\lambda_1 t} + (\lambda_5[Pb^{210}]' - \lambda_1[Ra^{226}]')e^{-\lambda_5 t}$$

$$[\Sigma Ra^{228}]^t = \lambda_2[Ra^{228}]\{(1+2/(\lambda_3-\lambda_2))e^{-\lambda_2 t} - 1/(\lambda_3-\lambda_2)\cdot e^{-\lambda_3 t},$$

where $[\Sigma Ra^{226}]^t$ and $[\Sigma Ra^{228}]^t$ stand for the beta-activity of Ra^{226}-series and of Ra^{228}-series, respectively, and λ_5 expresses the decay constant of Pb^{210}. Then by the summation of the two equations the total beta-activity of the layer, A_β^t, is obtained as follows:

$$A_\beta^t = 4.3\times10^{-4}[Ra^{226}]'\{3-(1-q)e^{-3.1\times10^{-2}t} + 8.7pe^{-0.10t} - 3.9pe^{-0.36t} \tag{5}$$

where $p=\lambda_2[Ra^{228}]'/\lambda_1[Ra^{226}]'$ and $q=\lambda_5[Pb^{210}]'/\lambda_1[Ra^{226}]'$.

By the same consideration as in the method (a) we can calculate the geologic age of a layer by measuring the total beta-activity of the layer, assuming q is also constant during the period of sedimentation.

(c) The Method Based on the Total Time Variation of the Abundance Ratios of Radium Isotopes in Sediments.—Let us consider a column parallel to the direction of growth of the sediment. The concentration of a radium is controlled by two factors, an increase of the isotope by sedimentation and a decrease by radioactive decay.

When dk and $d[Ra]^t$ express the increase of an isotope of radium by sedimentation and the total change of the isotope in the column, respectively, in a small time, dt, at $t=t$, the increase of the amount of the isotope at $t=t$ can be written by the following equation:

$$d(Ra)^t = dk - \lambda(Ra)^t\, dt,$$

where $(Ra)^t$ stands for the total amount of an isotope of radium in the column at $t=t$.

According to the condition (4), dk or $dk/dt = K$ in this equation is constant and we can solve the differential equation obtaining the total amount of the isotope in the column at $t=t$. Thus for Ra^{226} and Ra^{228} the following equations can be given:

$$(Ra^{226})^t = K_1(1-e^{-\lambda_1 t})/\lambda_1 \tag{6}$$

$$(Ra^{228})^t = K_2(1-e^{-\lambda_2 t})/\lambda_2 \tag{7}$$

When the determination is carried out at a

time t' after sample has been collected and when the time t' is sufficiently large in comparison with the half-life of Ra^{224} so that the sedimented Ra^{224} has completely decayed off at the time of determination, the total amount of Ra^{224} at this time will be obtained by integrating the equation (3) from t' to $t+t'$ giving the equation (8).

$$(Ra^{224})^{t+t'}=\{K_2/\lambda_4(\lambda_3-\lambda_2)\}\{\alpha(\lambda_3-\lambda_2-\lambda_3e^{-\lambda_2 t}+\lambda_2e^{-\lambda_3 t})+\beta\lambda_3(1-e^{-\lambda_3 t})\}, \quad (8)$$

where $\alpha=e^{-\lambda_2 t'}$, and $\beta=e^{-\lambda_2 t'}-e^{-\lambda_3 t'}$, respectively.

From the equation, (6) and (8), the total variation of the ratio, Ra^{224} to Ra^{226}, v.s. time in the column is represented by the following equation when we insert numerical values for constants:

$$(Ra^{224}/Ra^{226}_0)^{t+t'}=(K_2/18K_1)\{\alpha(0.26-0.36e^{-0.10t}+0.10e^{-0.36t})+0.56\beta(1-e^{-0.36t})\}/t+t' \quad (9)$$

where $e^{-\lambda_1(t+t')}$ is approximated to $1-\lambda_1(t+t')$.

In this equation K_2/K_1 is considered to be equal to the abundance ratio of the two isotopes in the water. Then the geologic age of the sediment as well as the mean rate of sedimentation can be estimated by measuring the ratio, Ra^{224} to Ra^{226}, in the total mass of the columnar sample.

The Rough Estimation of the Sedimentation Rate as well as the Sedimentation Intensity of Hokutolite.

Hokutolite is one of the radioactive sinter deposits from hot springs[4,5] and is being precipitated from spring waters at temperatures ranging from 98°C to 40°C. In most cases, it is growing layer by layer on the surface of the base rock, andesite and is considered to be the most suitable sample for our methods.

The content and the ratios of radium isotopes in the spring water are shown in Table I. Pb^{210} is also supposed to be present, but the content in the water has not yet been determined. In Table II are shown the mean content of Ra^{226} and ratio, Ra^{224} to Ra^{226}, in the two samples, Hokutolite A and Hokutolite B. The Hokutolite A is of a thickness of eleven millimeters and is grow-

TABLE I

CONTENTS AND RATIOS OF RADIUM ISOTOPES IN THE SPRING WATERS

Date	Content of Ra^{226}	The Atomic Ratio Ra^{224}/Ra^{226}	The Atomic Ratio Ra^{228}/Ra^{226}	Content of Th^{228}
October '53	2.0×10^{-11} g./l.	5.9×10^{-5}	ca. 5×10^{-2}	ca. 0
July '54	1.4 „	5.0 „	—	ca. 0

TABLE II

CONTENT AND RATIO OF RADIUM ISOTOPES IN HOKUTOLITE

Sample	Age observed	Content of Ra^{226}	The Atom Ratio Ra^{224}/Ra^{226}
Hok.—A	unknow	1.0×10^{-9} g./g.	1.0 0.2
Hok.—B	5 yr.	1.6 „	4.0 0.2

TABLE III

VERTICAL CHANGE OF RADIOACTIVE PROPERTIES IN HOKUTOLITE A

Nos. of pieces	Depth from the Surface (mm.)	Cont. of Ra^{226} (10^{-9}g./g.)	Atom. Ratio Ra^{224}/Ra^{226} (10^{-5})	Specific—Activity (c.p.m./g.)
1		1.9	6.0	6010
2		0.8	6.0	3500
3		1.9	3.5	2400
4		0.9	2.7	1480
5		1.8	0.87	960
6		—	—	820
7		1.5	0.10	555
8	3	—	—	—
9		1.4	0	—
10	4	1.1	0	—
11		—	—	710
13		0.9	0	—
14	6	—	—	350
16		0.7	0	—
17		—	—	330
19		0.8	0	—
20		—	—	455
23		—	—	460
25		0.8	0	—
26	9	—	—	410
29		—	—	—
32		0.8	0	310
33	11	1.5	0	405

4) R. Ohashi, Mineralogical Mag., 19, 73 (1920); I. Suganuma, Bull. Chem. Soc. Japan, 3, 69 (1928); E. Minami, Kobutsugaku Zasshi (J. Mineralogical Soc. Japan), 2, 1 (1954).

5) Hokutolite is composed of the mixed crystal of barium sulfate and lead sulfate, and was found first at the Hokuto springs in Formosa and then at the Tamagawa Springs (formerly called Shibukuro Springs) in Akita perfecture in Japan. The molecular ratio, lead sulfate to barium sulfate, in Hokutolite from Tamagawa is found to fluctuate between 0.2 and 0.02. The spring waters of Tamagawa contain radioactive elements of both uranium- and thorium-series which make the mineral distincly radioactive. The main constituents of the water are Al^{+++}, Fe^{++}, and Cl^-, with smaller quantities of SO_4^{--}, F^- and Fe^{+++}. Barium and lead are also contained in the water but their concentrations are in the order of p.p.m.

ing on the large base rock It is deposited from the flowing water with a temperature as high as 45°C. A small column is made carefully from this sample, and is cut, layer by layer, into thirty-three pieces from the surface to the bottom. The measurements of the content and the ratio of radium isotopes as well as the specific beta activity are performed on each of these pieces and the results are summarized in Table III.

Hokutolite B is, on the other hand, about 0.75 mm. thick and is known to be about five years old. This sample is growing on a small andesite block on which the spring water, with a temperature of 75°C, splashes vigorously.

The content and the ratio of radium isotopes of the water are determined by the following method. One hundred milligrams of barium are added to the sample water as barium chloride and barium sulfate is precipitated by the usual method. Barium chloride method reported by Ames et al[5] is employed in order to eliminate other radioactive elements coprecipitated with radium. The alpha-activity of the barium sulfate is measured continuously by a Lauritsen type electroscope and the variation with time of the activity is plotted on a graph paper. The content of Ra^{226} and the ratio, Ra^{224} to Ra^{226}, are easily calculated from the curve, but the calculation of the ratio, Ra^{228} to Ra^{226}, is not so easy because of the somewhat long half-life of Ra^{228}. As described later, the ratio, Ra^{228} to Ra^{226}, in the spring water, is evaluated by the more convenient way. In the determination of these values in Hokutolite, the same method is employed but barium chloride need not be added to the sample in this case.

(1) The Estimation of the Rate of Growth Near the Surface of Hokutolite.—From the equations, (4) and (5), it is calculated that the ratio, Ra^{224} to Ra^{226}, or the total beta-activity of a layer becomes zero or constant when about fifty years has passed since its precipitation. From Table III, it is shown that in the case of Hokutolite A this time corresponds to the period of sedimentation of the layer about 3 mm. thick. The mean rate of growth above this layer is then calculated to be about 6×10^{-2} mm. per year.

This fact is more clearly shown in Fig. 1 and Fig. 2, which are constructed on the basis of the following considerations: the experimentally determined ratio of radium isotopes as well as beta-activity for each piece shown in Table III are not the values for infinitely thin layers, but the mean values for the layers with some thickness. Considering the above estimated rate of growth, the thickness of each layer seems to correspond to about seven years sedimentation. To compare these facts with theoretical data, therefore, we must use mean "theoretical" values for every seven years. The ratio, Ra^{228} to Ra^{226}, in the water is evaluated by equalizing the mean theoretical ratio, Ra^{224} to Ra^{226}, for the first seven years to the observed ratio and this gives 8×10^{-2} for the value. This value is considered to be more reliable than the one experimentally determined in Table I and will be used in the following discussion.

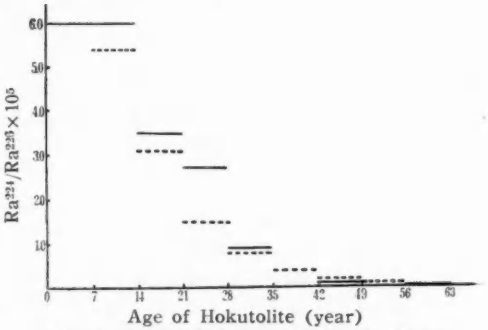

Fig. 1. Vertical change of the ratio, Ra^{224}/Ra^{226}, in Hokutolite-A.
Solid lines: Observed ratio, Ra^{224}/Ra^{226}, in each piece of Hokutolite-A up to No. 9 in Table III.
Dotted lines: Theoretical mean ratio for every seven years. Theoretical. value for first seven years is equalized to the observed one.

From Fig. 1 and Fig. 2, it is concluded that the rate of growth estimated above is approximately valid near the surface of the sample.

(2) The Estimation of the Mean Rate and Intensity of Sedimentation of Hokutolite for the Past One to Two Hundred Years.—From the above discussion the value for K_2/K_1 in the equation (9) is 8×10^{-2} and the time t', is known as 0.25 years for Hokutolite A and Hokutolite B, respectively. Using these data the theoretical time variation of the ratio, Ra^{224} to Ra^{226}, in the total mass of the deposit is plotted in Fig. 3 in a solid line. Comparison of the data in Table II with the curve in Fig. 3 gives the age and

6) D.P. Ames, J. Sedlet, H.H. Anderson and T.P. Kohman, The Transuranium Elements, (Natl. Nuclear Energy Series IV-14B) p. 1700 (1949).

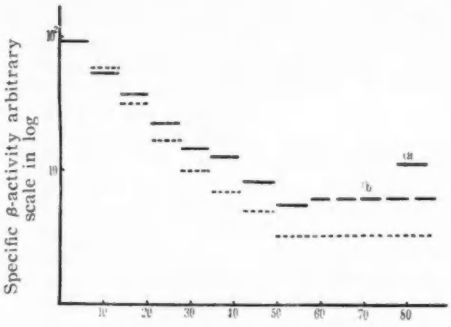

Fig. 2. The Vertical change of β-activity of Hokutolite.

Solid lines: Observed specific β-activiteis of each pieces of Hokutolite-A up to No. 11 in Table III.

Dotted lines: Theoretical mean β-activities for evry seven years. Pb^{210} is assumed to be in equilibrium with Ra^{223} in the water and the value for the first seven years is equalized to the observed one.

(a): observed value for No. 11, exceptionally high.

(b): observed mean value from No. 14 to No. 33.

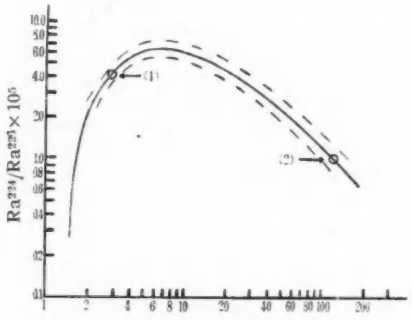

Fig. 3. The variation with time of the mean ratio, Ra^{224}/Ra^{226}, in total mass of Hokutolite.

Solid line: $K_2/K_1=8\times10^{-2}$

Dotted lines: above $K_2/K_1=9\times10^{-2}$, below $K_2/K_1=7\times10^{-2}$

(1) and (2): observed values for Hokutolite-B and-A, respectively.

the mean rate of sedimentation. Combining these results with the content of each element in Hokutolite and weight of the sample, the sedimentation intensity of each element can be estimated. Here the sedimentation intensities of radium and of Hokutolite as a whole are given. In the calculation of the sedimentation intensity of Hokutolite, the water content in the sediment is neglected. The reason is that the weight of Hokutolite A is approximately 4.5 gr./cm^3 while the specific gravity of Hokutolite is 4.5. These results are summarized in Table IV.

Discussion

The accuracy of the values calculated depends largely on the validity of assumptions first proposed. Among them assumption (4) is the most unlikely. A remarkable discrepancy between the values for the growth rate of Hokutolite A, between the values by the first two methods and the value by the third method, is evidently due to this. The fact that most of the Hokutolite samples consist of alternating white and brown layers suggests that sedimentation has proceeded not uniformly. Really it was shown by Mr. Sasaki[7] in our laboratory using the nuclear emulsion method that white layers are richer in radio-active elements than brown layers.

From these observations it is probable that the mean rate of growth of Hokutolite is smaller in recent years than in the older period.

On the other hand, the difference of the rate of growth between the sample A and sample B is considered mainly due to the difference of the conditions governing the sedimentation process. Some of them are shown in the beginning of this chapter. In addition, the content of Ra^{223} in the water precipitating Hokutolite A is about one-half of that in the water near Hokutolite B. The contents of barium and lead are probably decreased by the same proportion as radium though not yet assured.

As for the first assumption, that is, the constancy of the abundance ratio of radium

7) Symposium on Geochemistry held in Fukuoka October, 1954.

TABLE IV

THE SEDIMENTATION RATE AND INTENSITY OF HOKUTOLITE

Sample	Age calcd by the Method (c) yr.	Sedimentation Rate by the Method (a) & (b) Method (c) mm./yr.	mm./yr.	Sedimentation Intensity by the Method (c) of Ra 10^{-11} g./cm^2/yr.	Hokutolite 10^{-2} g./cm^2/yr.
Hok.−A	120±20	0.06	0.09±0.015	4±0.7	4±0.7
Hok.—B	3± 0.2	—	0.25±0.03	18±1	11±0.7

The Density of Hok.−B is assumed to be 4.5.

Experimental error in the determination of the ratio Ra^{224} to Ra^{226}, is only considered here.

isotopes, its validity cannot be ascertained experimentally within a short period. If radium isotopes are introduced into the spring water from the same mother rocks, sudden and appreciable change of their ratios would not take place in such a short period as one or two hundred years. In this case, however, the steady increase or decrease of the ratios, probably in both directions, may occur to some extent. In Fig. 3, the limit of the error is shown in two dotted lines as the ratio, Ra^{228} to Ra^{226}, in the water varies from 7×10^{-2} to 9×10^{-2}.

Uncertainties arising from other assumptions may be minimized by taking samples near the center of gross sediment.

The determination of the ratio, Ra^{224} to Ra^{226}, is done by the rather inconvenient method described before. The error is estimated to be about fifteen per cent when the ratio is less than 1×10^{-5}, while it decreases to about five per cent as the ratio increases. In our purpose, however, the uncertainty of this order could be allowed if one considers non-validities of the conditions assumed.

In the methods, (a) and (b), another important error is introduced by the crystalization of Hokutolite. The surface of Hokutolite becomes uneven as the crystalization takes place and it is very difficult to measure accurately the depth of a layer from the surface. This error is considered to amount to about ten per cent at the depth of 3 mm.

Comparing three methods with each other, (a) ond (b) are better than (c) in that the assumption for the uniform growth is not necessary to them and the time t is obtained rather distinctly, when the ratio, Ra^{224} to Ra^{226}, or the total beta activity becomes zero or constant. In the method (b), however, the uncertainty from the ratio, Pb^{210} to Ra^{226}, must be taken into consideration. In the case of the method (c), on the other hand, it is possible to estimate the mean rate of growth in the period ranging from a few years to one or two hundred years, while the first two methods can estimate the value only for about sixty years.

From these discussions it can be concluded that compared to the observed rate of growth, 0.15 mm./year the calculated rate for Hokutolite B, 0.25 mm./year, is fairly satisfactory. Perhaps, the value for Hokutolite A is also satisfactory with good approximation.

Summary

Under some assumptions, three methods for the estimation of sedimentation rate as well as sedimentation intensity of radioactive sediments are proposed. These methods are based on the time variation of the abundance ratios of radium isotopes in the sediments. The rate of sedimentation of a radioactive sediment, Hokutolite, is estimated for two samples by these methods. The result is 0.25 mm./year for one sample for which the observed value is known to be 0.15 mm./year. For the other sample of unknown age, the rate is estimated to be 0.09 mm./year.

The author wishes to express his sincere thanks to Prof. E. Minami and Dr. N. Saito, the University of Tokyo, for their encouragement and valuable suggestions. The work was supported financially by a scientific grant from the Ministry of Education as well as a grant from Research Association of Tamagawa Hot Springs, to which the author's thanks are due.

Department of Chemistry, Faculty of Science, Tokyo University, Tokyo

Some Remarks on the New Equation of State as Applied to the Critical Region

By Tetsuya ISHIKAWA

(Received March 9, 1955)

The indefiniteness of the critical state has been an interesting question for as long a time as since 1880, but the exact nature of the critical point does not yet seem to be established. The shape and the degree of flatness of the isotherms in the critical region are not those predictable from a van der Waals' type of equation which is conditioned by $(\partial p/\partial V)_{T=T_c}=0$, $(\partial^2 p/\partial V^2)_{T=T_c}=0$, and $(\partial^3 p/\partial V^3)_{T=T_c}=0$, but could be reconciled with either of the current theories: (1) Mayer-Harrison's "derby hat" theory[1] which predicts below the true critical temperature, T, flat, horisontal isotherms above the temperature of meniscus disappearance, T_m; (2) Rice's modified "derby hat" theory[2] which predicts a flat, horizontal critical isotherm with linear but sloping isotherms immediately above T_c; and (3) Zimm's singular point theory[3] which describes the critical point as a singularity at which not only $(\partial p/\partial V)_{T=T_c}=0$, $(\partial^2 p/\partial V^2)_{T=T_c}=0$, but also all the higher derivatives are zero. The precise pVT measurements in the critical region of xenon done by Habgood and Schneider[4], however, offer no support for Mayer-Harrison's theory since there is no obvious region of flat, horizontal isotherms above T_m, and also for Rice's theory since the observed coexistence border curve appears to be definitely rounded at the apex.

The present author[5] put forward a modified form of van der Waals' equation available for both gaseous and liquid phases:

$$p+a/V^{2-\varepsilon}=RT/(V-b),\ a=3p_cV_c^2,\ b=V_c/3,$$

where ε is a constant independent of pressure to the extent that the applied pressure affects no appreciable change in molecular association.

The introduction of ε into van der Waals' equation is sufficient to allow the critical factor, RT_c/p_cV_c, to be consistent with experiments, i.e., the reduced equation at the critical point, $RT_c/p_cV_c=2(1+3V_c^{\varepsilon})/3$, $\varepsilon=0.077\pm0.008$ when V is expressed in cc./mol., is valid for 66 kinds of normal and slightly polar substances, but such transformation of equation results in separating a simple van der Waals' critical point, which is conditioned by either of $b=V_c/3$ or $b=RT_c/8p_c$ with $a=27p_cb^2$, into a maximum and a minimum with never realizable portion, $\partial V/\partial p>0$, and with supersaturated vapour portion, the former being supposed to correspond with generally accepted phenomena in the liquid-vapour coexistence region. The divergency in the portion of $(\partial V/\partial p)_{T=T_c}>0$ may be saved, if the critical point is assumed to be the limiting case of liquid-vapour coexistence region by combining the equation of critical isotherm, $p+a/V^{2-\varepsilon}=RT_c/(V-b)$, with the horizontal line passing through the critical pressure, $p_c=3RT_c/2V_c(1+3V_c^{\varepsilon})$, where ε is not the value at the critical point, but the mean at the critical isotherm, provided that the continuity of state is true.

It is the fact, however, that there occurs no appreciable difference between ε at the critical point and the mean of ε values in the critical region, e.g., from Habgood and Schneider's data of xenon at the critical point, $t_c=16.590$°C, $p_c=57.636$ atm., and $d_c=1.099$ g./cc., ε is evaluated to be 0.06932, whereas the mean of ε values out of 29 measurements in their observed density range of 0.91503 to 1.30705 g./cc. is 0.06941; also from their preliminary data[5], the mean of ε values out of 16 measurements in the density range of 0.9934 to 1.2463 g./cc., for the range of which a meniscus is expected to disappear, is 0.06932; again from Beattie, Douslin, and Levine's data[7] for neopentane, $C(CH_3)_4$, ε at the critical point, $t_c=160.60$°C, $p_c=31.57$ atm., and $V_c=303$ cc./mol., is 0.07411, whereas the mean of ε values out of 17 measurements in their observed volume range of 259.7 to 377.4 cc./mol. is 0.07495.

1) T.E. Mayer and S.F. Harrison, *J. Chem. Phys.*, **6**, 87, 101 (1938).
2) O.K. Rice, *J. Chem. Phys.*, **15**, 314 (1947).
3) B.H. Zimm, *J. Chem. Phys.*, **19**, 1019 (1951).
4) H. W. Habgood and W. G. Schneider, *Can. J. Chem.*, **32**, 98 (1954).
5) T. Ishikawa, This Bulletin, **26**, 78, 530 (1953); ibid., **27**, 226, 570 (1954); ibid., **28**, 89 (1955); T. Ishikawa and M. Ikeda, ibid., **26**, 516 (1953).
6) W.G. Schneider and H.W. Habgood, *J. Chem. Phys.*, **21**, 2080 (1953).
7) J. A. Beattie, D.R. Douslin and S. W. Levine, *J. Chem. Phys.*, **19**, 948 (1951).

In the present case, to evaluate p(atm.) against a given V(cc./mol.) from the new equation of state, we take ε's at the respective critical points: for Xe, $2-\varepsilon=1.93068$, $b=V_c/3=39.82$cc./mol., $\log a=6.3923491$, and $T_c=16.590+273.16$°K; and for $C(CH_3)_4$, $2-\epsilon=1.92589$, $b=101.0$ cc./mol., $\log a=6.9392811$, and $T_c=160.60+273.16$°K, their results being illustrated (in full line) with the observed pressures (circles) in Fig. 1 and Fig. 2, in which are also shown, for the sake of comparison, the corresponding volumes of the maximum and the minimum.

With these consistent results for both cases, one is not able to deny the fact that the new equation has some intimate relationship with the actual state, but one can not elucidate any more, so long as $(2-\varepsilon)$ in the critical region is assumed to keep constant, so that, in the following case, we shall analyze the variation of ε with respect to the volume.

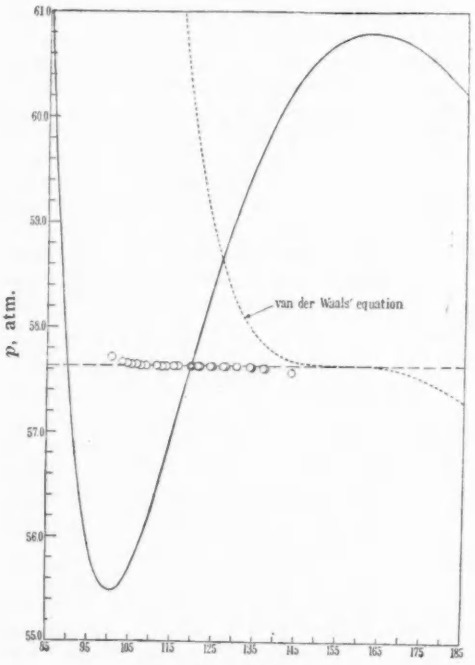

Fig. 1. p-V Diagram of xenon at the critical temperature.

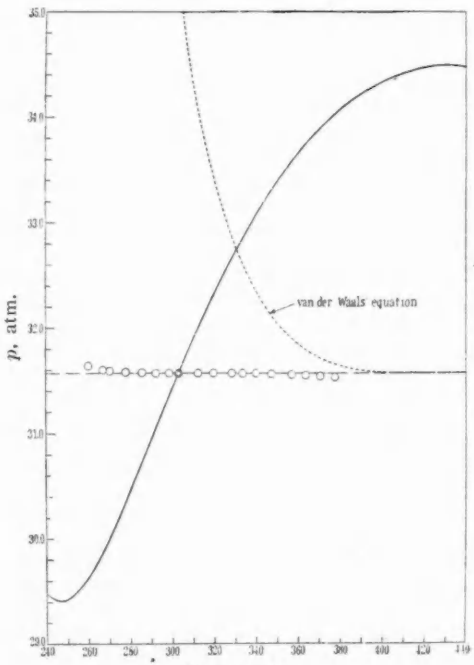

Fig. 2. p-V Diagram of neopentane at the critical temperature.

curves from van der Waals' equation (in dotted line) by putting $b=RT_c/8p_c=51.57$ cc./mol., $\log a=6.6168073$ for Xe, and $b=140.93$ cc./mol., $\log a=7.2286712$ for $C(CH_3)_4$.

As seen from Figs. 1 and 2, it can be acknowledged (1) that the inflection point in the portion of $(\partial p/\partial V)_{T=T_c}>0$ nearly coincides with the actual critical point (double circle), (2) that the minimum point is situated near the least volume in the liquid-vapour critical region, (3) that the maximum point is situated at the critical volume corresponding to van der Waals' equation ($b=RT_c/8p_c$), and (4) that the liquid-vapour critical region is the horizontal line which passes through the inflection point and ends close to the

For each substance, isothermal ε values at the critical temperature and at most 0.10° above and below the critical temperature have been computed from the measurements of the same workers cited above (see Tables I and II), and are diagrammatically shown in Figs. 3 and 4. As seen from Figs. 3 and 4, ε values within these temperature ranges seem to converge upon the respective unique curves, which are quite similar with each other, and each curve appears to consist of three parts, the first part being concave up to the critical point (double circle), or more precisely speaking, at first horizontal, or probably a minimum which is situated at the corresponding volume of the minimum

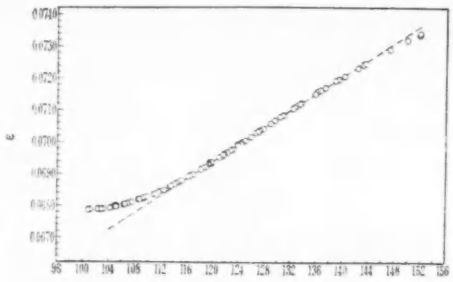

V, cc./mol.

Fig. 3. ε-V Diagram of xenon in the critical region.

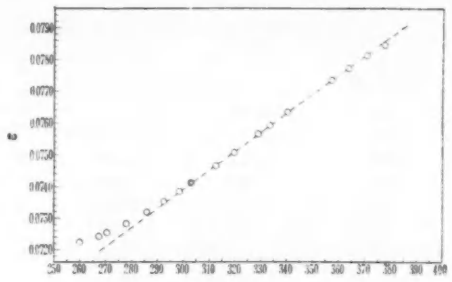

V, cc./mol.

Fig. 4. ε-V Diagram of neopentane in the critical region.

TABLE I

ISOTHERMAL ε VALUES OF XENON IN THE CRITICAL REGION

16.550°C		16.585°C		16.590°C		16.590°C	
V cc./mol.	ε	*V* cc./mol.	ε	*V* cc./mol.	ε	*V* cc./mol.	ε
102.27	0.06789	100.90	0.06787	100.46	0.06785	100.87	0.06786
104.33	0.06794	102.68	0.06789	104.30	0.06792	102.94	0.06787
106.44	0.06804	104.82	0.06793	106.48	0.06804	105.13	0.06797
108.62	0.06819	107.02	0.06807	108.74	0.06819	107.46	0.06811
110.94	0.06836	109.37	0.06825	111.16	0.06837	109.90	0.06828
113.36	0.06859	111.91	0.06847	113.50	0.06862	112.47	0.06849
115.87	0.06887	114.44	0.06872	116.18	0.06893	115.22	0.06879
118.49	0.06919	116.87	0.06900	118.83	0.06922	118.09	0.06914
121.13	0.06953	119.83	0.06937	121.61	0.06959	120.95	0.06950
123.94	0.06990	122.78	0.06973	124.40	0.06994	123.94	0.06989
126.75	0.07026	125.87	0.07014	127.33	0.07036	127.09	0.07032
129.65	0.07066	129.04	0.07056	130.30	0.07076	130.32	0.07076
132.66	0.07106	132.40	0.07102	133.58	0.07117	133.71	0.07120
135.80	0.07149	135.84	0.07148	136.64	0.07159	137.36	0.07168
138.95	0.07190	139.45	0.07194	143.49	0.07246		
		143.35	0.07244				
		147.20	0.07289				

16.600°C		16.620°C		16.490°C		16.690°C	
V cc./mol.	ε	*V* cc./mol.	ε	*V* cc./mol.	ε	*V* cc./mol.	ε
101.17	0.06787	103.27	0.06791	103.25	0.06790	103.25	0.06790
103.09	0.06789	105.32	0.06797	111.44	0.06844	111.44	0.06842
105.11	0.06798	107.43	0.06810	114.83	0.06877	114.83	0.06875
107.26	0.06808	109.61	0.06823	119.70	0.06937	119.70	0.06931
109.41	0.06824	111.97	0.06847	121.68	0.06961	121.68	0.06958
111.66	0.06842	114.39	0.06870	123.05	0.06979	123.05	0.06975
114.08	0.06867	116.90	0.06898	136.27	0.07156	136.27	0.07151
116.52	0.06895	119.53	0.06935	151.89	0.07336	151.89	0.07339
119.05	0.06926	122.21	0.06965	175.21	0.07563	175.21	0.07558
121.78	0.06960	125.04	0.07003				
124.53	0.06996	127.86	0.07040				
127.29	0.07034	130.69	0.07079				
130.12	0.07071	133.63	0.07119				
133.06	0.07112	136.82	0.07162				
136.03	0.07151	140.25	0.07204				
142.25	0.07230	143.21	0.07241				
		149.83	0.07320				

TABLE II

ISOTHERMAL ε VALUES OF NEOPENTANE IN THE CRITICAL REGION

V cc./mol.	160.50°C	160.58°C	160.60°C	160.62°C	160.70°C	mean
			ε			
259.7	0.07224	0.07224	0.07224	0.07223	0.07223	0.07224
266.7	0.07243	0.07243	0.07242	0.07242	0.07241	0.07242
270.3	0.07255	0.07255	0.07255	0.07355	0.07253	0.07255
277.8	0.07283	0.07283	0.07283	0.07283	0.07282	0.07283
285.7	0.07320	0.07319	0.07319	0.07318	0.07317	0.07319
292.4	0.07353	0.07353	0.07352	0.07352	0.07351	0.07352
298.5	0.07386	0.07385	0.07384	0.07385	0.07383	0.07385
304.9	0.07423	0.07422	0.07422	0.07421	0.07419	0.07421
312.5	0.07467	0.07467	0.07466	0.07466	0.07465	0.07466
319.5	0.07509	0.07509	0.07508	0.07508	0.07504	0.07508
328.8	0.07566	0.07566	0.07565	0.07565	0.07562	0.07565
333.3	0.07594	0.07593	0.07593	0.07592	0.07590	0.07592
340.1	0.07639	0.07635	0.07633	0.07633	0.07631	0.07634
357.1	0.07735	0.07735	0.07733	0.07731	0.07730	0.07733
363.6	0.07773	0.07772	0.07771	0.07770	0.07767	0.07771
370.4	0.07814	0.07813	0.07812	0.07811	0.07808	0.07812
377.4	0.07850	0.07847	0.07846	0.07845	0.07844	0.07846

of p-V curve, and finally a nearly straight line, the second part being undoubtedly a long straight line starting from the critical point, or in other words, at the critical point, the second, third, and higher derivatives of ε with respect to the volume appear to be zero, and the third part being convex up to the maximum corresponding to the volume at which the other form of van der Waals' equation ($b=V_c/3$) takes the critical pressure. The volume coincidences of the minimum with the minimum of p-V curve, and of the maximum with the inflection point of this form of van der Waals' equation have been confirmed by making use of Beattie, Barriault, and Brierley's data[8] for Xe, and of Beattie, Douslin, and Levine's data[9] for $C(CH_3)_4$. On the whole, it is clear that in the critical region $(\partial\varepsilon/\partial V)_T$ is always positive.

According to the Le Chatelier principle of mobile equilibrium[10], if the volume occupied by the molecules is increased, the state will tend to occur in the direction of increased number of molecules, or, if molecular association[11] is taken into account, in the direction of diminishing the degree of molecular association which will result in pressure increase, whereas in the critical region where the pressure is, by experience constant over a finite volume range, the state will occur to increase the degree of molecular association, i.e., to increase ε which depends on molecular association, so as to annul, as far as possible, the effect of volume increase, and if so, so long as a differential shift of ε occurs to be proportional to a differential shift of V in the same direction, the pressure will continue to be constant, or in other words, $(\partial^2\varepsilon/\partial V^2)_T=0$, $(\partial^3\varepsilon/\partial V^3)_T=0$, and so on at the critical point should be the necessary condition that the pressure in the critical region is constant over a finite volume range.

That the above condition is satisfied can clearly be acknowledged by comparing the observed constant pressure range in Fig. 1 or 2 with the straight line portion in Fig. 3 or 4 for each substance, and at the same time, the fact that there occurs no change of ε with respect to the volume just above and below the critical temperature in each case is a strong proof of the existence of a critical region, at least, within 0.10°C above the critical temperature.

The maximum point of ε which appears in the supersaturated vapour portion has been estimated to have the value of 14.4% increase for Xe, and the value of 17.5% increase for $C(CH_3)_4$ as referred to the respective critical values, each maximum corresponding to $V=341.62$ cc./mol. and $V=975.3$ cc./mol. respectively as computed from van der Waals' equation ($b=V_c/3$).

In conclusion, the author expresses his hearty thanks to Nagasaki American Cultural Center who has furnished him with American journals at his request.

Sasebo Commercial Junior College,
Sasebo, Nagasaki

8) J.A. Beattie, R.J. Barriault and J.S. Brierley, *J. Chem. Phys.*, **19**, 1219 (1951).
9) J. A. Beattie, D. R. Douslin and S. W. Levine, *J. Chem. Phys.*, **20**, 1619 (1952).
10) H.L. Chatelier, *Compt. rend.*, **100**, 441 (1885).
11) refer to T. Ishikawa, This Bulletin, **27**, 570 (1954).

High Viscous Alginic Acid

By Takeo TAKAHASHI and Koji KIMOTO

(Received March 4, 1955)

Introduction

Algin industry is a chemical industry newly developed in postwar Japan, and is regarded as a promising export industry in which seaweed is used as its raw material.

Many problems; however, remain to be solved. Especially maintaining the high viscosity of alginate through manufacturing processes is of great importance since this is the property to be utilized in most practical applications. The purpose of the present research is, by studying some properties of pure alginic acid and its salts, to confirm what causes the high viscosity and thus to make a contribution to the algin industry.

Alginie acid is a highly polymerized mannuronic acid in which the aldehyde groups of *d*-mannuronic acid are linked in β-glucoside bindings. The characteristic of this compound is the fact that in that one carboxyl group on each unit of monomer is free to react.

Owing to the various characteristics of alginic salts, this substance has lately been most effectively put in practical uses extensively in many fields, as foodstuffs, industrial and medical uses, toilet articles, etc.

Viscosity Measurement

A new viscosimeter of constant shearing force type (modified type of Ostwald's capillary viscosimeter) has been designed for a solution of alginate by Dr. Hajime Okada, and universally used in the algin industry of Japan. Experiments with various solutions revealed the fact that a viscosimeter of this type was suitable for measuring the viscosity of non-Newtonian fluid such as alginate. This apparatus is shown in Fig. 1. The liquid level head can be adjusted to obtain the desired shearing force, by moving up or down the capillary tube.

In this viscosimeter, the maximum shearing force is taken to be 27.6 dyne/cm. and in accordance with the length and diameter of capillary, the level head is determined as follows and the mark is graduated on the capillary tube

$$\text{Maximum shearing force} = 27.6 = PR/2L = H \cdot g \cdot R/2L = 980 \cdot H \cdot R/2L \quad (1)$$

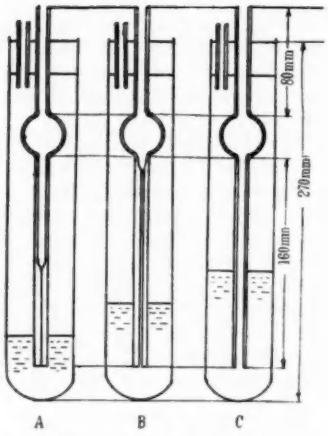

Fig. 1. A new viscosimeter of constant shearing force.

Each tube (A, B, C) should have a definite level head, which can be calculated from diameter and length of capillary.

$$H = 27.6 \times (2/980) \times L/R = 0.05633\, L/R \text{ cm.} \quad (2)$$

here, P = pressure

H = head of level

R = radius of capillary

L = length of capillary

Since the magnitude of viscosity of alginate solution changes from a few centipoises to poises, the viscosimeter tubes with different diameter of capillary are necessary. In such cases, each tube should have a definate level head, which can be calculated from diameter and length of capillary according to the above equation (2).

Viscosity Characteristics

Sodium alginate is a typical heteropolar high-molecular electrolyte having the following viscosity characteristics:

(1) The viscosity of the aqueous solution of alginate becomes maximum at the vicinity of neutral point. According to E. Heen[1], the electric charge of colloidal particles becomes maximum, so that the polar adsorption, hydrating property and viscosity suc-

1) E. Heen, *Koll. Z.*, **83**, 204 (1938).

cessively increase. This is the theory which explains the enormous viscosity due to "Elektroviskosen Effect".

Otherwise, H. Staudinger[2] estimated the phenomenon to be "Poly-ionische Viskositätserscheinung", i.e., by electrostatic action of high-valency colloidal ions, they agglomerate and viscosity increases.

(2) In the relation between reduced viscosity and concentration, the minimum point occurs at a certain diluted concentration. This phenomenon is not found on the homopolar high-molecular substance, so that it is due to the effect of ionized ions.

(3) If low-molecular electrolyte such as sodium carbonate or sodium chloride is added, the above minimum vanishes. This example is shown in Eig. 2. According to W. Kern[3],

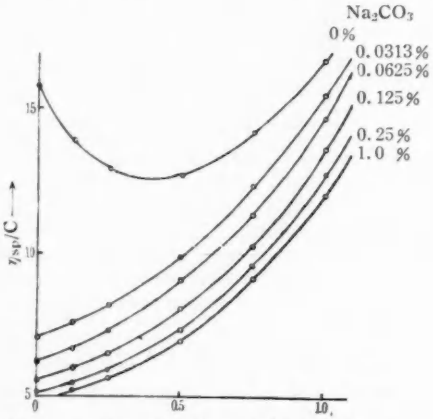

Concentration of sodium alginate (%)⟶

Fig. 2. Effect of addition of sodium carbonate on the relation between reduced viscosity and concentration.

reduced viscosity increases in the region of sol and gel, and then at the boundary becomes minimum. In the sol region "Ionaler Faktor" and in the gel region "Makromolekular Faktor" act powerfully.

Reduced viscosity=("Ionaler Faktor")
×("Makromolekulaler Faktor")

In the existence of low-molecular electrolyte, the "Ionaler Faktor" approaches to one, so that "Makromolekulaler Faktor" controls all the region.

The critical viscosity (at the transition point between sol and gel) of the aqueous solution of sodium alginates of different origin was measured and found to be about 3.5 to 3.6 c.p. The fact verifies the Staudinger's theory that the critical viscosity has the same value in lower-molecular as well as in high-molecular compound, if the compounds belong to the same homologue,

When the sodium carbonate is added until its concentration attains to 0.031%, the aqueous solution of sodium alginate shows no more minimum point in reduced viscosity-concentration curve. The reason is that the electric charge of the alginate particle is discharged by sodium ion added and has no characteristics of heteropolar high-molecule.

Viscosity and Temperature

Generally, according to Andrade[4], the viscosity of fluid has a relation against temperature as following equation:

$$\eta = Ae^{Q/RT} \tag{3}$$

here, η = relative viscosity
T = absolute temperature
R = gas constant
Q = activation energy
$\log \eta = \log A + Q/4.574T$

The viscosity measurement of an aqueous solution of sodium alginate at various temperature shows that the relation between the viscosity and temperature of such a non-Newtonian fluid may be expressed by Andrade's equation. The Fig. 3 shows the examples.

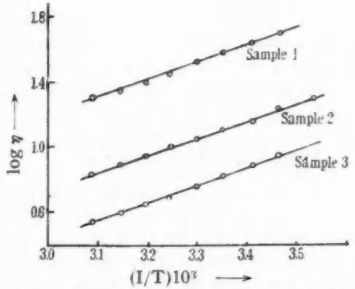

Fig. 3. Relation between $\log \eta$ and I/T
From inclination of staight line against abscissa, the activation energy can be calculated.

The activation energy (Q) for the fluidity of 1% solution of sodium alginate, when computed from the above equation, is approximately 5,000 cal. with some variations according to the concentration and viscosity of the solution.

Viscosity and Concentration

Many equations had been proposed by Einstein, Mark and Fikentscher, Arrhenius[5],

2) H. Staudinger, *Ann.*, **502**, 201 (1938).
3) W. Kern, *Z. Phys. Chem.*, A, **153**, 391 (1931).
4) Andrade, *Nature*, **125**, 580 (1930).
5) Arrhenius, *Z. Phys. Chem.*, I, 285 (1887).

Baker, Philippoff and Hess, Bredee Bergenand Booys, etc.

When applied to sodium alginate solution, Arrhenius' equation (4) gives value appropriate only at a high concentration. Especially when the alginate solution does not contain low molecular electrolyte, the deviation from the Arrhenius' equation becomes conspicuous.

$$\log \eta = k \cdot c \tag{4}$$

The Arrhenius' equation can not express the relation of viscosity and concentration (c) of the solution of heteropolar high-molecule such as sodium alginate, of which the viscosity is due to the ionic high molecule.

The Baker's equation[6],

$$\eta = (1+ac)^k \tag{5}$$

gives values that agree fairly with observed ones. However, the Baker's equation is not satisfied at a high concentration, contrary to Arrhenius' equation.

From the point of view of the two regions of sol and gel, there is no identical equation applicable through high and low concentration.

According to the author[7], in the lyophile colloidal solution such as alginate or carrageen, of which the viscosity is due to hydration with water, the viscosity may behave against concentration such as the depression of surface tension versus concentration. According to Freundlich's equation, it is able to express as following:

$$\eta_{sp} = \eta - 1 = \alpha \cdot c^{1/n} \tag{6}$$

$$\log \eta_{sp} = \log \alpha + (1/n) \cdot \log c \tag{7}$$

Schematically the relation between viscosity and concentration has two equations of the same type, only the value of constant, being different, as shown in Fig. 4.

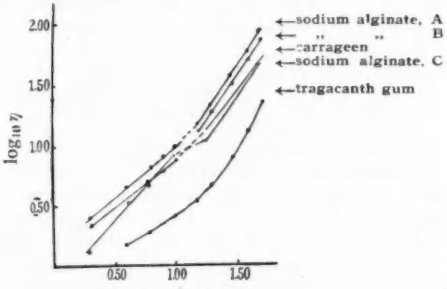

Fig. 4. Relation between viscosity and concentration has two equations of the same type, only differing the value of constants.

The critical concentration, which divides the equation into two, is about 0.15% and it coincides with the concentration, at which the hydration of alginate reaches maximum.

Recently Tetsuro Seiyama[8] proposed the following equation:

$$\eta = 1 + (a \cdot \phi \cdot c + A \cdot c^{1/2})/(100 - a \cdot c) \tag{8}$$

In this equation, the viscosity is assumed to be a linear function of $c^{1/2}$ under the assumption that the ionic atmosphere of high-molecular electrolyte is like that of low molecular electrolyte.

Colloidal State of Sodium Alginate in Aqueous Solution

In an aqueous solution of sodium alginate, the colloidal particle hydrates and swells. The Einstein's equation is derived dynamically from volume occupied by the solute particle, so that conversely, the specific volume of solute in solution can be computed theoretically from the equation.

According to Ichiro Sakurada[9], it follows by expansion of Baker's equation,

$$\eta = (1+ac)k = 1 + akc + [k(k-1)/2]a^2c^2 + \tag{9}$$

In diluted concentration, it may be allowed to neglect the term c^2 and follows,

$$\lim_{c \to 0} \eta = 1 + akc \tag{10}$$

also from Einstein's equation,

$$\lim_{c \to 0} \eta = 1 + 2.5\ (fc/100) \tag{11}$$

so that it follows,

$$ak = (2.5/100) \cdot f, \text{ or } f = 40 \cdot a \cdot k \tag{12}$$

By applying the equation (12) on alginate solution, the authors calculated the specific volume (f), which is shown in Fig. 5. The

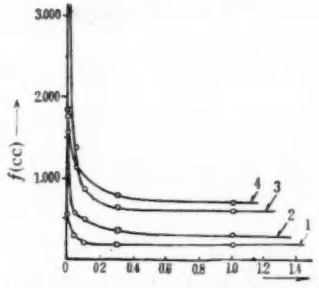

Concentration of Na_2CO_3 added (%)

Fig. 5. Relation between specific volume and concentration of Na_2CO_3.

value of f decreases radically until the concentration of sodium carbonate approaches

6) F. Baker, *J. Chem. Soc.*, **103**, 1653 (1913).
7) T. Takahashi, *Report of Imperial Industrial Research Laboratory*, **28**, No. 5 (1933).
8) T. Seiyama, *J. Ind. Chem. Japan*, **52**, 300 (1949).
9) I. Sakurada, *J. Ind. Chem. Japan*, **35**, 1103 (1932).

0.3% and then takes the constant value, differing with the polymerization degree.

Computing from the above value, we know that 1 g. of pure highly-polymerized sodium alginate can fix water of about 3,500 cc. in volume.

Fikentscher's equation[10],

$$\eta=1+a\cdot\phi\cdot c/(100-\phi\cdot c) \quad (13)$$

is transformed as follows:

$$c/\eta=100/a\phi-c/a \quad (14)$$

From the $c/\eta-c$ curve shown in Fig. 6, the values of $100/a\phi$ and $1/a$ can be calculated respectively.

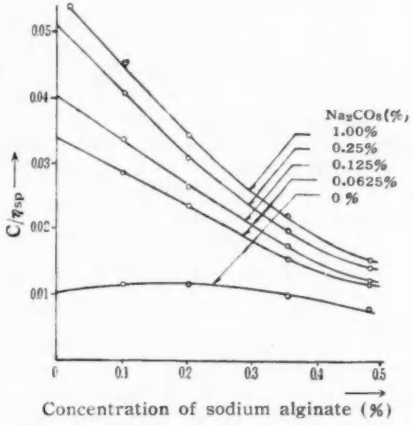

Eig. 6. Relation between reciprocal of reduced viscosity and concentration.

As a result, the value of a takes 6.5 to 8 at 1% of sodium carbonate, even if the polymerization degree of alginate differs greatly. If the particle is a spherical and non-electric body, the value of a is 2.5, according to Einstein's equation. This result shows distinctly that the particle of alginate must be in a bar shape.

Kuhn's equation (15)[11] refers to a bar molecule.

$$\eta=1+[2.5+(1/16)(1/d)^2]\cdot\phi\cdot c/100 \quad (15)$$

here, 1=length of a bar particle

d=longitudinal diameter in cross section of a bar particle

Placing

$$a=2.5+(1/16)\cdot(1/d)^2 \quad (16)$$

or $$1/d=4\sqrt{a-2.5}$$

and putting the above value of a into equation (16), the value of $1/d$ of sodium alginate becomes 8 to 9. The colloidal particle of alginate, therefore, seems to change its shape into a spheroid with major axis about 8 to 9 times the minor axis, if electrolyte, for example sodium carbonate, is added by 1% to the solution.

10) H. Mark and H. Fikentscher, *Koll. Z.*, **49**, 135 (1929).

11) W. Kuhn, *Z. Phys. Chem., A*, **158**, 78 (1931).

Electric Conductivity

The high molecular electrolyte is polyvalent as well as colloidal, and therefore its behaviour differs from the common electrolyte. The dissociation property can be studied by measuring either hydrogen ion concentration or electric conductivity, but on the high molecular electrolyte such as sodium alginate, the electric conductivity is the only method for investigation of dissociation.

On the purification of sodium alginate for measurement of conductivity, the method of coagulation by methanol is the most effective in removing the foreign minerals and other impurities. It takes at least three times of operation for purification to obtain alginate pure enough for electric conductivity measurement.

From the observed conductivity, the equivalent conductivity is computed according to the following formula:

Equivalent conductivity $=1{,}000\,k/c$

here, k=specific conductivity

c=equivalent concentration

The examples of experiments are shown in Fig. 7. Alkali metals and ammonium

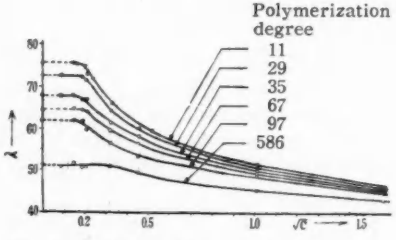

Fig. 7. Relation between equivalent conductivity and square root of concentration of sodium alginates having different polymerization degree.

salts of alginate in aqueous solution were found to show the typical characteristics of poly-valent colloidal electrolytes, i.e., the equivalent conductivity (λ) increases with the dilution of the solution, while, if furthermore diluted, it becomes constant or decreases.

The above phenomenon was already indicated as showing characteristics of high molecular electrolyte such as sodium alginate by Pauli and Sternbach[12] and Seiyama[13].

12) W. Pauli and Sternbach, *Koll. Z.*, **84**, 291 (1938).

13) T. Seiyama, *J. Ind. Chem. Japan*, **53**, 122 (1950).

According to the present authors[14] the equivalent conductivity decreases with increase of polymerization degree. If the equivalent conductivity takes a constant value at very much diluted solution, the ultimate equivalent conductivity (λ_0) may be extrapolated. When the λ_0 is plotted against a logarithm of polymerization (n), as shown in Fig. 8, the linear relation exists between

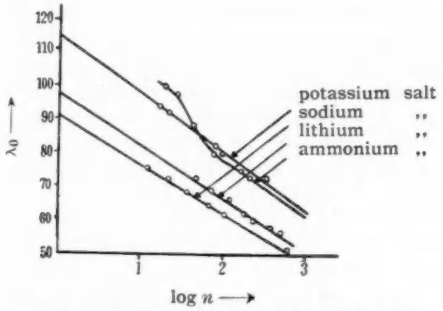

Fig. 8. Relation between equivalent conductivity at infinite dilution and logarithm of polymerization degree.

equivalent concuctivity and logarithm of polymerization degree.

$$\lambda_0^n = \lambda_0^1 - k \log n \qquad (17)$$

Here λ_0^n, λ_0^1 are equivalent conductivities at infinite dilution of alginate of polymerization degree n and 1, and k is the constant.

The above relation fits in case of alkali metals as well as magnesium and triethanolamine alginates.

Dissociation of Alginate

The equivalent conductivity decreases as the polymerization degree increases. This fact is to be interpreted as a result of change of ionic activity in high molecular electrolyte. Generally, the high molecular electrolyte has numerous ionic valency, so that it dissociates step by step, and it is impossible to apply the mass action law to dissociation of high molecular electrolyte as in the case of low molecular electrolyte.

According to Pauli and Valko[15], the dissociation degree is defined as average dissociation degree, and it is varied by distance between ionic radicals, i.e., density of ionic radicals in yarn-like molecule.

Furthermore, the ionic activity has a great role in dissociation of high molecular electrolyte. The alginate particle is not in the shape of a straight bar, but may dissolve in form of "Knäuel". As the polymerization degree increases, the density of ionic radicals increases and ionic activity decreases. This relation is shown in Fig. 9.

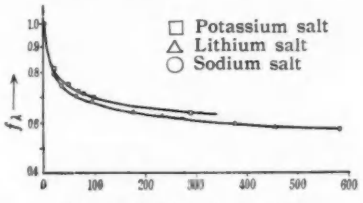

Fig. 9. Relation between coefficient of ionic activity (f_λ) and polymerization degree.

The sodium ion may be restricted in inner structure of colloidal ion of alginic acid, and as the polymerization degree increases, the activity of sodium ion decreases.

The ionic activity of alkali alginates decreases with increases of n, and this relation may be represented by equation (18):

$$f_\lambda^n = f_\gamma^1 - K \log n \qquad (18)$$

here f_λ^n and f_λ^1 denote the coefficients of ionic activity when $n=n$ and $n=1$ respectively, and K is a constant that depends on the concentration.

Furthermore, by measuring ashes in sodium alginate, the relation between the degree of ionization and n of alginic acid was also proved to be represented by an equation similar to the above.

The alginic acid dissociates partially in the aqueous solution and its chain molecule forms a "Knäuel". In its central part, the ionic radical is suppressed to ionize under the influence of ionic charge on the surrounding part, and retains the form of its inactive state.

When alkali acts upon alginic acid, at first the neutralization occurs on free and active ionic radicals in the outer part of alginic acid. As the neutralization proceeds, the ionic radical which formed salt, dissociates completely and the molecule expands owing to repulsive action among the negatively charged ions. Thus, the molecule decreases its ionic density, and approaches to the complete dissociation.

The authors gratefully acknowledge the generous grant for scientific research from the Ministry of Education, Japan, which made this study possible. They also wish to express appreciation to the collaborators in their laboratory.

Institute of Industrial Science,
Tokyo University, Chiba

14) T. Takahashi and K. Kimoto, *Rep. of the Institute of Industrial Science* (Tokyo Univ.), **1**, No. 4 (1951).

15) W. Pauli and Valko, *Elektrochemie der Kolloide*, 73 (1929).

Structure of Sulphamic Acid Molecule from a Three-dimensional Fourier Analysis

By Kenji OSAKI, Hiroyuki TADOKORO and Isamu NITTA

(Received May 9, 1955)

Introduction

Physical and chemical properties of sulphamic acid, or aminosulphonic acid HSO_3NH_2, stand in highly interesting contrast with those of sulphuric and other sulphonic acids. A crystal structure investigation of sulphamic acid has recently been undertaken by Brown, Cox and Llewellyn[1] who determined the dimensions of the unit cell as well as the space group but did not give any further detailed account of the structure. As it is of significance to know the molecular structure and arrangement in crystals of this substance, we have carried out the determination of atomic parameters by means of the three-dimensional Fourier syntheses. The present paper, of which an abstract was sent to the Stockholm Congress of the International Union of Crystallography in 1951, deals with some account of this investigation. After having sent our abstract we were informed of the paper by Kanda and King[2] of the determination of sulphamic acid and on later study of their paper we found that our results were in general agreement with theirs. However, as to the detailed structure of the molecule, there are some points of difference, which seem to be worth discussing here.

Determination of the Structure

Crystal Data.—Sulphamic acid, HSO_3NH_2; molecular weight, 97.09; the dimensions of the unit cell, from a series of symmetrical back-reflexion photographs, $a=8.066\pm0.001$ Å, $b=8.115\pm0.001$ Å, $c=9.255\pm0.003$ Å (Cu $K\alpha_1$, $\lambda=1.5405$ Å);* density, calculated 2.129, observed 2.126 gm/cm^3 (in toluene at 25°C) 2.03 gm/cm^3 (in ether at 12°C) (Cupery)[3]; eight molecules per unit cell, space group $D_{2h}^{15}-Pcab$.

In view of the conflicting circumstances in the Patterson projections of this space group, we computed the three-dimensional Patterson function $P(u\,v\,w)$ near the origin besides its sections at $w=0$, $\frac{1}{2}$, $\frac{1}{4}$ and $\frac{3}{4}$. Comparison among these functions together with ordinary Patterson projections immediately led us to an unambiguous solution of the spatial arrangement of the molecules, of which the structure was preliminarily assumed to be a regular tetrahedron similar to the SO_4-ion. Parameters thus obtained were improved through the calculation of structure factors and Fourier projections on the principal planes. As the refinement seemed insufficient, we calculated electron densities about each

TABLE I

ATOMIC PARAMETERS

	x/a	y/b	z/c	x(in Å)	y(in Å)	z(in Å)
S	0.0940	0.1668	0.1719	0.758	1.354	1.591
				(−0.003)	(−0.004)	(0.007)
O_I	−0.0486	0.0601	0.1767	−0.392	0.488	1.635
				(0.001)	(0.011)	(0.002)
O_{II}	0.0750	0.3057	0.0757	0.605	2.481	0.701
				(−0.002)	(0.015)	(0.015)
O_{III}	0.1758	0.2025	0.3055	1.418	1.643	2.827
				(−0.001)	(0.021)	(0.011)
N	0.2377	0.0438	0.0790	1.917	0.355	0.731
				(−0.046)	(0.036)	(−0.024)

Atomic parameters listed here are already corrected for finite series summation by the values in brackets.

1) C.J. Brown, E.G. Cox and F.J. Llewellyn, *J. Chem. Soc.*, **1940**, 1.

2) F.A. Kanda and A.J. King, *J. Am. Chem. Soc.*, **73**, 2315 (1951).

* The data of Kanda and King, if multiplied by the factor 1.0020, become $a=8.116$Å, $b=8.065$Å, $c=9.246$Å, *Pbca*, in good agreement with our values.

3) M.E. Cupery, *Ind. Eng. Chem.*, **30**, 627 (1938).

atomic centre using three-dimensional data. After two stages of refinement, F_o-corrections were introduced, the effect of which was considerable as given in brackets in Table I of the corrected parameters.

The nitrogen atom was first recognized in our case from the presence of single atom at a particularly larger distance~1.7 Å from the central sulphur atom, while the other three are at essentially same distance~1.4 Å. This choice was later verified by the electron density plot using the three-dimensional data; namely the peak corresponding to the nitrogen atom was found to be sensibly lower and broader than those for oxygen atoms (Fig. 1).

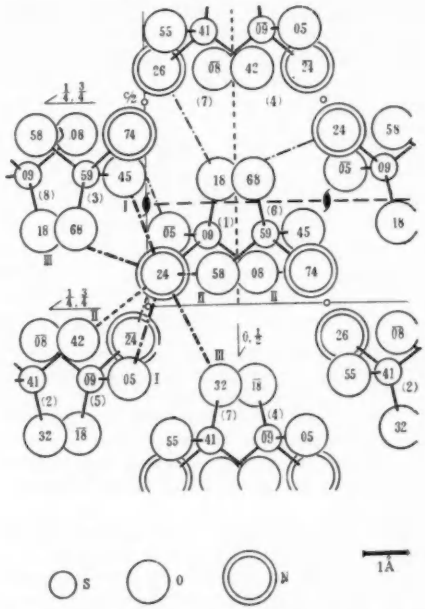

Fig. 2. Projection of part of unit cell upon (100). N-H·····O bonds only between molecule (1) and its neighbours are shown in chain lines, while dotted one show another close approach (2.84 Å) between O and N.

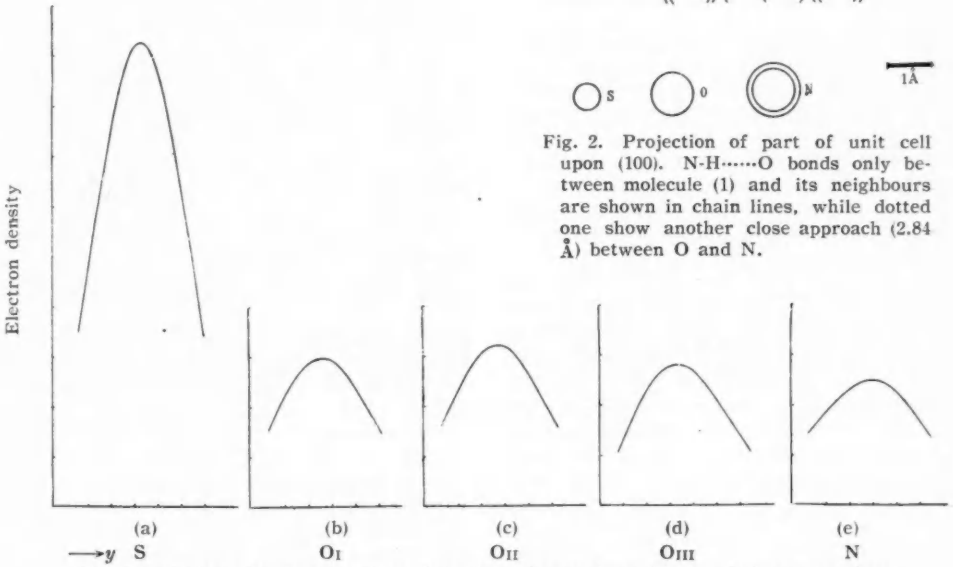

Fig. 1. Electron density plot along lines through atomic positions. Only curves along *b*-axis are shown.

Description of the Structure

The one nitrogen and the three oxygen atoms in the molecule of sulphamic acid constitute a nearly regular tetrahedron, and such tetrahedra are linked three-dimensionally to each other through hydrogen bonds of the type N-H·····O as shown partially in Fig. 2. The nitrogen atom of the molecule (1) (see Fig. 2) is surrounded, besides the three oxygen atoms of the same molecule, by six oxygen atoms, each from one of the neighbouring molecules, five being at distances ranging from 2.93 to 3.01 Å and the sixth at a distance of 2.84 Å. In spite of such a short distance, the sixth atom does not seem to be concerned with the hydrogen bond formation subst antially, because it lies rather in the extended direction of the sulphur-nitrogen axis of the molecule. The arrangement of the oxygen atoms around the nitrogen is illustrated by Fig. 3, in which the atoms are projected upon the plane of three oxygen atoms of the molecule (1). The five N-O directions except the sixth all make angles ranging from 100° to 114° with the N-S axis and this would

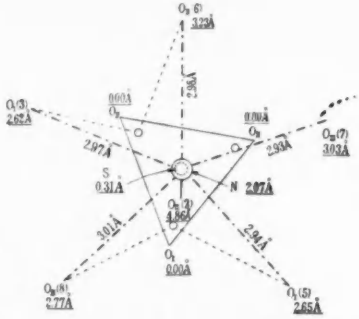

Fig. 3. Arrangement of the oxygen atoms surrounding a nitrogen atom of molecule (1), projected on the plane O_I O_{II} O_{III}. Underlined figures show the height of corresponding atoms measured from the plane of projection. Chain lines indicate the atom pairs linked by N-H·····O bonds.

suggest that all these N·····O pairs take part in the hydrogen bonding. A tentative location of three hydrogen atoms, which leads to one single and two bifurcated hydrogen bonds, are indicated in Fig. 3.* As for the non-hydrogen bonded nature of the sixth N·····O distance, it may be added that, in the case of potassium sulphamate crystal determined by Brown, Cox and Llewellyn[1] and by Jeffrey and Stadler[4] they have already found a short N·····O distance 3.04 Å, which they did not consider to be hydrogen bonded. Another instance is found in the case of orthorhombic hydrazonium sulphate[5], where a similarly disposed oxygen atom was not considered to be hydrogen bonded in spite of a shorter distance of 2.82 Å.

Discussion of the Molecular Structure

Though further refinements of atomic coordinates have not been carried out, the values of standard deviations σ listed in Table II seem to indicate already that we may discuss the molecular structure in some detail. The determined dimensions of the molecule are listed in Table III.

TABLE II
STANDARD DEVIATIONS

	S		O(average)	N
$\sigma(r)$	0.008Å		0.024Å	0.028Å
	S-O	S-N	O-O	O-N
σ(distance)	0.025Å	0.029Å	0.034Å	0.037Å

As to the shape of the NO_3 tetrahedron, the mutual deviations observed within the values of the three O-O's, or within those of the three O-N edges (see Table III) will be regarded as insignificant, whereas there is observed significant difference between the averaged values for the set of O-O and that for O-N. Thus we have in this crystal a somewhat elongated, but nearly regular tetrahedron.

The observed differences within three S-O distances are also insignificant and their mean value comes out 1.44 Å,* which deviates considerably from those given by Kanda and King[2], but agrees perfectly with the refined values obtained by Jeffrey and Stadler[4] in the case of potassium sulphamate.

TABLE III
BOND LENGTHS AND BOND ANGLES

Substances	S-N	S-O	O-O	N-O	∠NSO	∠OSO
Sulphamic acid						
present work	1.75_5	1.43	2.42	2.48	102°	114°
		1.44	2.42	2.50	102°	115°
		1.45	2.46	2.51	103°	118°
Kanda & King[2]	1.73	1.47	2.54	2.33	92°	114°
		1.48	2.57	2.49	100°	117°
		1.49	2.60	2.53	102°	119°
NH_4O_3S·NO·NO	1.791	1.464			102.2°	114.2°
Jeffrey & Stadley[4]		1.434			102.2°	114.2°
		1.434			105.7°	116.0°
KO_3S·NH_2	1.60	1.42	2.38	2.45	107°	111°
Jeffery & Stadler[4]		1.45	2.38	2.49	107°	112°
		1.45	2.38	2.49	108°	112°
β-isoprene sulphone		1.436	2.403			113.7°
Jeffery[6]						
SO_2 (microwave spectroscopy)[17]		1.433				

* This location turned out to be similar to that obtained by Kanda and King.

4) G.A. Jeffrey and H.P. Stadler, *J. Chem. Soc.*, 1951, 1467.

5) I. Nitta, K. Sakurai and Y. Tomiie, *Acta Cryst.*, **4**, 289 (1951).

6) G.A. Jeffrey, *Acta Cryst.*, **4**, 58 (1951).

The mean value of the three bond angles O-S-O is 116° which is considerably greater than the tetrahedral angle.

Our determined value of the S-N bond length is 1.75$_5$ Å in rather good agreement with that found by Kanda and King[2]. On the other hand Jeffrey and Stadler[4] have obtained a value 1.791 Å for the S-N distance in the dinitrososulphite ion and 1.60 Å for that in the sulphamate ion, of which the former was regarded by them to correspond very closely to the length of a pure single σ bond and the latter to that associated with a double bond. They discussed the accordance of their value 1.79 Å for N^+-S with that calculated from the well established values C-N=1.48 Å, C-S=1.81 Å and N-N=1.48 Å. A similar discussion to that of the case of dinitrososulphite ion will also be applied to the present case, although here the bond length is somewhat shorter and there are some differences in the distribution of valence forces around the nitrogen atom; for example, this is more or less tetrahedral and the configuration of three oxygen and three hydrogen atoms seems to be such as to form a trigonal prism, as shown in Fig. 3. As shown in Table III the observed N-S-O bond angles are nearly equal to each other and their mean value 102° is sensibly smaller than that 107° found by Jeffrey and Stadler[4] in the case of potassium sulphamate, of which the latter is more close to the tetrahedral angle 109.5°.

As to the bonding characteristics of the molecule as a whole, there are two extreme ideal structures conceivable; the one containing a hydroxyl and an amino group, $(H_2N)-SO_2-(OH)$, and the other of a zwitterion type, $(H_3N)^+-(SO_3)^-$. In the former case the lone pair of $2p$ electrons on the neutral amine nitrogen atom will be expected to possess a tendency to form a linkage of a partial double bond character with the central sulphur atom, as actually observed by Brown and Cox[1] and by Jeffrey and Stadler[4] in the case of sulphamate ion $(H_2NSO_3)^-$ in the potassium and ammonium salts. In the other case of zwitterion structure, on the contrary, the absence of such a lone pair of electrons will prevent double bond formation with the sulphur atom. The observed value 1.75$_5$ Å of the S-N bond distance, which corresponds more closely to a single covalent $S-N^+$ bond, will thus be accounted for essentially by the zwitterion structure $(H_3N)^+-(SO_3)^-$. In this respect our conclusion is in agreement with that of Kanda and King[2]. The location of three hydrogen atoms around the ammonium nitrogen was not determined directly. However, assuming that they are arranged so that the bond angles S-N-H and H-N-H form approximately tetrahedral angles and that they are all linked by forming hydrogen bonds with adjacent oxygen atoms of the surrounding molecules, it is possible to assign probable positions for them which are shown in Fig. 3 as already mentioned. It may be added that such assignment makes one hydrogen atom H_{II} lie on the line connecting the central nitrogen and an oxygen $O_{III}(7)$ and each of the other two, H_I or H_{III}, on the plane of $NO_I(5)O_{III}(8)$ or $NO_I(3)O_{II}(6)$, thus the latter H_I or H_{III} forming bifurcated bonds. Moreover, such configuration of the hydrogen atoms may be an electrostatically stable one because each hydrogen atom comes very near to each of the three oxygen atoms in the molecule.* Turning to the part SO_3, it has already been remarked that the S-O bond length found is in the mean to be 1.44Å, which is consistent with the remarkably constant values reported for S-O bonds in various molecules, and a similar discussion on the nature of the bond to that given by Jeffrey and Stadler[4] will also apply to the present case. Only it will be of some interest to notice that this zwitterion type of sulphamic acid molecule may be regarded as an addition compound of pyramidal ammonia molecule NH_3 and planar sulphur trioxide SO_3, as in the cases of NH_3-BF_3 and the like which have been extensively studied by Hoard, Geller and others.[7-14] The flat shape of the SO_3 pyramid may suggest a considerable contribution of the π-bond

* The values given in the Abstracts of the Second International Congress (I.U.C., 1951) are those before the correction for finite series and refinement of lattice parameters.

* Quite recently (at a meeting of the Physical Society of Japan held in Nagoya in April, 1955) K. Sano of the Yamanashi University, Japan, reported his nuclear magnetic resonance absorption experiment of this crystal. In this connection it is remarked that the above-mentioned location of the three hydrogen atoms as forming a regular triangle is only a tentative one and the possibility of a deviation from such a regular arrangement is not excluded.

7) S. Geller and J.L. Hoard, *Acta. Cryst.*, **3**, 121 (1950).
8) J. L. Hoard, T. B. Owen, A. Buzzell and O. N. Salmon, *Acta Cryst.*, **3**, 130 (1950).
9) S. Geller and O.N. Salmon, *Acta Cryst.*, **4**, 379 (1951).
10) S. Geller, R. E. Hughes and J. L. Hoard, *Acta Cryst.*, **4**, 380 (1951).
11) S. Geller and M.E. Miberg, *Acta Cryst.*, **4**, 381 (1951).
12) J. L. Hoard, S. Geller and W. M. Cashin, *Acta Cryst.*, **4**, 396 (1951).
13) S. Geller and J.L. Hoard, *Acta Cryst.*, **4**, 399 (1951).
14) J. L. Hoard, S. Geller and T. B. Owen, *Acta Cryst.*, **4**, 405 (1951).

nature in the S-O linkage. Recently Pauling[15] gave an interesting discussion on the interatomic distances and bond character in the oxygen acids and related substances. He gave for the S-O distance in the flat molecule of SO_3 the calculated value of 1.44Å, which also suggest the view that the nature of the S-O bond in sulphamic acid molecule is not very different from that in SO_3 molecule.

In order to obtain some further information on the structure of the molecule, we have carried out a dielectric measurement of this crystal at various temperatures using the alternating field of the frequency of 3 Mc. The results are $\varepsilon_a=5.2$, $\varepsilon_b=5.2$ and $\varepsilon_c=5.0$ (at 12~15°C), which are sensibly constant at various temperatures. By combining these data, comparable with those of ordinary ionic crystals of NaCl type, with those of refractive indices $n_a=1.568$, $n_b=1.563$ and $n_c=1.553$ (at 25±3°C) for 5461 Å of this crystal given by Bryant,[16] it is obvious that the infrared polarisabilities are fairly large, by far larger than ordinary molecular crystals containing amino or hydroxyl group, standing thus not in contradiction to the view of the zwitterion structure of the molecule in the crystalline state.

15) L. Pauling, *J. Phys. Chem.*, **56**, 361 (1952).

16) W. M. D. Bryant, *J. Am. Chem. Soc.*, **61**, 2551 (1939).

17) B. P. Dailey, S. Golden and E. B. Wilson, Jr., *Phys. Rev.*, **72**, 871 (1947).

Experimental Remarks

Crystals obtained from neutral aqueous solution were ground into thin rods of cylindrical shape as far as possible, the cross sections being 0.24×0.31 mm. for [100], 0.27×0.25 mm. for [010], 0.12×0.10 mm. for [001].

Oscillation photographs were taken using the multiple film technique with the Cu-K radiations. Intensities were estimated by comparing with standard density scales. Atomic scattering factors for S^{+3}, O^{-2}, N^{-2} were taken from the International Tables. The effect of outer electrons was found to be small when all (hkl) data were taken into account. Three-dimensional Fourier summations were carried out along lines parallel to the three principal axes using 120-section cosine tables, these lines passing in no case more than 0.10 Å apart from the peak obtained.

The authors express their gratitude to Dr. S. Uchida of Government Chemical Industrial Research Laboratory of Tokyo, who directed our attention to the importance of the X-ray investigation of this substance and gave us good crystals for this purpose, to Dr. R. Kiriyama for the measure ment of the dielectric constants of the crystal, and to Mr. Y. Sasada for his help in numerical computations. Grateful acknowledgment is made to the Ministry of Education for a grant.

Department of Chemistry, Faculty of Science, Osaka University, Osaka

The Michael Addition of Diethyl Malonate to Ethyl Crotonate-(carbonyl-C^{14})[1]

By Osamu SIMAMURA and Naoki INAMOTO

(Received May 24, 1955)

Michael and Ross have shown[2] that whereas diethyl methylmalonate adds to ethyl crotonate in the presence of one sixth equivalent of sodium ethoxide to yield diethyl α-ethoxycarbonyl-α, β-dimethylglutarate (normal product), the product is, with one equivalent of sodium ethoxide, diethyl α-ethoxycarbonyl-β, γ-dimethylglutarate (abnormal product). In a previous work[3] it has been established by a tracer technique with radioactive carbon-14 that the abnormal product is formed by the migration of an ethoxycarbonyl group from the diethyl methylmalonate moiety to the α-carbon atom of the crotonate in the course of the addition reaction. A mechanism of the formation of the normal or abnormal product according to experimental conditions has been put foward and the structural features which lead to the migration of the ethoxycarbonyl group have been discussed.

Work has now been extended to the Michael addition between diethyl malonate and ethyl crotonate-(carbonyl-C^{14}). In this case, the migration of an ethoxycarbonyl group from diethyl malonate should result in structurally the same product as the one formed without the migration. But, similarly to the case with diethyl methylmalonate described previously, the tracer method would reveal any migration which might take place.

Labelled ethyl crotonate (activity 8.6±0.6 μc/mol.) was refluxed with diethyl sodiomalonate in ether and the resulting diethyl α-ethoxycarbonyl-β-methylglutarate was hydrolyzed with sodium hydroxide to the corresponding tricarboxylic acid (activity 8.4± 0.6 μc/mol.). The decarboxylation of this acid by heating at 165° gave carbon dioxide which was found to be only slightly active, and β-methylglutaric acid with an activity of 8.0±0.5 μc/mol. The sequence of the reactions carried out is shown below and the measured activities (with standard errors) of the products at each step are also given under the formulae.

If the migration of an ethoxycarbonyl group had taken place freely in the course of the Michael addition from an adding molecule of diethyl malonate to the carbon atom α to the labelled ethoxycarbonyl group of ethyl crotonate, the tricarboxylic acid

$$CH_3CH{=}CHC^{14}OOC_2H_5 + CH_2(COOC_2H_5)_2 \xrightarrow{C_2H_5ONa} CH_3CHCH_2C^{14}OOC_2H_5 \quad (CH(COOC_2H_5)_2)$$

8.6±0.6 μc/mol. 9.5±1.1 μc/mol.

$$\longrightarrow CH_3CHCH_2C^{14}OOH \quad (CH(COOH)_2) \longrightarrow CH_3CHCH_2C^{14}OOH \quad (CH_2COOH) + CO_2$$

8.4±0.6 μc/mol. 8.0±0.5 μc/mol. 0.12±0.08 μc/mol.

1) Presented at the Meeting of the Kanto Section of the Chemical Society of Japan, in Tokyo, Sept. 18, 1954.

2) A. Michael and J. Ross, *J. Am. Chem. Soc.*, **52**, 4598 (1930).

3) O. Simamura, N. Inamoto and T. Suehiro, This Bulletin, **27**, 221 (1954).

Added in proof—D. Samuel and D. Ginsburg, *J. Chem. Soc.*, **1955**, 1288, have come to the same conclusion by the use of O^{18} as tracer.

obtained by hydrolysis of the addition product would have included a labelled malonic acid grouping, and therefore the carbon dioxide evolved on decarboxylation would have contained half the amount of the radioactivity in the original ethyl crotonate. Most of the activity being actually found in β-methylglutaric acid, it was demonstrated that such a migration of the ethoxycarbonyl group occurred only to an extremely limited extent and the addition proceeded almost normally.

According to the theory set forth previously, the non-migration of the ethoxycarbonyl group in the present case is due to the presence of an acidic hydrogen atom on the carbon with two activating ethoxycarbonyl groups in an adduct anion (I) initially formed from diethyl sodiomalonate and ethyl crotonate. This hydrogen atom immediately migrates to the carbon atom carrying a lone pair of electrons, giving rise to an isomeric anion (II), which is more stable than structure (I) owing to the conjugation of the lone pair of electrons thus produced with two ethoxycarbonyl groups. In the process of working up of the reaction mixture, anion (II) picks up a proton from the aqueous medium to give the final product (III). The present result demonstrates that the migratory aptitude of a proton to an atom with a lone pair of electrons exceeds by far that of an ethoxycarbonyl group.

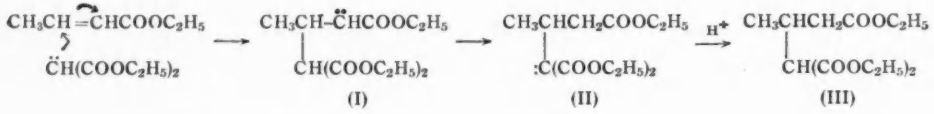

(I) (II) (III)

Added in Proof—After the submission of this article our attention has been drawn to the work of G. A. Swan, *J. Chem. Soc.*, 1955, 1039, who reported the results of similar experiments, which are in full accord with ours.

Experimental

Materials.—Ethyl crotonate-(carbonyl-C^{14}) was prepared as reported previously[3]. Diethyl malonate was purified by fractional distillation under diminished pressure.

The Michael Addition.—Sodium (0.24 g.) was melted by heating in xylene and powdered by shaking, the xylene decanted, the sodium washed with ether, and 50 cc. of ether and 0.5 g. of absolute ethyl alcohol added to prepare sodium ethoxide. To this mixture 1.52 g. of diethyl malonate was added. Ethyl crotonate-(carbonyl-C^{14}) (1.09 g., 8.6±0.6 μc/mol.) in 30 cc. of ether was then added to the stirred mixture and the mixture was refluxed for five hours. Acetic acid (0.7 g.) in 14 cc. of water was added with stirring, the ethereal layer separated, dried with anhydrous sodium sulfate, the ether removed on a water bath and the residue subjected to distillation under diminished pressure, giving 0.9 g. of diethyl α-ethoxycarbonyl-β-methylglutarate boiling at 127~128° at 4 mmHg. This was heated with 0.6 g. of sodium hydroxide in a mixture of 6 cc. each of water and alcohol for three hours on a boiling water bath. The alcohol was removed from the reaction mixture and the residue diluted with water to 40 cc. and passed through a column of Amberlite IR 120. A fraction with pH 2.2 was collected and evaporated to dryness over concentrated sulfuric acid in a vacuum desiccator, giving 0.6 g. of crude acid. This acid was recrystallized four times from ether and benzene, yielding 0.4 g. of α-carboxy-β-methylglutaric acid, m.p. 138–139°C (Found: neutralization equivalent 63.4; activity 8.4±0.6 μc/mol.).

Decarboxylation of α-Carboxy-β-methylglutaric Acid.—The decarboxylation of the labelled α-carboxy-β-methylglutaric acid described above and the absorption of the evolved carbon dioxide by aqueous sodium hydroxide were carried out in an apparatus similar to that for the Van Slyke-Folch oxidation[4]. The labelled acid (173 mg.) was placed in one limb of the apparatus and aqueous sodium hydroxide in another. The apparatus was evacuated and the limb containing the acid was heated gradually to 165°C and kept at that temperature for one hour. When the reaction was completed, ammonium chloride was added to the sodium hydroxide solution, and barium carbonate was precipitated by barium chloride, collected on a filter paper and assayed for radioactivity (Found: 0.12±0.08 μc/mol.). The residue from the decarboxylation was recrystal-

4) M. Calvin et al., "Isotopic Carbon", John Wiley & Sons, Inc., New York, 1949, p. 93.

lized three times from benzene, giving 60 mg. of β-methylglutaric acid, m.p. 86–87°C (Found: activity 8.0±0.5 μc/mol.).

Radioactivity Determinations. — Radiocarbon assays were carried out by oxidizing samples according to Van Slyke and Folch[5], and converting the resulting carbon dioxide to barium carbonate, which was counted with an end-window Geiger-Müller counter on an "infinite thick" layer, the counts being all corrected for background and compared with the count of a standard barium carbonate with a known molar activity.

Summary

The Michael addition of diethyl malonate to ethyl crotonate-(carbonyl-C^{14}) was carried out with one equivalent of sodium ethoxide. The addition product, diethyl α-ethoxycarbonyl-β-methylglutarate, was hydrolyzed to the corresponding acid. It was decarboxylated by heating to give β-methylglutaric acid, which was found to contain most of the radioactivity originally present in the ethyl crotonate. Thus, it was demonstrated that the migration of an ethoxycarbonyl group did not take place in contrast to the case with diethyl methylmalonate. The mechanism is discussed.

The authors are indebted to the Ministry of Education for a Grant-in-Aid for Scientific Research.

Department of Chemistry,
Faculty of Science,
Tokyo University,
Tokyo

5) D.D. Van Slyke and J. Folch, *J. Biol. Chem.*, **136**, 509 (1940).

SHORT COMMUNICATIONS

Isotopic Exchange Reaction Between Heavy Oxygen and Carbon Dioxide on Silver Catalyst

By Hisashi Mori, Kozo Hirota
and Yasushi Kobayashi

(Received March 17, 1955)

As reduced silver can catalyze the oxidation reaction of carbon monoxide even at such a low temperature as 80°C[1], it is of interest to study the behavior of oxygen and carbon dioxide on this metal. It was attempted, therefore, to ascertain whether or not the catalytic isotopic exchange reaction:

$$OO^* + CO_2 \rightleftarrows COO^* + O_2$$

(O^* denotes heavy oxygen)

was measurable by the static method, as done with platinum by use of slightly shifted oxygen[2]. The heavy oxygen was obtained by thermal diffusion column constructed in our laboratory by Mr. Y. Horibe[3] (total column length=15 m.).

The catalyst was prepared by the reduction of precipitated silver oxide at 120–240°C using the hydrogen gas, followed by repeated activation at 240°C. Throughout this research one and the same catalyst was used, but it was reduced again before each run. The original gas consisted of heavy oxygen (OO^* being 2.12% of total O_2) and carbon dioxide in nearly equal molar amount. Its total pressure was 127–148 mmHg, the partial pressure of O_2 being less than the decomposition pressure[4] of Ag_2O at 175–250°C. In the measurement of chemisorption of O_2 and CO_2, their initial pressure was taken to be 76–78 mmHg. As the volume of reaction tube was about 120 cc. (STP), the volume of oxygen in the original gas was about 7 cc. (STP), which was fairly little as compared with the catalyst quantity (74 g.). Such a proportion was adopted, so as to make the amount

Table I

Run No.	React. temp. °C	React. time min.	OO^{18} %	COO^{18} %	$\frac{CO_2}{O_2}$	Initial pres. mmHg	Adsorb. gas amount mmHg	Remark
1	175	90	2.1_4	1.0_4	0.99	141	19	b
		270	2.1_1	1.1_1			25	
2	188	20	—	—	0.97	142	17	b
		60	2.0_4	0.9_9			22	
		210	1.8_8	1.1_0			26	
3	200	15	2.0_7	0.8_9	1.08	127	15	a
		90	2.0_3	1.1_1			21	
		270	1.4_3	1.1_8			21	
4	200	15	1.5_4	1.0_5	1.28	130	0	c
		60	1.5_7	1.0_8			0	CO_2 after O_2
		180	1.2_6	1.1_4			0	
5	200	15	2.0_7	1.1_4	1.15	133	21	c,
		60	1.9_5	1.2_0			22	O_2 after CO_2
		180	1.5_3	1.2_1			22	
6	200	15	1.7_7	—	—	78	16.5	c, O_2 only
		180	1.6_4	—			16.5	
7	200	180	—	0.4_1	—	76	0	c, CO_2 only
8	220	60	1.8_0	0.8_0	1.03	137	16	a
		180	1.0_2	0.8_7			—	
9	220	10	2.0_9	1.0_1	0.93	148	16	b
		50	1.3_4	1.0_9			18	
		180	1.2_0	1.1_2			18	
10	250	15	1.6_2	—	—	76	6	b, O_2 only
		210	1.4_0	—			7	

of gaseous oxygen comparable to that chemisorbed.

Besides the continuous manometric reading, the progress of the reaction was investigated intermittently by mass-spectrometric analyses of the samples (about one cc. STP) taken out from the reaction tube at recorded times. Abundance ratios of O^{18}/O^{16} in O_2 and CO_2 contained in them were determined by the same mass-spectrogram (Type of the mass-spectrometer: Hitachi-RMB-1). The ratio could be determined within the accuracy of $\pm 0.05\%$ for O_2 and $\pm 0.03\%$ for CO_2.

Summarized results are shown in Table I, where a, b, and c in the last column denote the reducing temperatures 220,250, and 300°C, respectively. In runs 1, 2, 3, and 5 there is this curious result that the increase of O^{18} in CO_2 from its natural abundance, 0.40% as COO^{18}, is greater than the corresponding decrease of O^{18} in O_2. This tendency becomes more marked as the reaction temperature decreases. It can be explained, however, if we assume that, following the rapid adsorption of O_2 and CO_2, the exchange reaction and desorption of CO_2 soon occur before the desorption of a considerable amount of oxygen takes place. This assumption is plausible, because the chemisorbed amount of oxygen cannot be neglected in reference to the initial gas volume.

Though the data are not yet reproducible, due to the gradual increase of catalytic activity, the following conclusion can be derived.

i) Even when the catalyst is reduced at 300°C for five hours, some chemical species containing oxygen atoms remain in the subsurface or bulkphase of the catalyst; see runs 10, 6, 7, and 8.

ii) The exchange reaction proceeds evidently at 175–220°C, though the desorption of O_2 is very slow at 175–188°C; thus the rate-determining step is the desorption of oxygen atoms; see runs 1, 2, 3, 4, 5, 7, 8 and 9.

Detailed studies are now going on.

1) A.F. Benton and R.P. Bell, *J. Am. Chem. Soc.*, **56**, 501 (1934). T. Titani et al., *J. Chem. Soc. Japan*, **55** 13, 224, 305 (1934). N. Yamada, This Bulletin, **27**, 36, (1954).

2) N. Morita and T. Titani, This Bulletin, **12**, 104 (1937); **13**, 357 (1938).

3) Y. Horibe and S. Nishizawa, *J. Chem. Soc. Japan*, **76**, 26 (1955).

4) E.g., A.F. Benton and L.C. Drake, *J. Am. Chem. Soc.*, **54**, 2186 (1932); **56**, 255 (1934).

Chemical Department, Science Faculty, Osaka University, Osaka

Isotopic Composition of the Common Lead in Japan

By Hitoshi Sakai, Masatake Honda and Eiichi Minami

(Received June 28, 1955)

Fourteen lead samples, mainly consisting of galenas, from the various parts of Japan are analyzed for their isotopic compositions of lead. Using a commercial mass-spectrometer, Model 21-103A of Consolidated Engineering Co., the samples are analyzed in the form of lead tetra-methyl as described by Collins et al.[1] and Dibeler and Mohler[2]. Of four main peak groups in the mass-spectrogram of lead tetra-methyl, the first group consisting of Pb^+ and PbH^+ is used for the isotopic analysis. Since Pb^{204} peak is usually very small compared to those of other isotopes of lead, the superposition of Hg^{204} peak to that of Pb^{204} must be accurately corrected. For this purpose mercury dimethyl is synthesized from the same mercury as used in the pumping system of the instrument and the peak ratio of Hg^{204} to Hg^{202} is found to be 0.231 ± 0.001 for the same machine. This correction factor is used throughout the research.

The time variation of working conditions of the mass-spectrometer is checked by a standard sample and is proved to be negligibly small in the course of the experiment.

The results are summarized in Table I, and the maximum standard deviation is $\pm 0.5\%$ of the values.

A standard sample, galena, from Broken Hill, New South Wales, is analyzed by the same method and the values 16.07, 15.41 and 35.87 are obtained for the ratios Pb^{206}/Pb^{204}, Pb^{207}/Pb^{204} and Pb^{208}/Pb^{204}, respectively. They are in good agreement with Nier's data[3], 16.07, 15.40 and 35.5, respectively, for the corresponding ratio's obtained for a galena from the same district.

A number of lead ores of recent geologic ages from the various parts of the world has been analyzed by many researchers. For example, Tilton et al.[4] calculated the average composition of lead ores formed within the last 50 m.y. by least squares analysis of the data by Collins et al.[5]. They

TABLE I

ISOTOPIC COMPOSITION OF ORE LEAD IN JAPAN

No.	Locality	Mineral	Isotopic Composition of Lead $\frac{Pb^{206}}{Pb^{204}}$	$\frac{Pb^{207}}{Pb^{204}}$	$\frac{Pb^{208}}{Pb^{204}}$	Geologic Age
			(Atomic Ratio)			
1	Kamioka Mine, Gifu Prefecture	Galena	18.20±0.05	15.55±0.05	38.71±0.15	Cretaceous
2	Daira Mine, Akita Prefecture	Galena	18.32±0.05	15.43±0.05	38.45±0.15	Tertiary
3	Hanaoka Mine, Akita Prefecture	Galena	18.55±0.05	15.57±0.05	38.61±0.15	Tertiary
4	Arakawa Mine, Akita Prefecture	Galena	18.44±0.05	15.57±0.05	38.74±0.15	Tertiary
5	Hosokura Mine, Akita Prefecture	Galena	18.59±0.05	15.59±0.05	38.73±0.15	Tertiary
6	Tamagawa Hotsprings, Akita Prefecture	Hokutolite	18.63±0.05	15.61±0.05	39.04±0.15	—
7	Osaruzawa Mine, Akita Prefecture	Galena	18.54±0.05	15.58±0.05	38.82±0.15	Tertiary
8	Taishuu Mine, Nagasaki Prefecture	Galena	18.47±0.05	15.59±0.05	39.02±0.15	Cretaceous
9	Budō Mine, Niigata Prefecture	Galena	18.42±0.05	15.50±0.05	38.60±0.15	Tertiary
10	Mikawa Mine, Niigata Prefecture	Galeha	18.58±0.05	15.66±0.05	39.00±0.15	Tertiary Probably
11	Chichibu Mine, Saitama Prefecture	Galena	18.71±0.05	15.83±0.05	39.20±0.15	Tertiary
12	Ogoya Mine, Ishikawa Prefecture	Pyro-morphite	18.82±0.05	15.67±0.05	39.32±0.15	Tertiary
13	Sani-mura, Shioya, Ibaragi Prefecture	Galena	18.36±0.05	15.53±0.05	38.59±0.15	—
14	Tōya Mine Hokkaidō	Galena	18.52±0.05	15.56±0.05	38.68±0.15	Tertiary
	The average value of Galena sample:		18.48	15.59	38.76	

are 18.5, 15.6 and 38.4 for the ratios, Pb^{206}/Pb^{204}, Pb^{207}/Pb^{204} and Pb^{208}/Pb^{204}, respectively, and in good agreement with the average value of the recent lead from Japan. From Table I, however, it is seen that "secondary" lead ores, Hokutolite and Pyromorphite, as well as some of the galena have comparatively high content of thorium lead, of which the geological meanings are not yet known.

The samples in this research are kindly presented by Prof. T. Watanabe and Assist. Prof. K. Imai of the University of Tokyo and Mr. Sugizaki of the University of Nagoya. Prof. S. Araki and his associates of the University of Tokyo have given us useful suggestions on the operation of the mass spectrometer. The authors wish to express their sincere thanks to them.

1) C. B. Collins, R. D. Russell and R.M. Farquhar, *Can. J. Phys.*, 31, 402-418 (1953).
2) V.H. Dibeler and F.L. Mohler, *J. Res. Nat. Bur. Standards* V. 47, 337-342 (1951).
3) A.O. Nier, *J. Am. Chem. Soc.*, 60, 1571 (1938).
4) G.R. Tilton et al., *Bull. Am. Geal. Soc.*, in Press.
5) loc. cit.

Department of Chemistry, Faculty of Science, Tokyo University
Tokyo

Low-temperature Sublimation of Polonium Dithizonate

By Kenjiro KIMURA and Hisao MABUCHI

(Received June 28, 1955)

The formation of polonium dithizonate was first reported in 1950 by T. Ishimori and H. Sakaguchi[1], and, independently, by G. Boussière and C. Ferradini[2]. In the course of study on polonium chemistry using polonium-210, the present authors observed the following phenomenon.

A thin layer of ultra-micro quantities of polonium dithizonate was prepared in a stainless steel dish by evaporating the solution of the compound in carbon tetrachloride. When the dish was heated on a hot plate, the α-activity of the sample in the dish was rapidly diminished.

Since such a phenomenon has never been reported, it was explored in detail.

In order to know the cause of decrease in activity of the sample, a platinum plate was placed 3 cm above the dish and heating of the sample was carried out in a closed system. The platinum plate was checked for its radioactivity with a Lauritsen electroscope. The presence of α-activity of polonium-210 was detected and approximately 25% of the lost activity was found on the plate.

From this fact it is likely that the decrease in the activity is caused by the sublimation of polonium-210 in some chemical form, although further study is necessary to confirm whether or not this phenomenon is the sublimation in the strict sense.

The heating was carried out in a range of temperatures between 80°C and 200°C, and attempts were made to identify the sublimate by chemical procedures combined with the measurement of radioactivity.

The result of the experiment is summarized as follows:

(1) The sublimation occurs at temperatures above approximately 120°C under atmospheric pressure.

(2) When the sample is treated with hydrogen peroxide before heating, the α-activity of the sample in the dish does not decrease even at temperatures above 120°C.

(3) The sublimate on the platinum plate is very soluble in carbon tetrachloride, but only slightly soluble in water. Moreover, it is remarkable that the partition of polonium α-activity between carbon tetrachloride and water is dependent on the hydrogen ion concentration of the water layer. This is one of characteristic properties of metal chelate compounds.

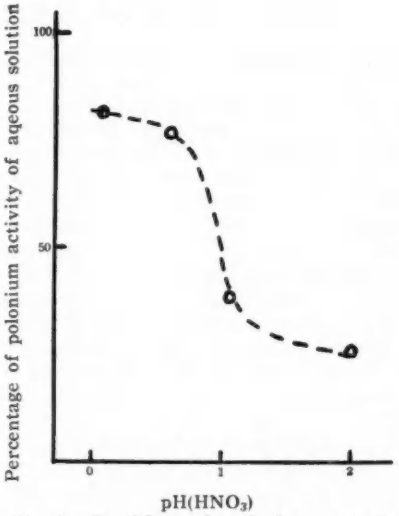

Fig. 1. Partition of polonium activity between carbon tetrachloride (2 cc.) and aqueous solution (20 cc.).

The figure shows the partition of polonium-210 between carbon tetrachloride and aqueous solution as a function of the pH of aqueous solution. In the study of the dithizone extraction of polonium the authors observed a similar change of the partition of polonium between carbon tetrachloride and aqueous solution.

From these results, the authors came to the conclusion that the sublimate is probably polonium dithizonate itself.

This phenomenon may be applied to the carrier-free separation as well as to the purification of polonium.

The detail of this study will be reported in a separate paper.

The authors would like to express their sincere thanks to Dr. Nobufusa Saito and Mr. Yuji Yokoyama for their valuable advice.

1) T. Ishimori and H. Sakaguchi; *J. Chem. Soc. Japan*, **71**, 327 (1950).
2) G. Boussière et C. Ferradini; *Anal. Chim. Acta*, **4**, 610 (1950).

Department of Chemistry, Faculty of Science, Tokyo University, Tokyo

Paramagnetic Resonance Absorption of Coals and Coal Extracts

By Yasaburo Yokozawa, Isao Miyasita, Masao Kugo and Keniti Higasi

(Received June 29, 1955)

Distinct paramagnetic resonance absorption has been observed in British and French coals[1,2,3]. As the nature of Japanese coal is regarded to be particular in many respects as compared with European one, it was considered worth while to enquire whether or not Japanese coal shows this absorption.

The paramagnetic resonance absorption was measured for a British coal as well as for eighteen samples from Hokkaido mines by use of a micro-wave of 3.2 cm. wavelength[4], the dielectric properties of Hokkaido coals having been reported elsewhere[5,6].

Paramagnetic resonance absorption peak with high intensity and narrow width was detected in all the samples examined. The amplitude of Japanese coal was somewhat less than that of the British specimen (Compare the height of the peaks on the left side of the photographs).

By heating the coals at 270°, 330°, 380°, 430° and 460°C, the height of the line was increased gradually with the elevation of temperature. The extracts and residues of the coals by pyridine, as well as the coal specimens heated up to 460°C were also examined and all of them showed the paramagnetic absorption.

It would be premature to discuss whether or not this absorption is ascribed to 'free radicals' of broken bonds[1] or to some other paramagnetic compounds similar to violanthrone and violanthrene[4,7], but it appears certain from this experiment that the problematic substance embracing unpaired electrons is fairly stable against the attack of pyridine solvent.

The writers wish to thank Professor G. Takeya for his kind interest in the present work.

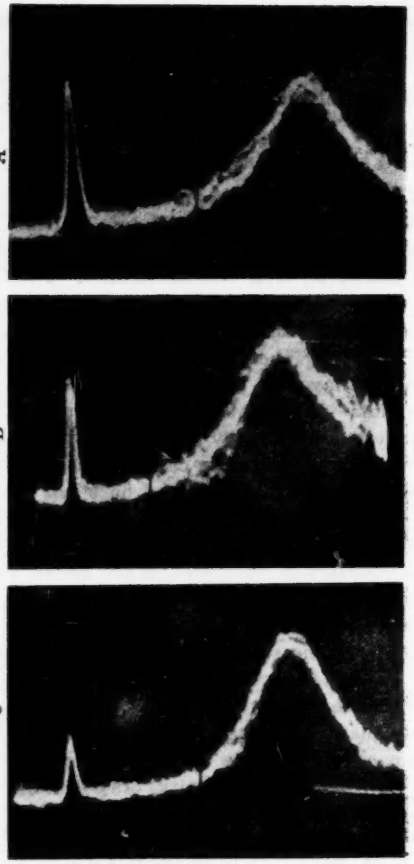

Fig. 1. Oscilloscope trace: absorption spectrum of coal and its pyridine extract. The hills seen on the right side are due to the absorption of cupric sulfate which was added as a standard.
A, British coal (Durham): fixed carbon 71.31, volatile matter 26.14, moisture 0.85, ash 1.70%.
B, Japanese coal (Yubari): fixed carbon 49.41, volatile matter 41.98, moisture 1.50, ash 7.11%.
C, Pyridine extract of B: C 84.50, H 6.48, O+N+S 7.73, ash 1.29%.

1) J.E. Bennett, D.J.E. Ingram and J.G. Tapley, *J. Chem. Phys.*, **23**, 215 (1955).
2) J. Uebersfeld, A. Étienne and J. Combrisson, *Nature*, **174**, 614 (1954).
3) A. Etienne and J. Uebersfeld, *J. Chim. Phys.*, **51**, 328 (1954).
4) Y. Yokozawa and I. Tatsuzaki, *J. Chem. Phys.*, **22**, 2087 (1954).
5) I. Miyasita, R. Miura and K. Higasi, This Bulletin, **28**, 148 (1955).
6) I. Miyasita, *Bull. Res. Inst. Appl. Elec.*, **5**, 123 (1953); **6**, 117 (1954); **7**, 17 (1955).
7) H. E. Blayden, J. Gibson and H. L. Riley, *J. Inst. Fuel*, Wartime Bulletin, 117 (1945).

Research Institute of Applied Electricity and the Faculty of Engineering, Hokkaido University, Sapporo